Summer 1997

Computer-Aided Design of Coupler-Driven Watt I and Tolerance Synthesis for Four-Bar Linkages

Haitao Li
Old Dominion University

COMPUTER-AIDED DESIGN OF COUPLER-DRIVEN WATT I AND TOLERANCE SYNTHESIS FOR FOUR-BAR LINKAGES

by

Haitao Li
B.S. July 1985, Beijing University of Science and Technology
M.S. July 1988, Anshan Institute of Iron and Steel Technology

A Dissertation submitted to the Faculty of
Old Dominion University in Partial Fulfillment of the
Requirement for the Degree of

DOCTOR OF PHILOSOPHY
ENGINEERING MECHANICS

OLD DOMINION UNIVERSITY
August 1997

Approved by:

_____
Sebastian Y. Bawab (Director)

_____
Han Bao (Member)

_____
Gene J-W. Hou (Member)

_____
Jen-Kuang Huang (Member)

ABSTRACT

COMPUTER-AIDED DESIGN OF COUPLER-DRIVEN WATT I AND TOLERANCE SYNTHESIS FOR FOUR-BAR LINKAGES

Haitao Li
Old Dominion University, 1997
Director: Dr. Sebastian Y. Bawab

Theory to rectify circuit defects in rocker-crank and double-rocker at the synthesis level is described based on the angular joint displacements. It complements the crank-rocker and double-crank circuit rectification to complete the circuit rectification of four-bar linkages. The procedure utilizes the algebraic method where special points followed by a line construction procedure are employed to validate the range of the critical angle that can identify the circuit defects as a function of the design positions prior to the completion of the linkage.

A complete procedure of the rectified synthesis of the coupler-driven Watt I six-bar linkage to pass through the pre-defined four design positions is presented. This is done by de-coupling the six-bar mechanism as a coupler-driven and crank-driven four-bar linkages with common links. The vector component mechanism modeling method is applied to these linkages where the dyad and triad synthesis approaches are adopted in conjunction with the vector-algebraic method to find the solutions. The linkage with the coupler-driver is initially synthesized and rectified, then followed by the crank-driven four-bar linkage. The six-bar linkage is thus insured to assemble free of circuit, branch, and order defects. Optimization techniques are used to render the best solution linkages according to the specified design criteria. The process is coded and added to a mechanism design platform - RECSYN that allows a designer to synthesize coupler-driven Watt I linkages and the new circuit rectification theory is also applied in the program.

A methodology to determine the optimum link length tolerance and joint clearance distributions in four-bar linkages for motion generation with specified structural error in order to manufacture the linkages is proposed. A stochastic model incorporated with tolerances and clearances for four-bar motion generation is proposed. The statistical characteristics of the random variables in the model are discussed. The mechanical error of four-bar motion generation as a function of statistical properties of random variables is defined. The tolerances and clearances are obtained as a result of solving an optimization problem with the objective function of link length tolerances and joint clearances and

structural error as constraints. A FORTRAN code is written based on the proposed theory and ADS is employed as an optimization design tool. With this program, optimum link length tolerance and joint clearance distribution can be computed when the user input the required linkage information and structural errors. Examples of assigning tolerance and clearance for four-bar motion generation are presented to demonstrate the application of the method.

To My Family

ACKNOWLEDGMENTS

I would like to express my gratitude to my advisor, Dr. Sebastian Y. Bawab for his technical advice, guidance, and support throughout my research. I wish to thank Dr. Han Bao, Dr. Gene J-W. Hou, and Dr. Jen-Kuang Huang for their review of this work and services as my committee members. I would also like to extend my appreciation and thanks to all those faculty members for their cooperation and input.

To my parents, I am very thankful for their support, trust, and encouragement. To my wife Xiaohong and daughter Jenny, I am greatly indebted to their love, support, and patience. I also wish to thank my brother and sister for their encouragement and support.

TABLE OF CONTENTS

PAGE

LIST OF FIGURES

PAGE

LIST OF TABLES

CHAPTER I

INTRODUCTION

1.1 Mechanisms and Linkages

A *mechanism* is a component of a machine consisting of two or more bodies arranged so that the motion of one compels the motion of the others. There exist a variety of mechanism types that include gears, belts and pulleys, chain drives, cams, and linkages, among others.

A *linkage* is defined as an assemblage of rigid bodies connected by kinematic joints to transmit power and motion. A linkage may serve as a component of a mechanism or machine. Thus the terms *linkage, mechanism* and *machine* are often used interchangeably (Wilson and Sadler, 1993).

A four-bar linkage with basic configuration is shown in Fig. 1.1. It consists of a base link, input or driving link output or driven link (also referred to as the follower) and a coupler link which couples the input and the output links.

The design process of a mechanism starts normally with the selection of a mechanism type. The selection is made based on the criteria such as cost, weight, durability, size, accuracy, time to implement the design, and solution availability. Linkages are generally simple, cost effective, light, durable and versatile compared to other types of mechanisms. Under some circumstances, the linkage may be the unique solution to carry out the design task. Unfortunately, the linkage design is very complex and time consuming, especially for mutiloop linkages such as six-bars.

In the past, the design of linkages required a good knowledge and experience of kinematics and patience when a designer had to rely on trial and error approaches. The situation has been improved tremendously with the adaption of the geometric solutions to numerical ones that can be delivered by computers. This enhances the attractiveness of linkages to replace other types of mechanisms.

Kinematics is the study of motion in mechanisms without reference to the forces that act on the system (Wilson and Sadler, 1993). The kinematics of linkages can be

---

The journal model is adapted for this dissertation in ASME.

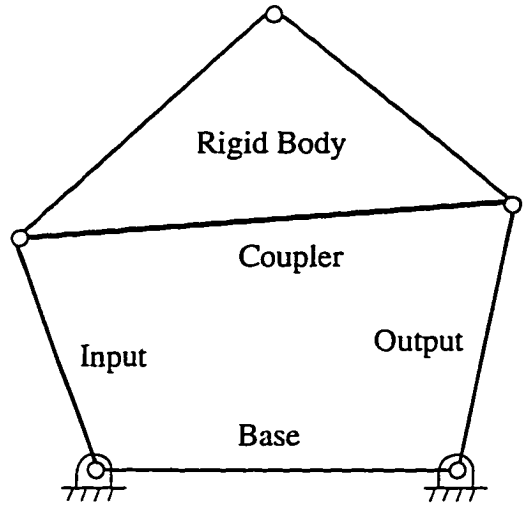

Figure 1.1 A Simple Four-Bar Linkage

divided in two main sections: analysis and synthesis. Analysis is concerned with the determination of displacement, velocity, acceleration and pulse (jerk) characteristics of existing mechanisms, while synthesis deals with the development of mechanisms which generate desired kinematic characteristics. The design of mechanisms involves both synthesis and analysis. When the analysis part is integrated with the synthesis part, spurious solutions can be eliminated. This method is known as the *Rectified Synthesis.*. An overview of linkage synthesis is provided in the following section.

1.2 Preface to Linkage Synthesis

Linkage synthesis can be divided into task, type, number, and dimensional synthesis. Task synthesis defines the task which a mechanism is designed to fulfill. Linkage tasks can be sub-categorized into *function generation*, *path generation*, and *motion generation*.

In function generation, the output and input links of a mechanism are coordinated by a prescribed function. An example of a function generator is shown in Fig. 1.2 where a valve is being directly actuated by an overhead cam (Mabie and Reinholtz, 1987). The linear motion of the valve x must be accurately defined as a function to the cam rotation angle θ.

In path generation, a point (called the tracer point) of the moving body is required to trace a specific path. Sometimes the angular position of the driving link is correlated with the tracer point position; this is called path generation with prescribed timing or path angle generation. An example is a web cutter shown in Fig. 1.3 (Hall, 1986).

In motion generation, both the position of a point within a moving body and the angular orientation of the body are specified; it is also known as a rigid body guidance. One example of motion generation is a front-end loader illustrated in Fig. 1.4 (Wilson and Sadler, 1993). In this case, the boom (rigid body) is actuated by two hydraulic cylinders, one on each side of the machine.

Type synthesis defines the type of mechanism designed to fulfill a given task. Number synthesis addressed the question of the number of links and connections needed to produce the required motion. The designer generally relies on intuition and experience as a guide to type and number synthesis. Very little supporting theory is available at this stage. Therefore, the designer should be familiar with the capabilities and typical applications of a variety of mechanisms: including gears, belts and pulleys, chain drives, cams, and linkages.

Dimensional synthesis deals with determining the actual link lengths of a linkage with pre-defined type and link number. In contrast to type and number synthesis, a great deal of theoretical background exists for dimensional synthesis of mechanisms. Burmester theory is a prime dimensional synthesis technique. Part of the work in this thesis relates to the dimensional synthesis of coupler-driven Watt I six-bar linkage.

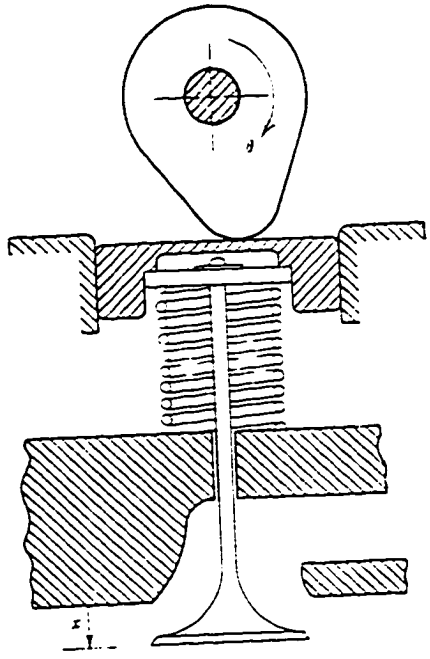

Figure 1.2 A Function Generator

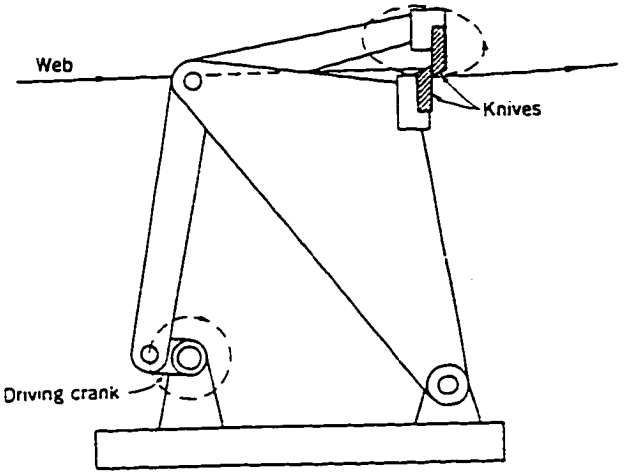

Figure 1.3 A Example of Path-Angle Generator - Web Cutter

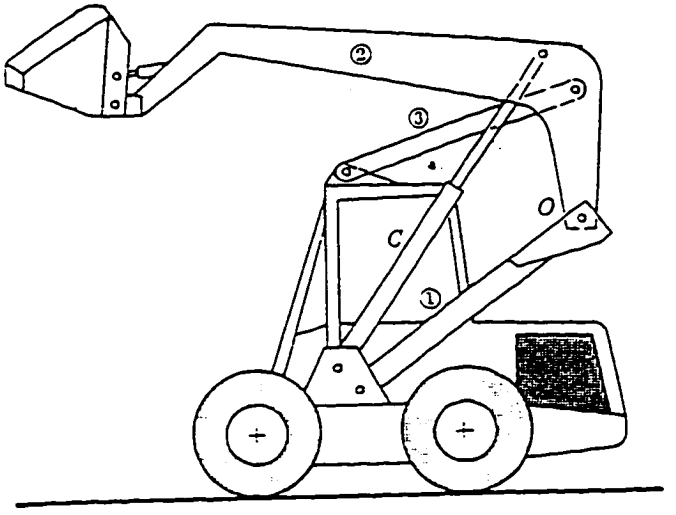

Figure 1.4 A Front-End Loader

Function generation, path generation, and motion generation can be referred to as precision position methods because linkages are designed to pass exactly through prescribed positions in each case. However, function generation and path generation synthesis problems can be transferred into motion generation synthesis problems (Waldron and Strong, 1979). The work in this dissertation is focused on motion generation.

Rigid body guidance of four-bar linkages has a maximum number of five precision positions that can be synthesized. However, the solution for the five positions is limited to a maximum number of nine points which makes it extremely difficult to validate a feasible solution. Therefore, it is more efficient to design linkages for three or four design positions.

A synthesized linkage is only guaranteed to be assembled at the precision positions and it may not be able to move smoothly between successive design position in the right order. This happens when several important factors are considered in the synthesis process. There are three types of possible problems or "defects" occur in a synthesized linkage to render the linkage kinematically unsuitable for the design task. These are known as *circuit defect*, *branch defect*, and *order defect*. A circuit defect happens when a linkage can not go through all the design positions without being disconnected and reassembled in different configurations. Hence, it is obvious that a linkage suffers from circuit defect has no practical use. Branch defect occurs when the sign of the transmission angle[1] changes at one of the design positions. A branch defects are generally undesirable since the rotation of the followers of linkages can not be controlled when the sign of the transmission angle changes unless there are some external or internal forces applied to them. There are some rare cases, such as the lock mechanism of a clamp, where the linkage requires a branch defect. However, since pure kinematics is discussed here, linkages has branch defect are considered unacceptable. A example of linkage suffering from circuit and branch defects is shown in Fig. 1.5. Order defect exists when the linkage passes through the design positions in a wrong order. There is no order problem for two position synthesis. Solutions with circuit defects, branch defects, and order defects will be eliminated in the rectified synthesis. Grashof criterion is also very important in the rectified synthesis process because both link rotatability and circuit defect are related to Grashof types. Finally, a synthesized linkage may not deliver the desirable kinematic property requirements such as velocities and accelerations. Therefore, post-synthesis analysis needs to conduct to those with requirements of higher order kinematic properties.

Normally, a linkage is synthesized to be driven by a link pivoted to the ground. For example, the linkages shown in Figs. 1.2 and 1.3 are referred to as *crank-driven linkages*. There are cases where the floating links (coupler) are the drivers. these linkages are called *coupler-driven linkages*. The front-end loader shown in Fig. 1.4 has a coupler-driven linkage. Most of the documentation on mechanism synthesis deal with crank-driven case while the synthesis procedure of the coupler-driven linkage is somewhat different as

---

[1] Transmission angle is decided based on the mechanical advantage. In case of crank driven four-bar linkage transmission angle is formed from the coupler to the driven crank. The transmission angle range is $-\pi$ to π.

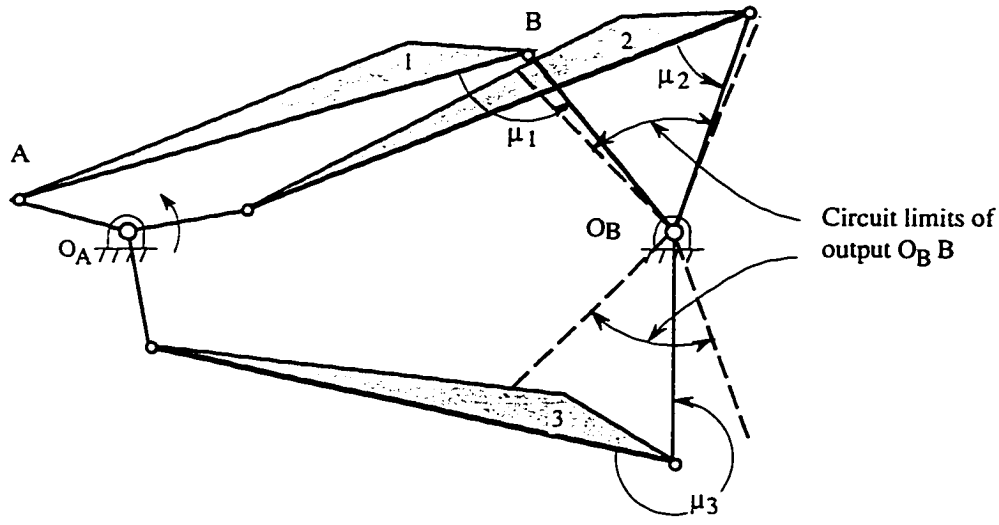

Figure 1.5 A Mechanism with Circuit and Branch Defects

described in Bawab et al. (1992). A technique of synthesizing coupler-driven Watt I six-bar linkages is documented in this work.

The four-bar, the simplest of the closed loop linkages, is able to perform relatively complex tasks. The synthesis theory for four-bar linkage has been well developed in the literature. Unfortunately, four-bar linkages have limited performance to satisfy difficult design criteria. The next least complex mechanism with one degree of freedom is the family of six bar linkages. The six bar linkages often provide attractive and compact solutions to more intricate tasks due to their two additional links. Six-bar linkages can be classified into two families, namely Watt I and II, and Stephenson I, II, and III as showed in Fig. 1.6 based on the connectivity between the two ternary links within the six-bars. The two ternary links are connected with each other in the Watt linkages, and separated in case of the Stephenson linkages. On the other hand, a Watt six-bar linkage consists of two four-bar loops and a Stephenson six-bar linkage is composed of one four-bar and one five-bar loops. Inasmuch as the additional links make the six-bar more versatile, they also add to the complexity of the design process. Synthesis of six-bar linkages is not as completed as that of four-bars.

1.3 Mechanism Errors

In the design process of a mechanism, the accuracy required of the mechanism must be taken into account. In the real application, it is impossible to design and build a linkage

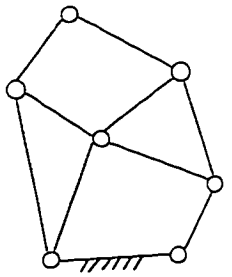

Watt I

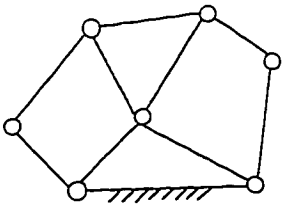

Watt II

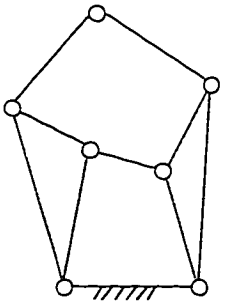

Stephenson I

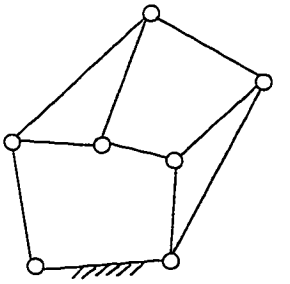

Stephenson II

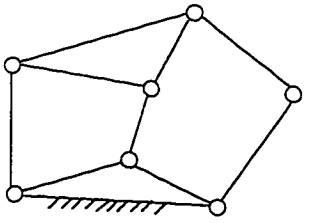

Stephenson III

Figure 1.6 Different Types of Six-Bar Linkages

that will theoretically generate a given motion. Often, however, the designer has to be satisfied with an approximation to the given motion. The difference between the desired motion and the actually produced one is known as *structural error.* In addition, there are errors due to manufacturing. The error resulting from tolerances of link lengths and joint

clearances is referred to as *mechanical error.* Literature on mechanism error is limited compared with that on mechanism synthesis. A research on mechanical error for four-bar motion generation will be conducted in Chapter VI.

1.4 Research Scope and Objectives

This section summarizes the work that will be completed in this document. The objectives of this research are to:

- Develop a theory to truly rectify the circuit defects at the synthesis level by controlling the critical angles for two, three, and four position motion generation; validate the theory by coding the theory in a mechanism synthesis and analysis package - RECSYN.
- Develop a rectified synthesis procedure for coupler-driven Watt I six-bar linkages for four position motion generation; implement the procedure in RECSYN to allow user to design a coupler-driven Watt I six-bar linkage.
- Propose the methodology to determine the optimal link length tolerance and joint clearance distributions of four-bar linkages for two, three, and four position motion generation in order to manufacture the linkages.

This dissertation is organized into seven chapters. Chapter II reviews the literature related to the research topics in this work. Chapter III summarizes the existing theory involved in the rectified synthesis of crank-driven four-bar linkages for two, three, and four design position motion generation. Chapter IV develops a complete theory to truly rectify circuit defects for two, three, and four position motion generation at synthesis level. In the case of four design positions, special points related to the poles are defined to mark the sections on the Burmester curve which result in circuit defects for rocker-cranks and double-rockers. Pole circles are employed to do similar work for three position. A line construction that is similar to Filemon construction is designed to apply to the driving circle-point to identify circuit defects for rocker-cranks and double-rockers. These techniques combined with those for crank-rockers and double-cranks described in Waldron (1976) will complete the circuit rectification. The whole process will be implemented into RECSYN for application and validation. Chapter V provides a rectified synthesis procedure for coupler-driven Watt I six-bar linkages for four position motion generation with the first half of reviewing the theory for coupler-driven four-bar linkage synthesis for four position motion generation by Bawab et al. (1992). The developed procedure is implemented in RECSYN to allow users to design a coupler-driven Watt I six-bar linkage. Examples showing the design process are also presented in this chapter. Chapter VI presents the methodology to determine the optimal link length tolerance and joint clearance distributions of four-bar linkages for two, three, and four position motion generation in

order to manufacture the linkages. A stochastic model incorporated with tolerances and clearances for four-bar motion generation is proposed. The tolerances and clearances are obtained as a result of solving a optimization problem with the objective function. Chapter VII comments on the developments presented here and provides recommendations for future work.

CHAPTER II

LITERATURE REVIEW

2.1 Summary

This chapter provides a review of the literature related to the research objectives. The literature includes the rectified synthesis of the crank and coupler-driven four-bar and six-bar linkages, defects in linkage solutions, rotatability of linkages, optimization in mechanism design, available software for computer-aided linkage synthesis and analysis, and linkage tolerance synthesis.

2.2 Rectified Synthesis

2.2.1 Linkage Synthesis

The synthesis theory for four-bar linkage is already well documented with contributions lead by Burmester, Freudenstein, Waldron, Erdman, and Sandor, among others.

The original problem of determining the points of a plane which describes those satisfying the four design positions was formulated by Burmester (Burmester, 1888). The resulting solution to this problem is a cubic curve which was named "Burmester Curve" in his honor. Burmester theory was limited in application of linkage design before the appearance of digital computers since finding solutions required tedious calculations and drawings which made the design process long and, at times, seemingly endless. Furthermore, the large computations required to calculate the coordinates of a single point of the Burmester curves made direct calculation of the curve coordinates impractical. Thus the generation of the Burmester curve had to be a graphical procedure as outlined by Beyer (1963) and Hall (1961) until the early 1960s. Keller (1965) provided a streamlined approach to graphical construction of the Burmester curves; however, the amount of labor involved is still too huge for it to be practically applied.

Alternate approaches to Burmester curve include trial-and-error, mechanism atlases, and graphical techniques in the past (Chase, 1984). The trial-and-error method consists of repeatedly modifying and analyzing a pre-defined linkage until a best solution is obtained. The atlas method is a technique using a brute force search. This method can be found in

Hrones and Nelson (1951) who demonstrated approximately 10,000 coupler curves for practical application. Graphical approaches were powerful and popular in linkage design before the advent of computer-assisted techniques; Tao (1964) offered excellent sources of this method. Of all the preceding methods, Burmester theory and graphical techniques are the only ones that can provide a closed form solution for problems up to five precision positions.

Modern resurgence of interest in linkage synthesis dates from the work of Freudenstein and Sandor (1961) who adopted the earlier geometric solutions to numerical solutions to be solved on a computer. Two parallel method of generating the Burmester curves exactly by computer computation gained popularity. The first is a purely algebraic approach provided by Suh and Radcliffe (1978) and Waldron and Kumar (1977). The equations for the curves are developed based on a series of coordinate transformations on which a constant curvature condition is imposed. The second is a complex number technique pioneered by Sandor (1959) and updated by Erdman (1981), Erdman and Sandor (1984), and Chase (1984). In this method, a set of simultaneous loop displacement equations are solved to generate the curve coordinates. Both methods result in identical Burmester curves for four position motion generation.

Each of the preceding methods has its own advantages. The algebraic approach can formulate the equations of the Burmester curves which is of cubic form. Therefore, this method has the ability to synthesize multiply separated positions which enables the user to specify the velocity or the acceleration instead of displacement at a precision position (Sparks, Walters and Tesar, 1968). The complex number method offers a relatively straightforward solution procedure for generating the coordinates of a point on the curve. In addition, the circle point curve for path angle generation, a higher order curve, can be obtained using the complex number method. In this work, the algebraic formulation is exclusively used.

On the Burmester curves generated, there are two special points of the curve, the slider point and the concurrent point, which give solutions containing infinite links. Beyer (1963) showed a graphical approach in locating these points. Kaufman (1972) derived the positions of the slider and concurrent points, using the complex approach for prescribed rotation of the tracer point link. Radcliffe (1980) derived similar work for the position of the slider point using the algebraic approach.

Instead of the traditional crank-driven four-bar mechanism design, Bawab et al. (1992) invented a rectification synthesis methodology of coupler-driven four-bar mechanisms for four-position motion generation. In the process, the coupler-driven four-bar linkage is synthesized as crank-driven without rectification, then one of its two cognate

crank-driven four-bar is formed by a series of transformation equations according to the characteristics of the Roberts' linkages. Bawab and Thiruvenkatachari (1995) also designed coupler-driven four-bars for two and three position motion generation.

Many works have been done on the synthesis of six-bar mechanism. McLarnan (1963) discussed the function generation of six-bar mechanisms including Watt II, Stephenson II, and Stephenson III chains. He developed algebraic equations in term of the design parameters and applied the Newton-Raphson technique to solve them. However, the solution is hardly able to converge due to the high sensitivity of the Newton-Raphson technique of the initial guess. Since the direct algebraic approach for multi-loop linkage synthesis involves solving high order, transcendental equations, several authors worked on the alternate synthesis strategy by making use of the existing four-bar linkage synthesis procedures. Patwardhan and Soni (1977) designed a Watt I six-bar linkage using graphical methods. The design process consists of synthesizing a four-bar linkage for a prescribed coupler curve and then synthesizing another four bar linkage for function generation. Dewey and Soni (1973) designed a Stephenson III function generator by applying the inversion method as in the synthesis of four-bar function generators. Kaufman (1971) used a similar method to synthesize a Watt I linkage for path generation with prescribed timing at five precision positions. In his method, a moving pivot was selected on the floating link to be the tracer point of four-bar, followed by four-bar synthesis using Burmester theory. The whole procedure is smilar to the one outlined in Patwardhan and Soni (1977).

Rao, Erdman, and Sandor (1971), Erdman and Sandor (1984) and Chase (1984) used the complex-number method to synthesize different types of six-bar linkages. White (1987) developed a procedure to rectify Stephenson III six-bar linkage. The guidelines of assuring good deviation angles, branching, correct order, and rotatability of the crank are set in the process. Bawab et al. (1996) described a rectified synthesis procedure of crank-driven Watt I six-bar mechanisms with well defined transmission angles for four-position motion generation. This is achieved by decomposing the six-bar mechanism into groups of dyads and triads which are rectified using the algebraic method of synthesis.

Bawab and Li (1995) presented a procedure to synthesize coupler-driven Watt I six-bar linkage to pass through the pre-defined four design positions. This is done by de-coupling the six-bar mechanism as tone coupler-driven and one crank-driven four-bar linkages with common links. The vector component mechanism modeling method is applied to these linkages where the dyad and triad synthesis approaches are adopted in conjunction with the algebraic method to find the solutions. The linkage with the coupler-driver is initially synthesized and rectified followed by the crank-driven four-bar linkage.

The six-bar linkage is thus insured to assemble free of circuit, branch, and order defects. The theory of coupler-driven Watt I six-bar linkage synthesis is implemented through an interactive synthesis package.

In the process of rectified synthesis, potential solutions with defects will be eliminated. These defects are circuit defects, branch defects, and order defects. A detailed literature survey will be presented in the following sub-section.

2.2.2 Linkage Rotatability

Linkage rotatability can be exclusively determined by the Grashof's inequality as expressed by Equation 2.1.

$$L_{min} + L_{max} \leq L_a + L_b \qquad (2.1)$$

where

L_{min} and L_{max} are the minimum and the maximum link-lengths respectively and L_a and L_b are the intermediate link-lengths.

A four-bar linkage that satisfies this inequality is referred to a Grashof four-bar linkage; otherwise, it is a non-Grashof four-bar linkage. Grashof four-bar has at least one link that can rotate fully while none of the link of a non-Grashof four-bar is able to make a full rotation. There are four types of Grashof linkages which are classified by the position of the shortest link relative to ground. If the input crank of the mechanism is the shortest link L_{min} then it is a crank-rocker (Fig. 2.1); if the shortest link is ground then it is classified as a double-crank (drag link); if the coupler is the shortest link then it is termed as double rocker;and if the output crank is the shortest then it is called a rocker-crank.

Gupta (1980) and Kazerounian and Gupta (1982) developed generalized algebraic-geometrical techniques for synthesizing crank-rocker and double-crank function generators with optimum transmission angles, such that the maximum and minimum transmission angles deviate equally about 90^0. Barker (1983) presented a classified scheme for the different types of Grashof and non-Grashof four-bar linkages. Barker and Jeng (1985) used Barker's scheme to determine the range of motion of the links within the four-bar linkages. Harber (1986) used numerical solution techniques to define the regions of the plane that give different Grashof types of mechanisms in three position synthesis. Ting (1994) and Ting and Liu (1991) studied the rotatability for five-bar and N-bar linkages. Their work is based on the inequality constraints that must exist between the link-length ratio. This is similar to Grashof's criterion. Midha et al. (1985) used the triangle inequality concept to study the mobility conditions of individual circuit for planar linkages. Norton (1992) used the same concept to develop a graphical method for synthesizing four-bar mechanisms in which the mobility angle of the side link is prescribed.

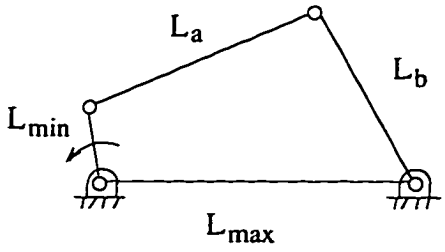

Figure 2.1 A Crank-Rocker Four-Bar Linkage

For six-bar linkages, Hunt (1978) presented a graphical study of some of the mobilities encountered. Watanabe and Feinabashi (1984a) and Watanabe et al. (1987) developed "composition loops" in Stephenson six-bar mechanism. Each loop was bound by a limit point at which the four-bar coupler curve of the mechanism was at an extreme.

2.2.3 Defects During Linkage Synthesis

A circuit of a linkage is defined as all possible orientations of the links which can be formed without disconnecting any of the joints (Chase and Mirth, 1993). A planar four-bar can have up to two circuits, while a Watt linkage has a maximum of four (Gibson and Marsh, 1989). A linkage is described to have a circuit defect when it can not go through all the design positions without changing circuits. The number of linkage circuits is related to the Grashof types in four-bars. Grashof four-bars have two circuits while non-Grashofs have one. Therefore, non-Grashof four-bars do not suffer from circuit defects and Grashof linkages can potentially suffer from circuit defects. A branch defect occurs when the sign of the transmission angle changes in at least one of the design positions.

Circuit defects and branch defects were discussed as a single name of branching or branch problems in the literature prior to Chase and Mirth (1993) who defined the terminology of the circuit and circuit defect, and branch defect. Circuit and branch problems have been first studied geometrically by Filemon (1971, 1972). She has developed a construction technique that identified all the feasible driving crank when applied to the driven crank. The driven and the driving cranks produce a linkage that can traverse through the design positions without a change of branch. Waldron and his associates developed a number of papers related to the circuit and branch rectification. Waldron (1974a and 1974b) implemented a graphical method that found the precision position poles and then identified the infeasible region on the Burmester curve of the follower (output) link. Filemon construction was then applied to discard the infeasible area and the driver (input) link was selected to complete the rectification. Waldron (1975a)

improved the applicability of the graphical method by clearly stating the steps involved in the rectification. However, both Filemon's and Waldron's methods only prevent circuit defects in crank-rocker and double-crank linkages. Waldron and Stephenson (1979) applied the branch rectification concepts to path-angle and function generation mechanisms. Kwong et al. (1981), and Kazerounian and Gupta (1982) developed techniques for synthesizing crank-rockers and double-cranks with desirable transmission angles free of both circuit and branch defects.

Several authors identified branch defects fewer identified circuit defects by preventing selected pairs of links from passing through collinear positions. Bagci (1974) eliminated the branch and circuit defects in the synthesis of function generations by separating the geometric inversions. The separated geometric inversion was obtained when the roots of the equation defining the angle of the follower link as a function of the driver link were solved. Gupta and Tinubu (1983) developed graphical analytical techniques to eliminate the branch and circuit defect for a function generator. Later, Tinubu and Gupta (1984) presented a procedure to eliminate the branching and circuit defect in a function generating mechanism using optimization techniques. This was based on the minimization of structural error. Prasad and Bagci (1974) and Krishnamurty and Turcic (1988,1992) used the Jacobian determinant to avoid branch and circuit defects in multi-loop mechanisms by eliminating changes in sign in Jacobian matrices derivable from the mechanism's loops.

Waldron (1976) demonstrated that a four-bar linkage satisfying the Grashof inequality experiences a circuit defect when one of the interior angles opposite to the shortest link changes signs. A Grashof mechanism will be free of a circuit defect if and only if the sign of one of these two angles is invariant. This is illustrated in Fig. 2.2. Waldron and Strong (1978a) defined an improved version of the methods used to directly identify the sections of Burmester curve having branch and circuit defect which are function of design positions. They identified the feasible and infeasible regions by inspecting the subscripts of the special points to replace the cumbersome angle sign table previously used in Waldron (1976). However, the solution only covers the elimination of circuit defects in crank-rocker and double-crank four-bar linkages. Circuit defects of double-rocker and rocker-crank linkages are eliminated indirectly by inverting the four-bar linkage into the base.

Mirth and Chase (1995) presented a general procedure for four-bar circuit and branch rectification as follows. The circuit property change-points are found, sectioning the Burmester curves into regions to indicate the Grashof types. Sections corresponding to non-Grashof mechanisms are known to be free of the circuit defect. A single trial solution mechanism is selected within each remaining section. If the trial solution mechanism is free

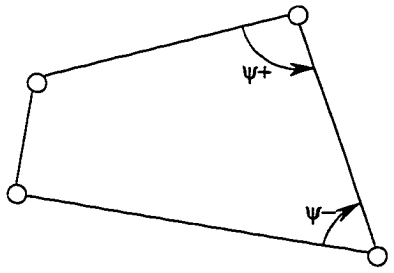

Figure 2.2 Angles Controlling Circuits in Four-Bar Linkages

of the circuit defect, its corresponding section is feasible. Otherwise, the section is discarded. For the regions free of circuit defects, the sign of the Jacobian determinant as described in Prasad and Bagci (1974) and Krishnamurty and Turcic (1988) can be legitimately used to determine if the mechanism has changed branch within the circuit. Circuits of Watt six-bar linkages were discussed separately. Circuit rectification approach for Watt II six-bar linkages were also presented based on the circuit characteristics of the two constituent four-bars. In case of Watt I, geometric inversion is applied to obtain the corresponding Watt II. This approach falls into a verification category. Bawab (1992) also discussed branch and circuit defects of a four-bar linkage in connection with the transmission angle and the angles opposite the shortest link, respectively. Although this method can be credited to synthesis level for crank-rocker and double-crank cases, it is conducted at the analysis level in the case of rocker-crank and double-rocker linkages. Bawab et al. (1992) rectified the circuit defects and branch defects of coupler-driven four-bars based on the properties of their crank-driven cognate four-bar linkages. The relationship of circuit between a coupler-driven four-bar and its crank-driven cognate four-bar was documented. Dou and Ting (1996) studied the circuits and branches in geared five-bar chains based on the joint rotatability criteria.

Bawab and Li (1996) proposed a new circuit rectification strategy at the synthesis level by controlling the change of sign of one of the angles opposite to the shortest link as in Waldron (1976). They utilized the algebraic method where special points are employed to eliminate the solutions with circuit defects as a function of the design positions. Complete rectification is accomplished at the mid-synthesis level by controlling the critical angles of the linkage that identify the existence of circuit defects. This work completes the unsolved part in Waldron and Strong (1978a) for rocker-cranks and double-rockers. A detailed description of this method is discussed in Chapter IV.

The definition of order defects is comparably straightforward. A linkage suffers an order defect when it is not able to go through all the design positions in a desired order. A linkage can be designed to pass through the design positions without any branch or circuit defects; however the solution may not acceptable unless the linkage passes through these design positions in the correct order for this reason the solution to the order defect is important in the solution rectification of linkages. A number of authors have discussed the order problem. Order problems is resolved as a part of solution rectification based on the requirement that the input linkage has to rotate continually in the same direction for all design positions that lie on the same circuit. Waldron (1975a, 1975b, and 1977), Waldron and Strong (1978a, 1978b) divided the Burmester curve for four design positions into segments that produce consistent ordering, image-poles being the dividing points for the circle-point Burmester curves. Similar work was done for the center point curve. Waldron and Stephenson (1979) addressed the order in path-angle generation and function generation synthesis. Chase and Fang (1991) used the complex method to locate the segments of the curve with the continuous rotation. Their work depended on finding the switch points which were equivalent to the image poles used by Waldron. Mirth (1994) has addressed the general order criteria for the precision position synthesis of single degree of freedom planar linkages. He has presented the complete order conditions for linkages with four design positions that lie on one to four separate branches.

2.3 Optimization in Mechanism Synthesis

A great deal of efforts have been made to apply optimization technique to design mechanisms. Generally, the synthesis problem is formulated as a classical optimization problem: the link lengths of a pre-defined linkage topology are modified to find the best fit to an objective function and a set of constraints. Works on linkage synthesis using optimization strategies are reviewed here.

Fox and Willmert (1967) presented an optimal design of four-bar linkages whose coupler point would generate a given curve and whose crank rotations would be as close as possible to the desired values. Prasad and Bagci (1974) used matrix iteration or Gaussian relaxation methods to minimize the error of two points in the moving lamina forming the design position for a single or a multi-loop mechanisms for rigid-body guidance. Bagci and Lee (1975) presented an optimum synthesis method for the paths generation and rigid-body positions of plane linkages. Dimensions of the optimum mechanism were determined by minimizing the error in the loop-closure equations for N design positions. Linear superposition was implemented to linearize the design equations. Kramer and Sandor (1975) used a selective precision point synthesis method to optimize the design of planar mechanisms for path, motion, or function generation with different arbitrary limits of

accuracy at the various design points. An improved general theory for the least-squares error synthesis of function-generating mechanisms was developed by Sutherland and Roth (1975). This theory leads to a rapidly converging iterative-type algorithm for solving the problem. In the optimization of four-bar linkages, the transmission angle of a function generator is optimized for a specified portion of the entire range of motion of the input and output links (Shoup and Pelan, 1971).

Rose and Sandor (1973) equalized the extreme errors between accuracy points by imposing additional constraints upon the problem. This leads to equalized (and thus minimized) extreme of structural error and thereby the iterative steps required in conventional optimization were avoided. Chen and Chan (1974) applied Marquardt's least-square compromise scheme to synthesize function-generating mechanisms. Eschenbach and Tesar (1971) used a transmission angle inequality constraints to define a bounded region for link-lengths. Expressions for the maximum deviation of the transmission angle from a 90 degree angle was presented and optimized by Freudenstein and Primrose (1972). Freudenstein and Chew (1971) optimized a ratio of the maximum to the minimum links and the transmission angle in a crank rocker linkage. Freudenstein (1978) obtained an expression for the link-length ratio. The general problem of determining the five parameters specifying a four-bar linkage which synthesizes a given function and at the same time satisfies some limiting conditions was considered by Levitski et al. (1972). Alizade et al. (1975) used the penalty function technique to optimize the kinematic synthesis of function generators. Gupta (1977) designed a four-bar function generator by minimizing the maximum deviation of the transmission angle from 90 degrees. This is called "mini-max". Some of the authors that used the "mini-max" approach were Tsai (1983a, 1983b), Khare and Dave (1980), Chiang (1986a, 1986b), and Gupta and Kazerounian (1983). Bawab et al. (1996) developed an automatic synthesis procedure of crank-driven four-bar mechanisms for two, three, or four-position motion generation based on optimization theory and rectified synthesis.

The literature on optimization of complex linkages is limited. To optimize a six-bar linkage for transmission angle, the transmission angle must be defined first. According to Hartenberg and Denavit (1964), transmission angles are defined to be the angle between the relative and absolute velocity vectors at the joints of the follower links. Yan and Wu (1989) identified the design positions that could create transmission angles of zero degrees. Watanabe and Funabashi (1984b) studied the motion-transmission angle. A transmission index was obtained for the durations in the displacement due to small changes in the input. Bawab et al. (1996) designed Watt six-bars by optimizing link length ratio and transmission angle.

2.4 Computer-Aided Mechanism Synthesis and Analysis

Kemler and Howe (1961) introduced perhaps the earliest published reference on computer applications in mechanism design by illustrating calculations of displacements, velocities, and accelerations in quick-return mechanisms. One of the early contributions which used the computer for linkage synthesis was that of Freudenstein and Sandor (1959) and Sandor (1959) who adapted and reformulated the graphical-based techniques of Burmester theory in Burmester (1888) for computer solution. With the advent of high-level programming languages coupled with continuous enhancements and improvements in the development of Graphical User Interfaces (GUI), several programs have been written to implement the mechanism synthesis and analysis. Some of these mechanism synthesis are:

KINSYN was developed by Kaufman (1972, 1973). This program implements the closed form complex approach as presented in Freudenstein and Sandor (1959) to generate four-bar linkages for motion, path, and function generation. It also has ability of linkage animation. Development and implementation on a custom hardware system has been a big drawback in KINSYN and its versions are available in the commercial market.

LINCAGES, LINCAGES-4, LINCAGES-6, and LINCAGES-N are a series of software developed by a group of people at University of Minnesota lead by Erdman. These packages are capable of synthesizing and analyzing four-bar, five-bar, six-bar, and N-bar linkage based on complex number Burmester theory. They are adapatable to various facilities such as IBMPC, VAX, Apollo, Intergraph, etc., and very user friendly. This program has a user friendly interface. Different versions of LINCAGES are available on the commercial market (Erdman, 1985).

RECSYN was initially developed by Chuang, Strong, and Waldron (1981). This package uses the algebraic method, and it was the first program that provided "Solution rectification" for branching, order and circuit defects. It was later modified by Srinivasan et al. (1988) to include optimization in synthesis of design positions. Improved versions (Bawab, 1992) with synthesis of crank-driven six-bar linkages and coupler-driven four-bar for four positions for different driver links and enhancements in existing capabilities has been a tangible feature of RECSYN. The software was developed to highlight and validate the rectified synthesis theory, and is not available commercially. Coupler-driven four-bar for two and three position motion generation was added by Thiruvenkatachari (1996). The synthesis procedure of coupler-driven Watt I developed in this work is also implemented on RECSYN.

MECSYN was developed by Sivertsen and Myklebust (1980) This program synthesizes four-bar linkages and the Stephenson linkages by inversion and well.

Analysis packages came out a little earlier than synthesis software, some of them, among others, are:

IMP - Integrated Mechanism Program was developed by Sheth and Unicker (1971) at University of Wisconsin, Madison. Along with the modified version IMP-84, IMP provides powerful analysis ability for kinematic, static, and dynamic force for both 2-D and 3-D system.

SAM 3.0 (Simulation and Analysis of Mechanisms) offers powerful and easy motion and force analysis of arbitrary 2-D mechanisms. This is a commercial software developed by ARTAS-Engineering Software. SAM is equipped with a large library of basic elements and is based on a unique mathematical foundation that treats open loop, closed loop, multiple loop and complex mechanisms similarly.

DRAM and **ADAMS** were developed by Smith, Orlandea, and Chace. DRAM is used to planar kinematic, static, and dynamic force analysis while ADAMS is for 3-D (Erdman 1985).

Working Model is a window based commercial software dealing with 2-D mechanism analysis and animation as well as mechanical dynamic simulation (Rubin, 1995).

2.5 Tolerance Synthesis of Linkage

Considerable work has been done to analyze the mechanical error due to tolerances on link lengths and the clearances in the joints for planar mechanisms during the past few decades. Basically, two distinct approaches, deterministic and stochastic, are applied in the analysis. The deterministic methods that are based on worst case scenario of individual tolerances are conservative and do not reflect the real behavior of mechanisms. They were mainly used in the pioneering investigation (Tuttle (1960), Knappe (1963), and Hartenberg and Denavit (1964)). Tuttle (1960) assumed the mechanism output error has a linear relationship with joint clearances in his analysis without considering link dimension tolerances. Knappe (1963) decided the effect of link length variation on the output using partial derivatives and obtained the output error effect by simply adding the deviations due to individual parameters. Hartenberg and Denavit (1964) assumed extreme values of link length tolerance, which yields conservative results. Neither of these studies takes both tolerances and clearances into account simultaneously.

In contrast, the stochastic approach has been found to be more suitable for both analysis and synthesis of mechanical error (Garrett and Hall (1969), Dhande and Chakraborty (1973), Chakraborty (1975), Dhande and Chakraborty (1978), Rao and Reddy (1979) and Rhyu and Kwak (1988)). Garrett and Hall (1969) took not only the link length variations or "tolerances" but also joint clearances into account in their analysis of a

four-bar function generator. A statistical approach with 3σ[2] mobility band level of confidence was adopted to achieve a desired functional relationship between input crank and output follower.

A stochastic model was introduced by Dhande and Chakraborty (1973) as shown in Fig. 2.3 where one pin and race are assigned to each member of the stochastic model. The equivalent linkage that takes the effects of tolerance and clearance into account is drawn in dotted lines in Fig 2.3. There are totally twelve random variables associated with the model, i. e. four link lengths and four pairs of x and y coordinates of the pin centers in the clearance circles, however there are two disadvantages in this model. Since the local coordinate system is so chosen that the x axis is coincident with the centerline of the link ending in the race, it makes it difficulty to measure the related angles in absolute space. On the other hand, the input angle is treated as a deterministic variable which is not the actual case because the pin center is randomly located in the clearance circle of the bush. They treated tolerances and clearances as optimization parameters and hence obtain their optimum values by dynamic programming using the allowable output deviation as a constraint. The four-bar generators studied in Garrett and Hall (1969) were borrowed as examples, and consistent results were obtained.

Chakraborty (1975) improved the above method by including the second order term of Taylor's expansion and analyzing the synthesized linkage for the maximum mechanical error. Dhande and Chakraborty (1978) investigated mechanical error for spatial linkages using stochastic model. Rao and Reddy (1979) optimally minimized the mechanical and structural errors of function generators using the stochastic model in Dhande and Chakraborty (1973).

Rhyu and Kwak (1988) modified the model shown in Fig. 2.3 by allocating races to the floating and fixed links and pins to the cranks for a four-bar function generator. The local coordinate systems are fixed onto the floating and fixed links, and the input angle is considered as random. Twelve random variables exist in the model which are four link lengths and the x and y coordinates of the pin centers in the clearance circles with respect to their local coordinate systems. The thirteenth random variable, length from the path generating point to the joint center on the coupler at the input side, is added for path generator of Rhyu and Kwak (1988). A tradeoff solution is obtained from the multiobjective optimization problem with two competing objective functions, mechanical error and manufacturing cost. Examples for both function generation and path generation were presented.

---

[2] σ stands for the standard deviation of normal distribution

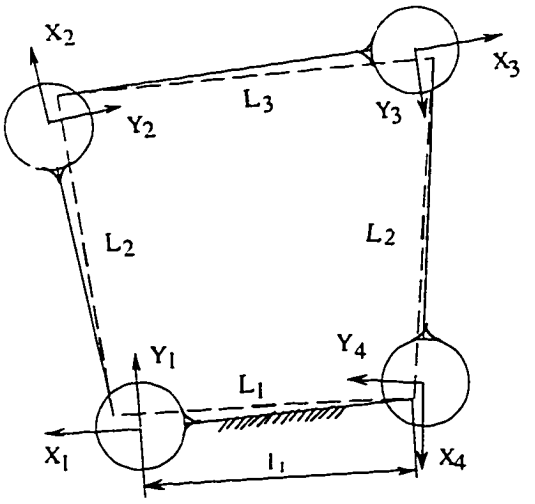

Figure 2.3 Stochastic Model in Dhande and Chakraborty (1973)

While most of the studies focused on the function generation, literature on path generation is limited. Baumgarten and Werff (1985) used probability theory and finite element method to analyze the effect of manufacturing tolerances on the performance of path generators. The same stochastic model as used by Dhande and Chakraborty (1973) was employed in Mallik and Dhande (1987) to develop a synthesis procedure to distribute tolerances and clearances to ensure that the output error of coupler point path did not exceed the specified limits.

Among the rest of investigations on mechanical error of linkages, Sharfi and Smith (1983) designed a simple method to allocate tolerances and clearances based on the assumption that all of them have equal effects upon output deviation. Their method can be applied to both four-bar function generation and multi-loop function generators as well. Fenton et al. (1989) developed a technique to allocate dimensional tolerances for multiple loop planar mechanisms by combining various link groups. The preliminary set of tolerance bands is estimated, and then optimized through a Jacobian chain to satisfy the output requirements. Faik and Erdman (1991) discussed the tolerance sensitivity distribution in the solution space proposed by Barker (1983) of four-bar linkages. This sensitivity distribution allowes the designer to synthesize a four-bar with predicted tolerances to satisfy a certain accuracy on link angles. However, neither position sensitivity analysis nor joint clearances were considered. Venkataraman et al. (1992) developed an optimal synthesis method of four-bar mechanism for four position rigid-body guidance with discrete selective variation on the design position, however the tolerances

and clearances were not assigned to linkage members. The Rayleigh quotient of the sensitivity Jacobian was used to define the performance quality of the mechanism in Ting and Long (1996) and the ideal tolerance distribution can be made based on the quotient.

Although motion generation (rigid body guidance) is widely used in actual application, there is no documented research on the mechanical error of four-bar linkage for motion generation to authors' knowledge.

CHAPTER III

RECTIFIED SYNTHESIS OF CRANK-DRIVEN FOUR-BAR LINKAGES FOR MOTION GENERATION

This chapter presents an overview of the rectified synthesis theory developed for crank-driven four-bar linkages for two, three, and four design position rigid body guidance[3] which is used as the fundamental in the subsequent chapters. The synthesis is developed with techniques to avoid applicable branch, circuit, and order defects. Synthesis can be performed from the circle point or the center point plane. The material in this chapter is mainly a summary of the work of Bawab (1992) based on Waldron (1974 to 1979) and Srinivasan et al. (1988). The theory is implemented to a graphical interactive package RECSYN. Section 3.1 discusses the existence of a branch defects and the techniques to identify and eliminate them. Circuit defects and available circuit rectification methods are provided in Section 3.2. The rectified synthesis for two design position motion generation is illustrated in section 3.3. Section 3.4 and 3.5 describe the rectified synthesis procedures for three and four position motion generation, respectively. Finally, Section 3.6 introduces the concept of the automatic synthesis and optimization strategy involved. It also presents a detailed optimization method applied to the automatic synthesis of four-bar linkages for two, three, and four position synthesis.

3.1 Branch Defect

The *Branch defect* is said to occur when the transmission angle of the linkage changes sign in order for the moving lamina of the linkage to pass through the design positions. The definition of transmission angle based on mechanical advantage along with Filemon construction is covered in this section.

3.1.1 Mechanical Advantage, Transmission Angle, and Toggle Position

A branch defect happens when the transmission angle changes signs. The sign convention of transmission angles ψ is $-\pi < \psi \leq \pi$, thus the limits of sign changing are 0 and π. When the transmission angle reaches one of the limits, the input link can no longer

[3] Rigid body guidance is also referred to as motion generation

moves in that direction and the output link is free to rotate in either direction without external or inertial forces being considered. This is known as the toggle position. At toggle positions, a linkage has zero mechanical advantage. The mechanical advantage (MA) of the mechanism can be expressed as the ratio of the input angular velocity to the output angular velocity as expressed in Eq. (3.1) (Yan and Wu, 1989).

$$MA = \frac{\omega_i}{\omega_o} = \frac{\overline{I_{ro}I_{io}}}{\overline{I_{ri}I_{io}}} \tag{3.1}$$

where ω_i is the angular velocity of the input link, and ω_o is the angular velocity of the output link. I_{ri}, I_{ro}, and I_{io} are the instant centers between the ground link r and the input link i, the ground link r and the output link o, and the input link i and the output link o, respectively, as shown in Fig. 3.1.

A toggle position exists when the mechanical advantage (MA) of a linkage is equal to zero. For the crank-driven four-bar linkage presented in Fig 3.1, the transmission angle is identified as angle I_{ic} I_{co} I_{ro} (angle ψ) (Bawab, 1992).

Figure 3.2 illustrates the two toggle positions of the four-bar linkage A*ABB* corresponding to ψ being either 0 or π and Fig. 3.3 shows that a changing of branches may exist at each of the two toggle positions.

Branch defects and toggle positions are generally undesirable and should be avoided. However, there are some rare cases in the real application, such as the lock mechanism of a vice grip clamp, where the linkage with branching is applied. In order to

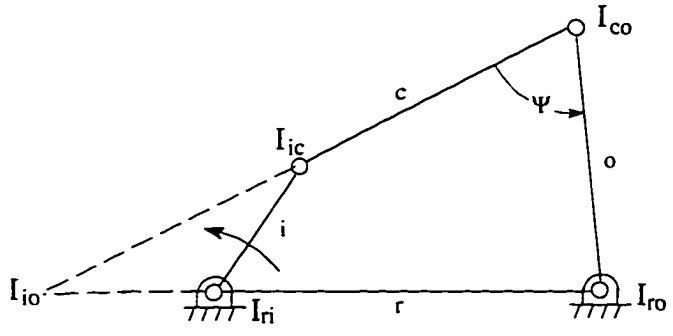

Figure 3.1 Transmission Angle of a Crank Driven Four-Bar

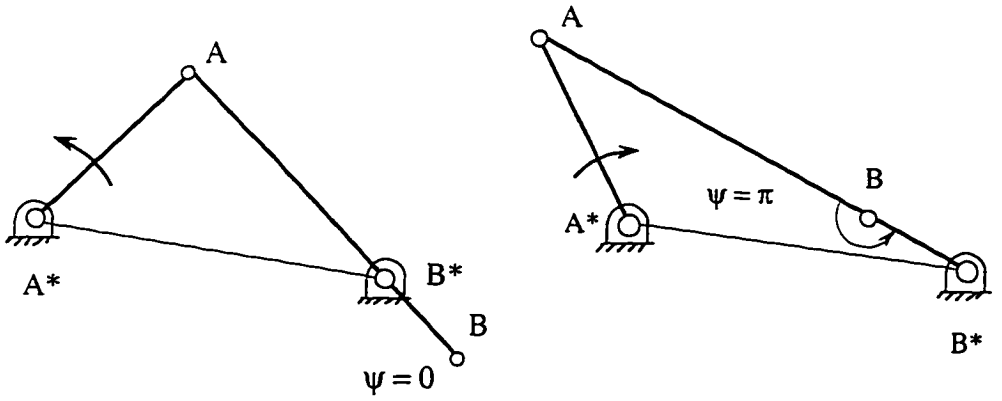

Figure 3.2 Toggle Positions of a Four-Bar Linkage

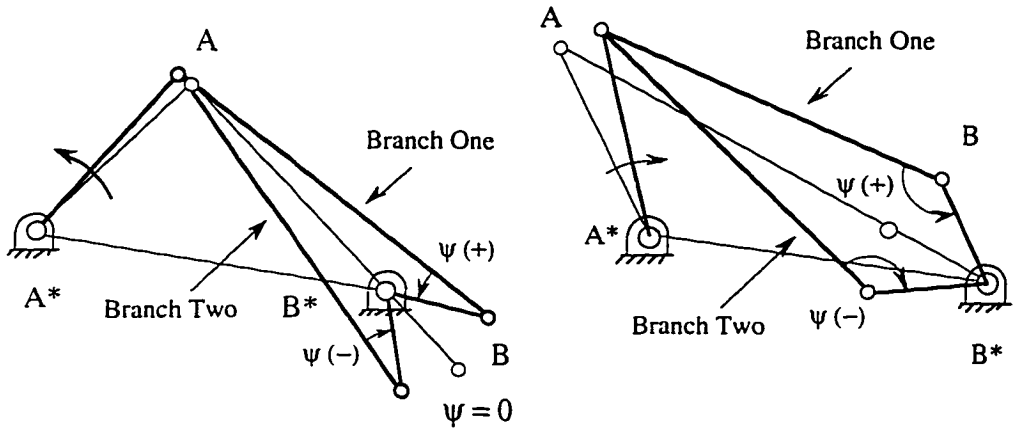

Figure 3.3 Branch defects in Four-Bar Linkages

synthesize a linkage to be free of branch defects (toggle positions), a three step technique can be adopted. The first step is to select an appropriate driven crank[3]. Then the infeasible regions which guarantee a branch defect are identified using the Filemon construction as described in next sub-section. Finally, the input link is selected from the permissible regions to complete the linkage.

[3] The selection of driven crank will be given in the later sections for various number of design positions.

3.1.2 Filemon Construction

There is a technique invented by Filemon (1971) which can be applied to the circle-point of a driven crank to determine the feasible and infeasible areas for the driving crank circle-point in terms of branch defects. This is called Filemon construction in her honor.

Fig. 3.4 illustrates the Filemon construction from the circle-point plane. The feasible region for the selection of the driving dyad is identified by lines l and m with slopes η_l and η_m, respectively. B^*B_i is the driven link where the subscript i = 1, 2, 3 and 4 denotes the positions. The line B_iP_i is drawn on the coupler and is collinear with B^*B_i in position 1. P_i (p_X, p_Y) gives the coordinates of the design position in the frame X and Y axes, respectively. B_i (X, Y) is the location of the circle-point in position i and B* (X*, Y*) is the location of the center-point of the driven crank. η_{ij} denotes the angle through which the coupler turns relative to the driven crank in order to reach position j from position i. The angle η_i is calculated as follows:

$$\cos\eta_i = \frac{(X_i - x^*)(p_{Xi} - X_i) + (Y_i - y^*)(p_{Yi} - Y_i)}{\sqrt{[(X_i - x^*)^2 + (Y_i - y^*)^2][(p_{Xi} - X_i)^2 + (p_{Yi} - Y_i)^2]}}$$

$$\sin\eta_i = \frac{(X_i - x^*)(p_{Yi} - Y_i) - (Y_i - y^*)(p_{Xi} - X_i)}{\sqrt{[(X_i - x^*)^2 + (Y_i - y^*)^2][(p_{Xi} - X_i)^2 + (p_{Yi} - Y_i)^2]}}$$

$$\eta_i = 2.0 \tan^{-1}\left[\frac{\sin\eta_i}{1+\cos\eta_i}\right] \qquad (3.2)$$

and η_{ij} is given as:

$$\eta_{ij} = \psi_j - \psi_i \qquad -\pi < \eta_{ij} < \pi$$

$$i = 1, 2, 3, 4 \quad \text{and} \quad j = 2, 3, 4$$

The lines l and m divide the coupler plane into the feasible regions (unshaded area) marked with U and unfeasible (shaded area) regions marked with V. In other words, any point in the shaded region V chosen as a driving crank circle-point will cause the transmission angle η to change signs when the coupler moves through all the design positions. Conversely any point in the region U chosen as a driving crank circle-point will give a linkage for which η does not change sign. Therefore, for a given driven crank, the Filemon construction eliminates the regions resulting in branch defects for the selection of the driving crank circle-point.

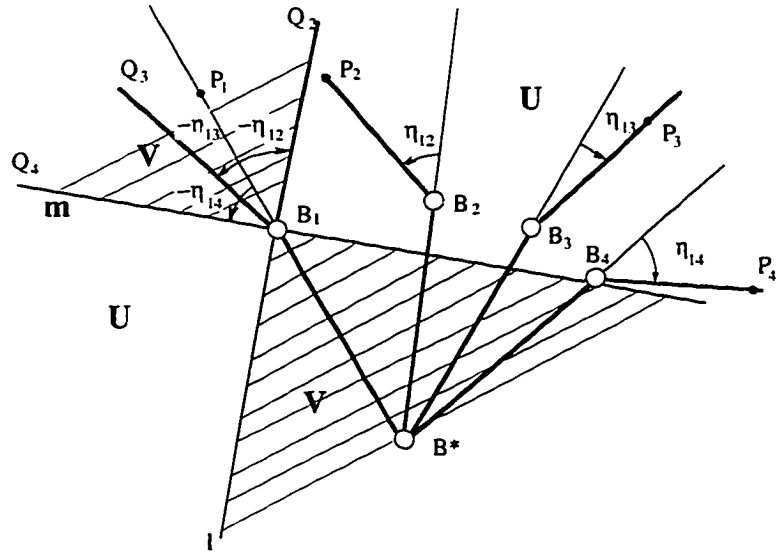

Figure 3.4 Filemon Construction for Four Position

It is, however, necessary to obtain the Filemon infeasible region in the center-point plane in order to synthesize mechanisms from the center point plane. Unfortunately, the simplicity of using constructions involving only circles or lines is lost, because the lines in the circle point plane map as conics in the center point plane. For this reason the Filemon infeasible regions are not plotted in the center point plane and rather conducted through the circle-point plane.

3.2 Circuit Defect

A circuit of a linkage is defined as all possible orientations of the links which can be formed without disconnecting any of the joints (Chase and Mirth, 1993). A synthesized linkage with no rectification is only guaranteed to be assembled at the precision positions without having the continuity considered. Therefore, the linkage may not able to pass all the design positions without being disconnected and reassembled in different configurations. This is referred to as a circuit defect. Linkages suffering circuit defects have no practical application and have to be excluded. The relationship between circuit defects and branch defects in four-bars is a function of Grashof types as discussed in the next subsection.

3.2.1 Circuit Defects and Branch Defects

Circuit defects and branch defects are seemingly quite different from each other by definition. A linkage with a circuit defect needs disconnecting and reassembling, while it is

not necessarily the case for a branch defect. Fig. 3.5 illustrates the distinction between the circuit and the branch defect.

A circuit of a linkage is defined as all possible orientations of the linkage that can be obtained without disconnecting any of the joints. If the joint must be disconnected in the process of moving from one position to another then the joints must lie on two different circuits. A branch is defined as a continuous series of positions a linkage is capable of achieving between stationary configurations on a circuit (Chase and Mirth, 1993).

A 'Stationary Configuration' is defined as the configuration of the mechanism where the derivative of the angle of the output link, with respect to the input link, becomes infinite [Hunt, 1978]. When a linkage is in a stationary configuration, no amount of force or torque applied to the input link is sufficient to cause it to pass out of this configuration. If two design configurations are separated by a stationary configuration then a simple torque or force applied to the input link will be unable to push the linkage through the stationary configuration that separates these two design configurations.

The number of circuits in a four-bar linkage relies on its Grashof type. Therefore, it is important to classify the linkage type of a four-bar linkage in order to identify circuit defects. A non-Grashof four-bar has only one circuit, hence there is no circuit problem in such type of linkages. On the other hand, the Grashof linkages have two circuits.

In the case of a crank-rocker or a double-crank linkage, the input link rotates fully with respect to the reference and the change of the configuration between the coupler and

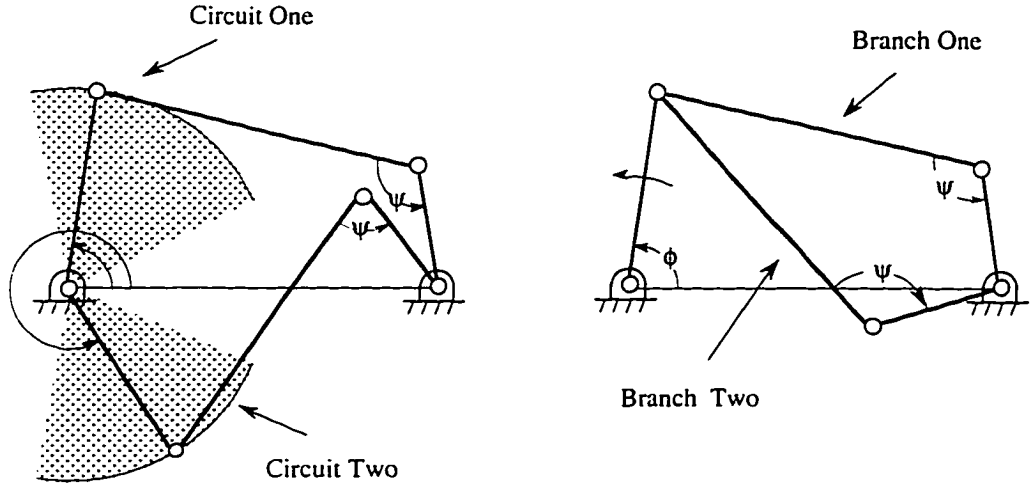

(a) Circuit Defect (b) Branch Defect

Figure. 3.5 Circuit and Branch Defect in Four-bar Linkage.

output link requires a change of sign of the transmission angle. Thus a change of circuit needs a change of branch and elimination of either one will eliminate the other. This is illustrated in Fig. 3.6.

But in the case of a double-rocker or a rocker-crank linkage, the input link does not fully rotate with respect to the reference; the elimination of a branch defect is not sufficient to eliminate circuit defects, and these defects must be identified and eliminated separately. Fig. 3.7 shows this distinction.

3.2.2 Elimination of Circuit Defects

As discussed in the previous subsection, circuit defects are closely related to the Grashof types. Branch defects and circuit defects happen simultaneously in crank-rocker or double-crank four-bar linkages. Therefore, Filemon construction can be applied to the driven dyad to eliminate both defects in case of these two Grashof types. This is indeed an application of Waldron's (1976) theory by controlling the sign of an angle opposite to the shortest link. In addition, there are certain regions for three position motion generation and some sections on the Burmester curve for four position motion generation that can be pre-determined to have a circuit defect since they result in no feasible area of driving circle-point from Filemon construct. More details will be found in the subsequent subsections about three and four position motion generation synthesis.

In the case of the circuit defects in rocker-crank and double-rockers, circuit defects have to be dealt with separately after branch defect identification. There are generally three

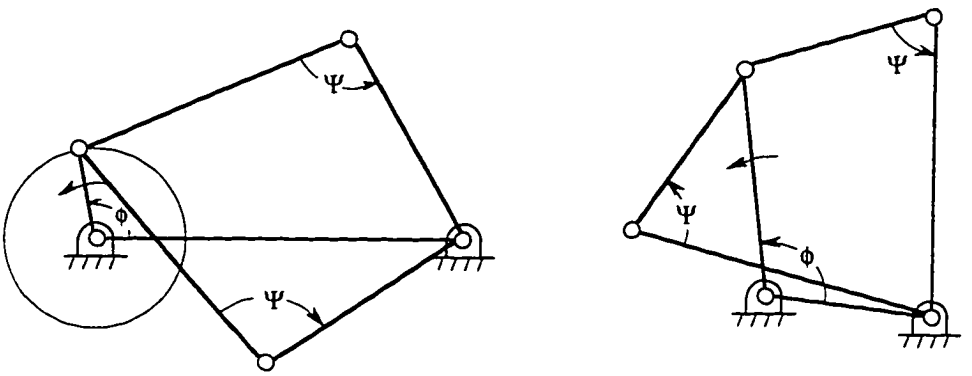

a) Crank rocker b) Double crank

Figure 3.6 Circuit and Branch Defect in a Crank-Rocker and Double-Crank Linkages

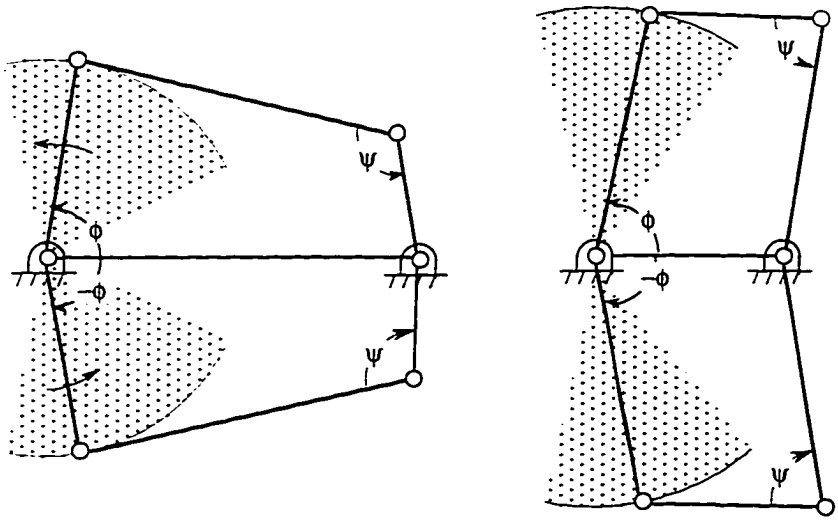

a) Rocker-crank b) Double Rocker

Figure 3.7 Circuit and Branch in Rocker-Crank and Double-Rocker Linkages

methods available to identify circuit defects for these two types of Grashof four-bars. One is to inverse them into either crank-rocker or double-crank four-bars as suggested in Waldron (1976) and then apply the Filemon construction. This is valid since linkage circuit is independent of geometric inversion. Unfortunately, this is a tedious process and is not practical. Another method is a brute force technique that examines the ranges for the input link described in Bawab (1992). If the input link position for all the design positions falls in one circuit, then the circuit defect does not exist for that linkage. Otherwise, the linkage has a circuit defect. These two methods are more of analysis category. A new is proposed by Bawab and Li (1996) where a so called line construction is applied to the driving center-point as presented in Chapter IV of this work.

3.3 Theory of Two Finitely Separated Position Synthesis

Theoretically, the number of solutions mechanisms with two position synthesis is six folds of infinities. The synthesis can be carried out from either circle-point plane (moving plane) or center-point plane (fixed plane). The relationship between the moving frame and the fixed frame is documented in Bawab (1992). In order to rectify the synthesized linkage free from branch and circuit defects, the driven crank must be chosen first no matter which plane is used. In addition, a uniform notation for the various angles used during the synthesis will be employed throughout this document. As illustrated in Fig. 3.8, the angle θ is the angle formed between the design position and the fixed frame,

the angle ϕ is the angle between the crank and the fixed frame and the angle η is the angle between the coupler and the crank. Thus, $\theta = \eta + \phi$.

3.3.1 Synthesis from the Circle-Point Plane

In a two position synthesis, any point on the moving plane can be chosen as the driven crank circle-point. For two design positions $P_1\ (p_{X1}, p_{Y1}, \theta_1)$ and $P_2\ (p_{X2}, p_{Y2}, \theta_2)$, a circle point $A_1\ (X_1, Y_1)$ with respect to the fixed coordinate frame X-Y is selected as shown in Fig. 3.9. The coordinates of the circle point corresponding to the second design position, $A_2\ (X_2, Y_2)$, can be calculated as follows :

$$\begin{bmatrix} X_2 \\ Y_2 \\ 1 \end{bmatrix} = \begin{bmatrix} \cos(\theta_2-\theta_1) & -\sin(\theta_2-\theta_1) & p_{X2}-p_{X1}\cos(\theta_2-\theta_1)+p_{Y1}\sin(\theta_2-\theta_1) \\ \sin(\theta_2-\theta_1) & \cos(\theta_2-\theta_1) & p_{Y2}-p_{X1}\sin(\theta_2-\theta_1)-p_{Y1}\cos(\theta_2-\theta_1) \\ 0 & 0 & 1 \end{bmatrix} \begin{bmatrix} X_1 \\ Y_1 \\ 1 \end{bmatrix} \tag{3.3}$$

The locus of the center points lies on the perpendicular bisector of the line joining the circle points in the two design positions. The locus can be found using the equation :

$$Y = AX + B \tag{3.4}$$

where

$$A = -\left(\frac{X_1 - X_2}{Y_1 - Y_2}\right) \quad \text{and} \quad B = \left(\frac{X_1 + X_2}{2}\right)\left(\frac{X_1 - X_2}{Y_1 - Y_2}\right) + \frac{Y_1 + Y_2}{2}$$

Any point on the locus can be selected as a driven crank center-point, and this completes the driven crank selection. After the selection of the driven crank, the Filemon construction is applied to the circle point A_1 to eliminate the infeasible regions for the selection of the circle point of the driving crank. The Filemon construction is used to eliminate regions in which the joint angle η changes sign to ensure that the mechanism can pass through the design positions without branch defect. After the selection of the driving-crank circle point, the circle point corresponding to the second position is found and then the locus of the center point of the driving crank is constructed. This locus is the perpendicular bisector of the line joining the two design positions of the circle point. During the selection of the center point, the different Grashof types are identified using Grashof's rule, to enable the user to obtain the desired Grashof type of linkage. The

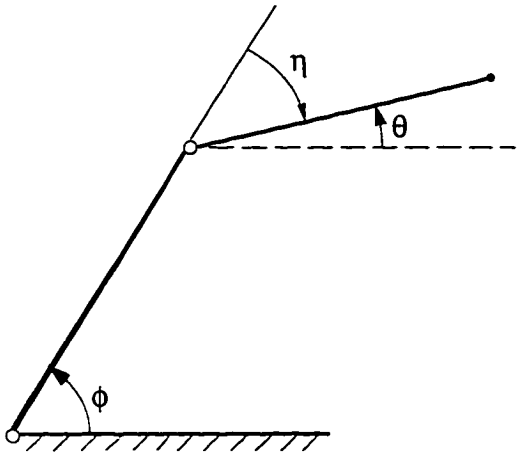

Figure 3.8 Angles Label the Driven Crank

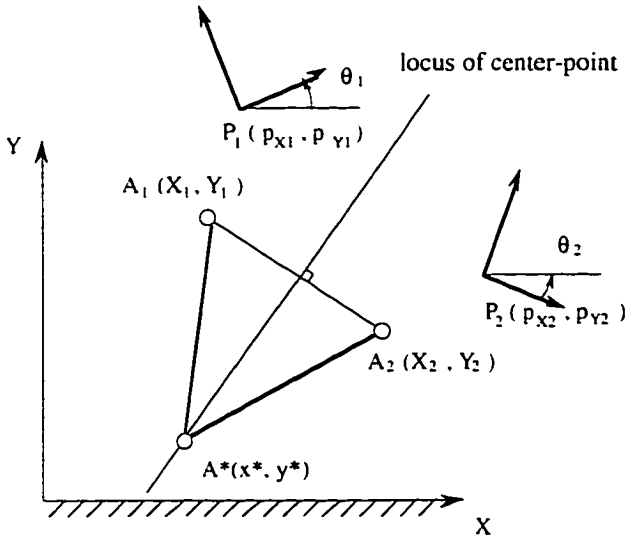

Figure 3.9 Crank Selection from Moving Plane

synthesized linkages need to be further checked for circuit defects. For the reason discussed in the previous section, circuit problems do not exist in crank-rockers and double-cranks; in case of double-rocker or rocker-crank, circuit problems can be checked by the method of examining the ranges for the input link described in Bawab (1992). Order problems do not exist in two position synthesis since the appropriate order can be

realized by adjusting the input direction. Hence, the four-bar linkage synthesized by the above procedure will traverse the design positions free from defects.

3.3.2 Synthesis from the Center-Point Plane

Instead of starting the synthesis from moving plane, the linkage synthesis can be done in the fixed plane by choosing the center-point of driven crank first. The necessary procedure, however, is inevitably similar to that from circle-point plane. Details of the work is covered in Srinivasan et al. (1988).

3.4 Theory of Three Finitely Separated Position Synthesis

With one more design position added compared to with two position synthesis, the solutions of the linkages is reduced to four-fold of infinities. Again, the synthesis can be done from either circle-point plane or center-point plane with the driven crank selected first to rectify the branch defects. Unlike two position synthesis, however, the selection of the driven crank in some regions can guarantee a branch defect when attempting to reach the design positions. These regions can be identified in both the center-point and the circle-point plane using the circles passing through poles and image poles respectively as proofed in Bawab (1992). All the calculations are made with respect to the first position in this section, which is coincident with the moving frame.

3.4.1 Synthesis From the Circle-Point Plane

In three position synthesis, there exist regions in the moving plane that are infeasible for the selection of the driven crank circle-point. These infeasible regions are identified by the circles drawn using pairs of image poles as the diameter in the circle-point plane. This is because any point selected from the infeasible areas will have the angular range formed from the coupler to the driven crank greater than π, which consequently results in no feasible regions from Filemon construction.

The angular displacement of the coupler relative to the crank ψ_{ij} from position i to j with respect to circle-point X_1 at position 1 can be related to the image pole pair $P'_{ik}P'_{jk}$ as illustrated in Fig. 3.10. It can be found that the angle subtended at circle-point X_1 by the image pole pair $P'_{ik}P'_{jk}$ is $\psi_{ij}/2$ measured from $X_1P'_{ik}$ to $X_1P'_{jk}$. If a circle is drawn to pass through the image poles $P'_{ik}P'_{jk}$, with the sign convention used such that $-\pi < \psi_{ij} < \pi$, the sign of ψ_{ij} can be found at every point in the solution space as given in Fig. 3.11.

Since $\psi_{ik} = \psi_{ij} + \psi_{jk}$, it is necessary for the range of rotation to be of the same sign. For instance, if ψ_{ij} and ψ_{jk} are positive, then ψ_{ik} must be positive to have a feasible

point: i.e. a negative ψ_{ij} means that $\psi_{ij} + \psi_{jk} > \pi$. This fact combined with the knowledge of sign of ψ_{ij} gives us a method to identify the infeasible regions. These regions are illustrated in Fig. 3.12. The procedure for identifying these infeasible regions is outlined below for design positions i, j, k. Any point in the unhatched regions is feasible for the selection of the circle-point with respect to position I. The center-point of the driven crank

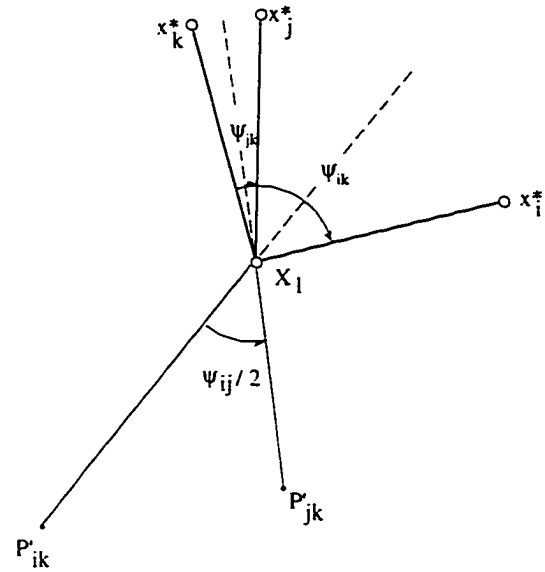

Figure 3.10 Angle Subtended by Image poles $P'_{ik}P'_{jk}$

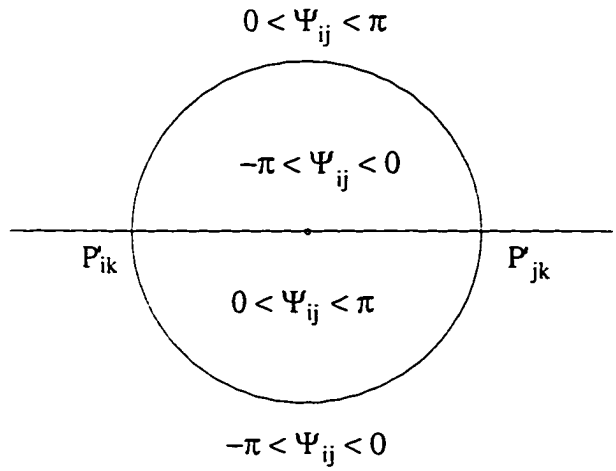

Figure 3.11 Regions of different signs of ψ_{ij}

can be found as an intersection between the two loci of the center-points corresponding any two pairs of the three sets of design positions i-j, i-k, or j-k. For instance, for the design position pair i-j and i-k the equations of the loci of the center-point (Eq. (3.8)) are obtained using Eq.(3.4):

$$\begin{aligned} Y &= m_1 X + c_1 \\ Y &= m_2 X + c_2 \end{aligned} \tag{3.8}$$

where

$$m_1 = -\left(\frac{X_i - X_j}{Y_i - Y_j}\right)$$

$$c_1 = \left(\frac{X_i + X_j}{2}\right)\left(\frac{X_i - X_j}{Y_i - Y_j}\right) + \frac{Y_i + Y_j}{2}$$

$$m_2 = -\left(\frac{X_i - X_k}{Y_i - Y_k}\right)$$

$$c_2 = \left(\frac{X_i + X_k}{2}\right)\left(\frac{X_i - X_k}{Y_i - Y_k}\right) + \frac{Y_i + Y_k}{2}$$

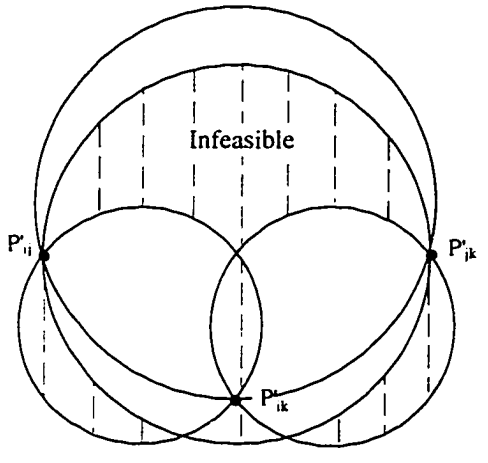

Figure 3.12 Feasible Regions for the Driven Crank Circle-Point

Therefore, the coordinates of the driven crank center-point can be calculated from Eq. (3.8) as:

$$x^* = -\left[\frac{c_2 - c_1}{m_2 - m_1}\right]$$

$$y^* = -\left[\frac{m_2 c_1 - m_1 c_2}{m_2 - m_1}\right] \qquad (3.9)$$

The center-point computed from equation (3.9) along with the selected circle-point completes the driven crank synthesis. Filemon construction is applied to eliminate branch defects for the selection of the driving-crank circle-point. The Grashof type for any linkage with its circle-point chosen from the feasible areas of Filemon construction is identified. In the case of crank rockers and double cranks, there is no order problem since the desired order can be obtained by driving the crank in either the clockwise or anti-clockwise direction. In addition, since the circuit and branch defects are defined to be the same, the elimination of circuit defects leads to the elimination of branch defects. Hence, a synthesized crank-rocker or double-crank linkage is secured to be defect free. However, in the case of a double-rocker or rocker-crank, a cyclic sequence other than ijk or kji would be unacceptable because changing the direction of rotation of the driving crank does not ensure that it passes through the design positions in the correct order. Rectification theory does not handle this problem because it is a combination of both the circuit and the order problems, which in this case are interrelated. Although it would be desirable to handle this case, it does not seriously jeopardize the quality of linkages obtained. Also, circuit problems need to be checked using the aforesaid circuit problems identification method to finish the rectified synthesis process.

3.4.2 Synthesis From the Center-Point Plane

Infeasible regions similar to the ones existing in the circle-point plane are also present in the center-point region. Pole circles (Waldron and Strong, 1978b) identify the infeasible regions. The procedure details can be referred to Srinivasan et al. (1988).

3.5 Theory of Four Finitely Separated Position Synthesis

With the number of design positions increased to four, the solution for the circle-points and center-points is no longer areas but rather curves. These curves are the cubic Burmester circle-point and center-point curves. The equations of the Burmester curves in both moving and fixed planes, and the associated branch, circuit and order rectification strategy are discussed in this section.

3.5.1 Burmester Circle-Point Curve

The algebraic method to obtain the solution circle-point for four precision design positions is provided in this subsection.

A dyad that assembles at position i (i = 1, 2, 3, and 4) of the four design position is show in Fig. 3.14. Suppose the length of the crank is R, then the relationship between the circle-point A_i (X_i, Y_i) and center-point A* (x*, y*) can be expressed by Eq. (3.10).

$$(X_i - x^*)^2 + (Y_i - y^*)^2 = R^2 \tag{3.10}$$

All computations are performed relative to the first design position, i.e. the moving frame is coincident with the first one, thus,

$$\begin{aligned} p_{X1} &= p_{Y1} = \theta_1 = 0 \\ X_i &= p_{xi} + x\cos\theta_i - y\sin\theta_i \\ Y_i &= p_{Yi} + x\sin\theta_i + y\cos\theta_i \qquad i = 2, 3, 4 \end{aligned} \tag{3.11}$$

where p_{Xi}, p_{Yi}, θ_i are the coordinates and angular orientation of the design positions relative to the first design position, and (X_i, Y_i) are the coordinates of the circle point corresponding to the i^{th} design position.

Substituting Eq. (3.11) into Eq. (3.10) and rearranging terms yields:

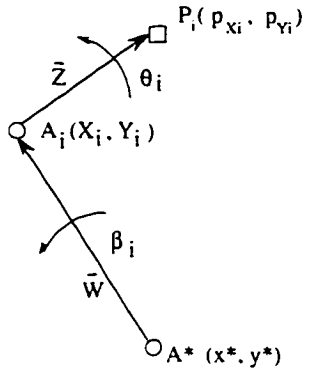

Figure 3.13 Dyad of a Four-Bar Linkage

$$x^*\left[x(1-\cos\theta_i)+y\sin\theta_i-P_{Xi}\right]+y^*\left[-x\sin\theta_i+y(1-\cos\theta_i)-P_{Yi}\right]$$
$$+x(P_{Xi}\cos\theta_i+P_{Yi}\sin\theta_i)+y(-P_{Xi}\sin\theta_i+P_{Yi}\cos\theta_i)+\frac{P_{Xi}^2+P_{Yi}^2}{2}=0$$
$$i=2,3,4 \qquad (3.12)$$

or

$$x^*(xa_i+yb_i-P_{Xi})+y^*(ya_i-xb_i-P_{Yi})$$
$$+xc_i+yd_i+e_i=0 \qquad i=2,3,4 \qquad (3.13)$$

where

$$a_i = 1-\cos\theta_i'$$
$$b_i = \sin\theta_i'$$
$$c_i = P_{Xi}'\cos\theta_i'+P_{Yi}'\sin\theta_i'$$
$$d_i = -P_{Xi}'\sin\theta_i'+P_{Yi}'\cos\theta_i'$$
$$e_i = \frac{P_{Xi}'^2+P_{Yi}'^2}{2}$$
$$P_{Xi}'=P_{Xi}-P_{X1}\cos\theta_i'+P_{Y1}\sin\theta_i' \quad \& \quad P_{Yi}'=P_{Yi}-P_{Y1}\sin\theta_i'-P_{X1}\cos\theta_i'$$
$$\theta_i'=\theta_i-\theta_1 \qquad i=2,3,4$$

Equation (3.13) represents three equations with two unknowns (x*, y*). In order to obtain a non-trivial solution, these equations must be linearly dependent. Therefore,

$$\left|(a_i x+b_i y-P_{Xi}) \quad (-b_i x+a_i y-P_{Yi}) \quad (c_i x+d_i y+e_i)\right|=0 \qquad i=2,3,4$$

or

$$A_1x^3+A_1xy^2+A_2yx^2+A_2y^3+A_3xy+A_4x^2+A_5y^2+A_6x+A_7y+A_8=0 \qquad (3.14)$$

where

$$A_1 = -\left|a_i\ b_i\ c_i\right|$$
$$A_2 = \left|b_i\ a_i\ d_i\right|$$

$$
\begin{aligned}
A_3 &= -\left|a_i\, P'_{Yi}\, d_i\right| - \left|b_i\, P'_{Yi}\, c_i\right| + \left|P'_{Xi}\, b_i\, d_i\right| - \left|P'_{Xi}\, a_i\, c_i\right| \\
A_4 &= -\left|a_i\, b_i\, e_i\right| - \left|a_i\, P'_{Yi} c_i\right| + \left|P'_{Xi}\, b_i\, c_i\right| \\
A_5 &= \left|b_i\, a_i\, e_i\right| - \left|b_i\, P'_{Yi}\, d_i\right| - \left|P'_{Xi}\, a_i\, d_i\right| \\
A_6 &= -\left|a_i\, P'_{Yi}\, e_i\right| + \left|P'_{Xi}\, b_i\, e_i\right| + \left|P'_{Xi}\, P'_{Yi}\, c_i\right| \\
A_7 &= -\left|b_i\, P'_{Yi}\, e_i\right| - \left|P'_{Xi}\, a_i\, e_i\right| + \left|P'_{Xi}\, P'_{Yi}\, d_i\right| \\
A_8 &= \left|P'_{Xi}\, P'_{Yi}\, e_i\right|
\end{aligned}
$$

$$i = 2,3,4$$

Equation (3.14) which is cubic forms the circle-point Burmester curve. This is illustrated in Fig. 3.13. This curve can be of two types, a single branch or a double branch curve. The Burmester curve can be presented numerically by finding the solution to Eq. (3.14) at small intervals of consistent length if possible. However, it is almost impossible to obtain consistent intervals in the x-y reference frame. This can be improved by rotating and translating the x-y reference frame to an S-T reference frame which has the S axis coincide with the asymptote. In order to transfer from the x-y reference frame to the S-T reference frame, the x-y frame must be rotated by an angle α to an intermediate U-V reference frame such that U is parallel to the asymptote of the curve. Then the U-V reference is translated to the S-T reference. This is shown in Fig. 3.14. Once the circle-points are computed, they are transferred back to the x-y frame. If α is the angle of rotation from the x-y frame to the U-V frame. Then,

$$
\begin{aligned}
x &= u\cos\alpha - v\sin\alpha \\
y &= u\sin\alpha + v\cos\alpha
\end{aligned}
\qquad (3.15)
$$

where

$$
\begin{aligned}
\sin\alpha &= \frac{A_1}{\sqrt{A_1^2 + A_2^2}} \\
\cos\alpha &= -\frac{A_2}{\sqrt{A_1^2 + A_2^2}}
\end{aligned}
$$

Substituting Eq. (3.15) into (3.14) gives

$$A_1'(u^2+v^2)v + A_2'uv + A_3'u^2 + A_4'v^2 + A_5'u + A_6'v + A_7' = 0 \qquad (3.16)$$

where

$$A_1' = \sqrt{A_1^2 + A_2^2}$$

$$A_2' = \frac{A_3(A_2^2 - A_1^2) + 2A_1A_2(A_4 - A_5)}{A_1'^2}$$

$$A_3' = \frac{A_5A_1^2 + A_4A_2^2 - A_1A_2A_3}{A_1'^2}$$

$$A_4' = \frac{A_4A_1^2 + A_5A_2^2 + A_1A_2A_3}{A_1'^2}$$

$$A_5' = \frac{A_2A_6 - A_1A_7}{A_1'}$$

$$A_6' = \frac{A_1A_6 + A_2A_7}{A_1'}$$

$$A_7' = A_8$$

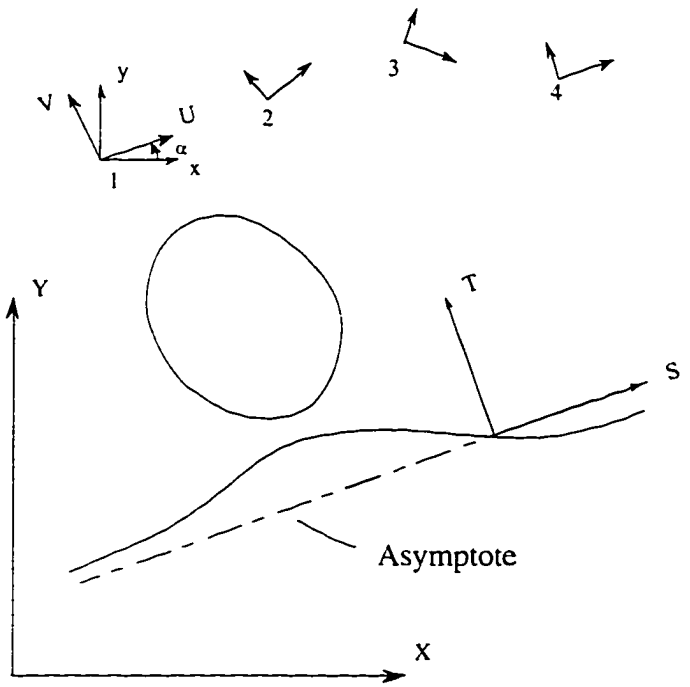

Figure 3.14 Burmester Circle-Point Curve in Various Frames

Next apply the translation equations

$$\begin{aligned} u &= s + a \\ v &= t + b \end{aligned} \tag{3.17}$$

where

$$a = \frac{A_3'^3 - A_4'A_3'^2 + A_6'A_3'A_1' - A_7'A_1'^2}{A_1'(A_1'A_5' - A_2'A_3')}$$

$$b = -\frac{A_3'}{A_1'}$$

To move from the U-V reference to the S-T reference. The Burmester circle-point curve becomes

$$A_1''(s^2 + t^2)\ t + A_2''st + A_3''s^2 + A_4''t^2 + A_5''s + A_6''t + A_7'' = 0 \tag{3.28}$$

where

$$\begin{aligned} A_1'' &= A_1' \\ A_2'' &= 2aA_1' + A_2' \\ A''_3 &= A'_1 b + A'_3 = 0 \\ A_4'' &= A_4' - 3A_3' \\ A_5'' &= 2abA_1' + A_2'b + 2aA_3' + A_5' \\ A_6'' &= A_1'(a^2 + 3b^2) + A_2'a + 2A_4'b + A_6' \\ A_7'' &= A_1'a^2b + A_1'b^3 + A_2'ab + A_3'a^2 + A_4'b^2 + A_5'a + A_6'b + A_7' \end{aligned}$$

To construct the curve, "s" is varied with a preset increment from an initial starting value to form the cubic curve with "t" being the dependent variable. The resulting equation is of the form

$$t^3 + a_1t^2 + a_2t + a_3 = 0 \tag{3.19}$$

where

$$a_1 = \frac{A_4''}{A_1''}$$

$$a_2 = \frac{A_1''s^2 + A_2''s + A_6''}{A_1''}$$

$$a_3 = \frac{A_3'' s^2 + A_5'' s + A_7''}{A_1''}$$

The problem reduces to solving "t" in Eq. (3.19) for each "s" value. A good solution procedure is to use Cardan solution. Let

$$Q = \frac{3a_2 - a_1^2}{9}$$

$$R = \frac{9a_1a_2 - 27a_3 - 2a_1^3}{54}$$

$$S = \sqrt[3]{R + \sqrt{D}}$$

$$T = \sqrt[3]{R - \sqrt{D}}$$

$$D = Q^3 + R^2$$

The value of discriminant D determines the solution. If

(i) $D > 0$, then one real root exists

$$t_1 = S + T - \frac{a_1}{3}$$

(ii) $D = 0$, then three real roots with at least two equal

$$\phi = \cos^{-1} \frac{R}{\sqrt{-Q^3}}$$

$$t_3 = 2\sqrt{|Q|} \cos\left(\frac{\phi + 4\pi}{3}\right) - \frac{a_1}{3}$$

(iii) $D < 0$, then all three roots are real

$$\phi = \cos^{-1} \frac{R}{\sqrt{-Q^3}}$$

$$t_1 = 2\sqrt{|Q|} \cos\left(\frac{\phi}{3}\right) - \frac{a_1}{3}$$

$$t_2 = 2\sqrt{|Q|} \cos\left(\frac{\phi + 2\pi}{3}\right) - \frac{a_1}{3}$$

$$t_3 = 2\sqrt{|Q|}\cos\left(\frac{\phi + 4\pi}{3}\right) - \frac{a_1}{3}$$

In order to determine whether the circle-point curve is a single branch or a double branch, it is necessary to examine the region in which there are three real roots. Eq. (3.18) can be rearranged so that "s" is the variable.

$$(A_1''t + A_3'')s^2 + (A_2''t + A_5'')s + (A_1''t^3 + A_4''t^2 + A_6''t + A_7'') = 0 \qquad (3.20)$$

Since all of the values of "s" must be real, the discriminant of the quadratic equation must be greater than or equal to zero. Thus,

$$D_s = a_1t^4 + 4a_2t^3 + 6a_3t^2 + 4a_4t + a_5 \geq 0 \qquad (3.21)$$

where

$$a_1 = 4A_1''^2$$

$$a_2 = A_1''(A_3'' + A_4'')$$

$$a_3 = \frac{-A_2''^2 + 4A_1''A_6'' + 4A_3''A_4''}{6}$$

$$a_4 = -\frac{A_2''A_5''}{2} + A_1''A_7'' + A_3''A_6''$$

$$a_5 = -A_5''^2 + 4A_3''A_7''$$

Equation (3.21) can have either two or four real roots. The number of roots determines the number of target lines which are parallel to the asymptote. The number of real roots depend on the discriminant D_t of Eq. (3.21).

$$D_t = \left(a_1a_5 - 4a_2a_4 + 3a_3^2\right)^3 - 27\left(a_1a_3a_5 + 2a_2a_3a_4 - a_1a_4^2 - a_5a_2^2 - a_3^3\right)^2 \qquad (3.22)$$

If $D_t < 0$, then two real roots exists and therefore a single branched curve is obtained.

If $D_t > 0$, then four real roots and therefore a double branched curve is obtained.

After the circle points are computed in the S-T frame, they are transformed back into the x-y domain. The coordinate transformation equation for this is

$$\begin{Bmatrix} x \\ y \end{Bmatrix} = \begin{bmatrix} \cos\alpha & -\sin\alpha \\ \sin\alpha & \cos\alpha \end{bmatrix} \begin{Bmatrix} s+a \\ t+b \end{Bmatrix} \tag{3.23}$$

where

$$\sin\alpha = \frac{A_1}{\sqrt{A_1^2 + A_2^2}}$$

$$\cos\alpha = -\frac{A_2}{\sqrt{A_1^2 + A_2^2}}$$

(s, t) the coordinates of the point in the S-T frame of reference

(x, y) the coordinates of the point in the X-Y frame of reference

a, b translation from U-V reference frame to S-T frame of reference

It may be noted, in the application of the circle-point curve, that although the circle-point-curve extends to infinity on either side along the S-axis about the origin, it is not necessary to extend the curve over a very large range as the curve could be well approximated by a small number of straight line segments as the curve dies down asymptotically. Further, for far away circle points, the crank lengths turn out to be large, which are generally not of interest.

3.5.2 Defect Rectification

Some segments on the Burmester circle-point curve are guaranteed to have branch defects which are function of design positions. These segments are identified with the aids of the special points corresponding to the image poles.

In Fig. 3.15, the Burmester circle-point curve intersects the circle with diameter $P'_{ik}P'_{jk}$ at the image poles and two special points T_{ij} and U_{ij}. Q_{ij} is another special point intersected by the image pole line with the Burmester curve. The last special point a circle-point corresponding to a center-point located at infinity (slider-point). The equations to locate the special points are presented in Bawab (1992). These special points, Q_{ij}, T_{ij} and U_{ij} . are the boundary of the segments for the change of the sign of transmission angle displacement ψ_{ij} from position i to j. The rule to determine the sign of ψ_{ij} is the same as that demonstrated in Fig. 3.11.

The solid (thick) line illustrated in Fig. 3.15 is the feasible solution in term of branch defect. However, the identification of the feasible region becomes more confusing when all six image poles are included. Therefore, it is easier to find the feasible region

when dealing with the maximum range of motion of ψ which must be less than π. Assume that the sequence of the positions is i j k l. Then the transmission angles are ψ_{ij}, ψ_{jk}, ψ_{kl} and ψ_{li}, where $-\pi < \psi < \pi$. If all the ψ's are of the same sign, then the range of rotation is greater than π (Fig. 3.16a). If one of the ψ's is of opposite direction, then the range of rotation becomes less than π (Fig. 3.16b).

Prior to the selection of the driven circle-point, the sections on the circle-point curve that have branch defects can be algebraically identified with the aid of the special points. The order of rotation of the coupler relative to the crank is bounded by the poles in the center-point planes. However, the Q's are the special points in the circle-point plane corresponding to the poles. Therefore the Q's bound segments of the curve on which the order of rotation of the coupler relative to the crank is constant, i.e. a segment bounded by Q_{ij} Q_{ik} must have the sequence i k l j or i j l k. Fig. 3.15 shows that ψ_{ij} is π at the special points T_{ij} or U_{ij}. Thus, if positions i and j are adjacent in the order of coupler rotation relative to the crank, T_{ij} or U_{ij} marks the boundary of the feasible segment of the curve; otherwise T_{ij} or U_{ij} lie in the infeasible segment of the curve. The result is shown in Fig. 3.17.

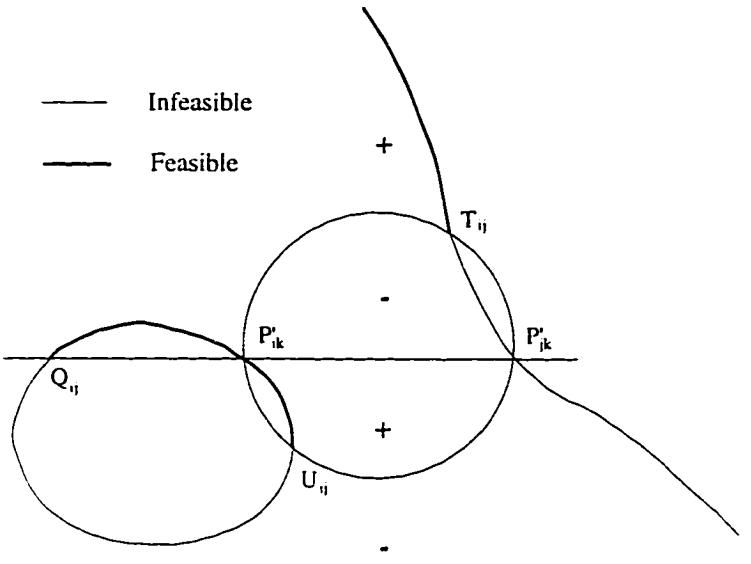

Figure 3.15 Special Points and Feasible Segments in Circle-Point Curve

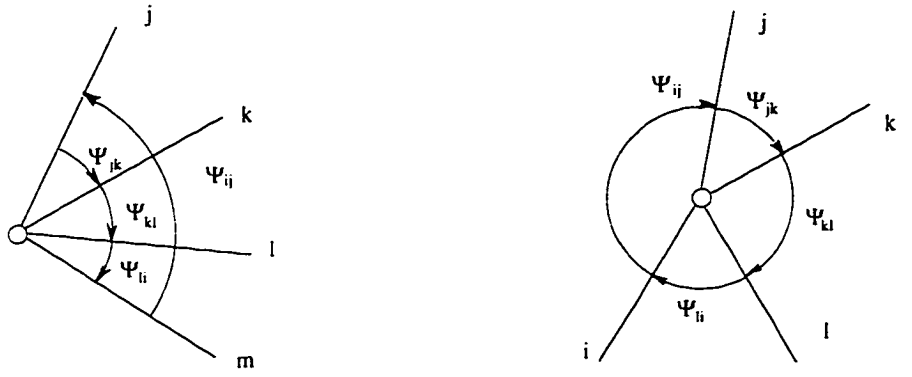

(a) Range Less Than π (b) Range Greater Than π

Figure 3.16 Rotational Range Between the Moving Lamina and Crank

A driven crank circle-point is chosen from the feasible portions on the Burmester curve as shown in Fig. 17 to start the linkage synthesis. The corresponding center-point can be obtained with reference to any three out of the four design position using the approach of three position case discussed in Section 3.31. The driving circle-point should be selected from the sections of the curve overlapping with the feasible areas of Filemon construction. This will generate four-bar linkage free from branch defects. Since circuit defects defer from branch defects in rocker-cranks and double-rockers, their identification must be exerted by checking the range of input positions as discussed earlier.

The order for a linkage to pass through the design positions can only be determined after the driving crank is synthesized although the segments with correct order on the Burmester curve may be identified at the very beginning. This is because that the image poles bound segments of the curve on which the order of rotation of the crank relative to the frame is constant, i.e. a segment bounded by P'_{ij} or P'_{jk} must have the sequence i k l j or i j l k. Based on that concept, the regions with order 1 2 3 4 (i j k l) are identified and selected as the feasible regions of driving circle-point for order defects (Fig. 3.18).

3.5.3 Burmester Center-Point Curve

The derivation of the center-point equation is similar to that of the circle-point equation except that we seek to define a set of equations such that the circle-point coordinates (x, y) are the independent variables rather than center-point (x*, y*). By the same token, the cubic center-point curve equation can be derived as

$$\left(B_1 x^* + B_2 y^*\right)\left(x^{*2} + y^{*2}\right) + B_3 x^* y^* + B_4 x^{*2} + B_5 y^{*2} + B_6 x^* + B_7 y^* + B_8 = 0 \qquad (3.24)$$

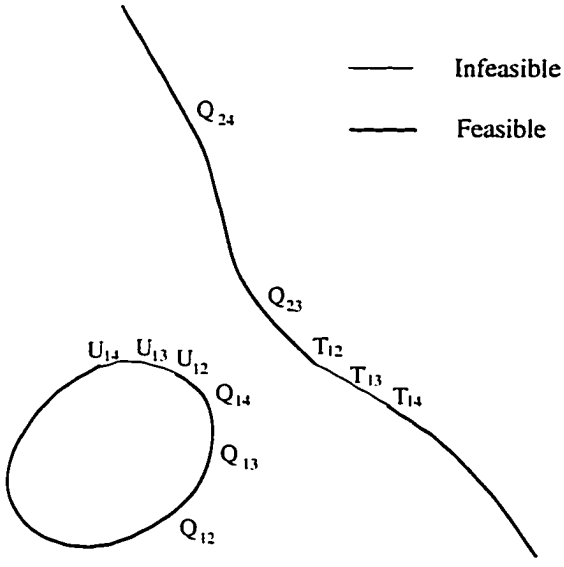

Figure 3.17 Regions with Branch Defect on the Circle-Point Curve

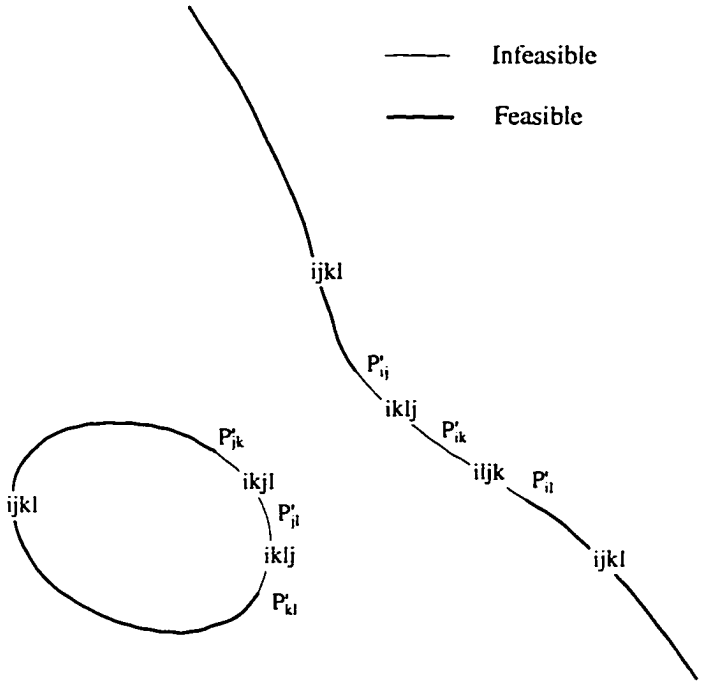

Figure 3.18 Segments for Order Defect on Circle-Point Curve

The coefficients of Eq. (3.24) are found the same way as the coefficients of the circle-point equation. As in the case of the circle-point equation, the x-y reference frame may be rotated and translated to the S-T frame of reference to construct the curve. The rectification techniques for the circle-point curve can then be mapped onto the center-point curve.

3.6 Automatic Synthesis

In order to synthesize a linkage to pass through the design positions with specified geometrical constraints on the moving and fixed points, the designer must be familiar with the theory of linkage synthesis and must go through the trial and error process of synthesizing until an acceptable linkage is obtained. This is referred to as manual synthesis. On the other hand, an automatic synthesis technique can be formed to find the best linkages by formulating the process as an optimization problem.

In most applications, it is necessary to synthesize a linkage to pass through the design positions and have a good transmission angle and link-length ratio that are treated as objective function. In addition there might be a fixed region boundary in which the fixed pivots (center-points) and moving pivots (circle-points) must lie. These restrictions are treated as constraints. Also, the Filemon feasible regions and the feasible regions where branch and order defects are eliminated are considered as constraints.

3.6.1 Objective Function

In the dimensional synthesis of linkages, the objective to improve the characteristics of the linkage is formulated to satisfy a set of constraints. The objective is the one that best describes the design variables. Constrained optimization problem for automatic synthesis can be transformed into a set of unconstrained problems by using a penalty function that assigns a large penalty factor for the set of violated constraints and no penalty for the set of feasible constraints. Here, the Broydon-Fletcher-Goldfarb-Shanno (BFGS) method with penalty function approach is used as the optimization technique with the Golden-Section method being the one dimensional search (Vanderplaats, 1984). The penalty function is written as:

$$P(x, R) = f(x) + \lambda(R, G_j(x)) \tag{3.25}$$

where

$f(x)$ = the objective function

R = Set of penalty parameters

λ = Penalty term

$G_j(x)$ = set of violated constraints ($G_j(x) > 0$)

According to the literature, a good criteria for a good linkage is one which has all transmission angles as close as possible to 90 degrees. Another criteria that determines the

validity is for the linkage to have the ratio of minimum link-length to the maximum link-length close to one for minimum space. However the link-length ratio is not as critical as the transmission angle. The objective function is formed form the transmission angle and the link-length ratio by applying a weight factor to the transmission angle part of the objective function. The weighting factor is appointed between zero and one. A weighting factor of zero implies that the user considers good transmission angle to be far more important than the link-length ratio, and a weighting factor of one implies otherwise. For any given weighting factor and link-length ratio, a linkage with the best transmission angle that satisfies the link-length ratio is found.

Thus the original optimization problem is defined as:

Minimize

$$f(x,\mu) = W f_1(x) + (1-W) f_2(\mu) \qquad (3.26)$$

subject to constraints

$$G_j(x) \leq 0 \qquad j = 1,2,3,....m$$

where

$f(x,\mu)$	=	Objective Function
x	=	Design variables which correspond to the coordinates of the fixed, moving pivots
μ	=	The Minimum transmission angle μ_1 and the maximum transmission angle μ_2
W	=	Link-length to transmission angle weighting factor
$f_1(x)$	=	Link-length ratio function
$f_2(\mu)$	=	Transmission angle ratio.

The link length ratio function is given somewhat arbitrarily by:

$$f_1(x) = e^A$$

where

$$A = \frac{10(x_1^{max} - x_1)}{x_1}$$

x_1^{max}	=	Maximum link-length ratio of the desired linkage.
x_1	=	User desired limit for the link-length ratio.

The transmission angle function is given by:

$$f_2(x) = e^B$$

where

$$B = 10\,\mathrm{Max}\left\{\left|\frac{\pi}{2}-\mu_1\right|,\ \left|\frac{\pi}{2}-\mu_2\right|\right\}$$

μ_1 and μ_2 are the limit for the transmission angles

An exponential function is used to improve the convergence characteristics of the objective function.

3.6.2 Constraint Equations

Fixed region boundaries within which the fixed pivots (center-points) and the moving pivots (circle-points) must lie are treated as constraints. These constraints are assumed to have a rectangular shape and could be generalized to a convex polygon shape. As defined in the previous section the constraints for the optimization problem is given by:

$$G_j(x) \le 0 \qquad j= 1,2,3,....m$$

Consistent with the above definition constraints G_1 to G_8 are defined to ensure that the fixed pivots are within the user defined fixed boundary constraints. The minimum coordinates of the rectangle are x_{min}^{fix} and y_{min}^{fix}, and the maximum coordinates of the rectangle are x_{max}^{fix} and y_{max}^{fix}. The coordinates of the center-point of the driven crank is given by (x^*_1, y^*_1) and the center-point of the driving-crank is given by (x^*_2, y^*_2)

$$\begin{aligned}
G_1 &= x_{min}^{fix} - x^*_1 \\
G_2 &= x^*_1 - x_{max}^{fix} \\
G_3 &= y_{min}^{fix} - y^*_1 \\
G_4 &= y^*_1 - y_{max}^{fix} \\
G_5 &= x_{min}^{fix} - x^*_2 \\
G_6 &= x^*_2 - x_{max}^{fix} \\
G_7 &= y_{min}^{fix} - y^*_2 \\
G_8 &= y^*_2 - y_{max}^{fix}
\end{aligned} \qquad (3.27)$$

Similarly the constraints G_9 to G_{16} are defined to ensure that the moving pivots are within the user defined moving boundary constraints. The minimum coordinate of the rectangle are x_{min}^{mov} and y_{min}^{mov} and the maximum coordinates being x_{max}^{mov} and. y_{max}^{mov}

$$G_9 = x_{min}^{mov} - x_1$$

$$
\begin{aligned}
G_{10} &= x_1 - x_{max}^{mov} \\
G_{11} &= y_{min}^{mov} - y_1 \\
G_{12} &= y_1 - y_{max}^{mov} \\
G_{13} &= x_{min}^{mov} - x_2 \\
G_{14} &= x_2 - x_{max}^{mov} \\
G_{15} &= y_{min}^{mov} - y_2 \\
G_{16} &= y_2 - y_{max}^{mov}
\end{aligned} \tag{3.28}
$$

The Filemon infeasible regions and circuit defects are also treated as constraints. The angle γ that the coupler makes with the horizontal is given by

$$\gamma = \tan^{-1}\left[\frac{y_2 - y_1}{x_2 - x_1}\right] \tag{3.29}$$

For the driven circle-point (x_2, y_2) and the driving circle-point (x_1, y_1), ψ_1 and ψ_m represent the Filemon angles as shown in Fig. 3.19.

For circle-point (x_2, y_2) located in the Filemon infeasible region, the constraints G_{17} and G_{18} are given as:

$$
\begin{aligned}
G_{17} &= \gamma - \psi_1 \\
G_{18} &= \psi_m - \gamma
\end{aligned} \tag{3.30}
$$

On the other hand, the constraints G_{17} and G_{18} are set to zero when the circle-point (x_2, y_2) located in the Filemon feasible region x. It should be noted here that the Filemon angles given are in the circle-point plane.

The elimination of circuit defect is performed in a fashion similar to that explained for manual synthesis. The constraints for the circuit defect is specified by:

$$
\begin{aligned}
G_{19} &= 0 \text{ without circuit defect.} \\
G_{19} &= \infty \text{ with circuit defect.}
\end{aligned} \tag{3.31}
$$

3.6.3 Two Position Automatic Synthesis

In two position synthesis the number of design variables to be optimized is six. Three corresponding to the driven crank synthesis and three corresponding to the driving crank synthesis. Depending on the constraint boundary specified by the user, the synthesis is conducted either from the center-point plane or the circle-point plane. The synthesis is

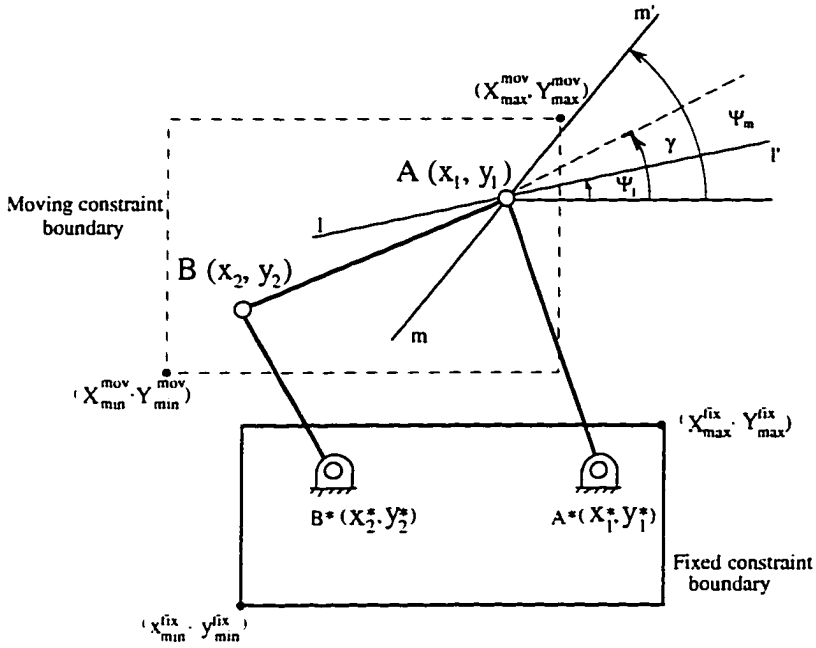

Figure 3.19 Description of the Constraint Specification

performed from the circle-point plane if the user only defines the constraint boundary for the moving pivots.

It is assumed that the circle-point plane is the plane of synthesis. To start with, a grid point (x, y) is selected in the search and the locus of the center point corresponding to the circle-point is found, and only one design variable needed to define a center-point (see Fig 3.20). If no part of the locus lies within the fixed constraint boundary, then the grid point is discarded and another grid point is tried. This process continues until some part of the center-point locus lies within the constraint boundary or all the grid points are exhausted. In that case, it is assumed that there is no solution within the user defined constraint boundary. A similar search procedure is applied for the driving crank synthesis.

In the selection of a driving crank, grid points that are in the Filemon feasible region are selected. If the initial linkage satisfying the constraints is found, it is identified on the basis of its Grashof type and then checked for circuit defects. If the linkage does not exhibit a circuit defect, the objective function of this linkage is computed and the search is continued. Throughout the search, the linkages with improved objective function replace the existing ones. Therefore all the grid points in the plane are evaluated and the nine best linkages are stored for optimization to improve their solutions.

3.6.4 Three Position Automatic Synthesis

In three position synthesis, the number of design variables to be optimized is four. Two variables corresponding to the driven crank synthesis and two variables corresponding to the driving-crank synthesis.

A grid point (x, y) is selected as driven crank circle-point from within the constraints specified, such that the point does not lie in the infeasible regions for branch defects, and its corresponding center-point is found. This accounts for the two variables associated with the driven crank synthesis. If the center point selected does not lie within the constraints specified, then the grid point is discarded and another grid point is tried. After the selection of the driven crank, the driving crank is selected from regions other than those eliminated by the Filemon construction. As in two position synthesis, the nine best linkages are stored for further optimization.

Since there exists regions that are infeasible for the selection of the driven crank, there is a constraint G_{20} due to the joint angle ψ changing signs in these regions. To check for the feasibility of driven crank circle-point (x_2, y_2), the vertical line passing through x_2 is used as illustrated in Fig 3.21. The y coordinate of intersection points (maximum of 6) of the vertical lines with the circles is computed and sorted in the order of increasing y.

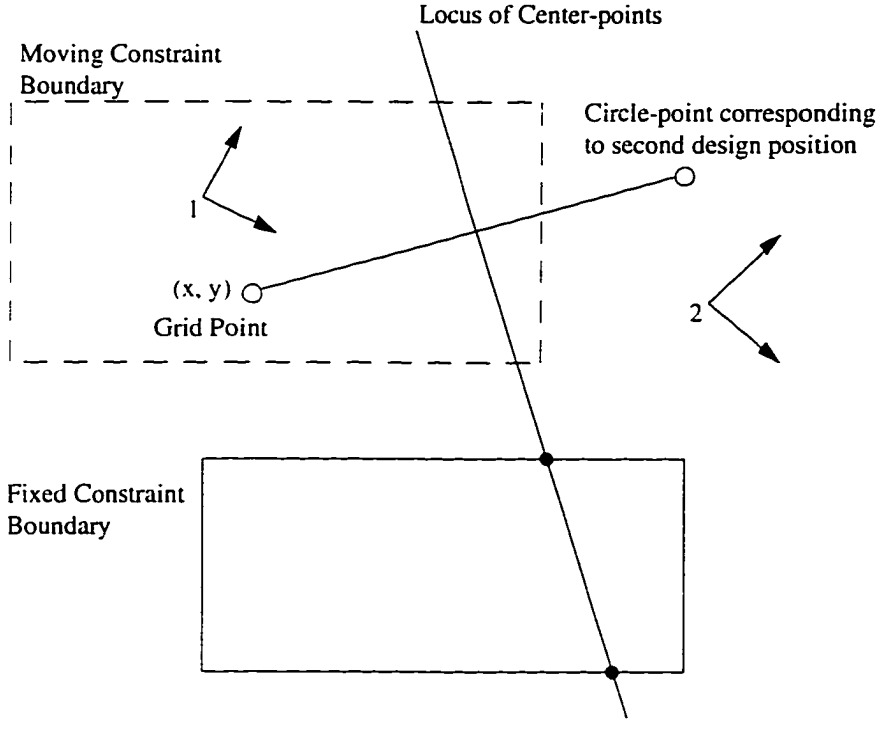

Figure 3.20 Initial Guess Selection for Two Position Automatic Synthesis

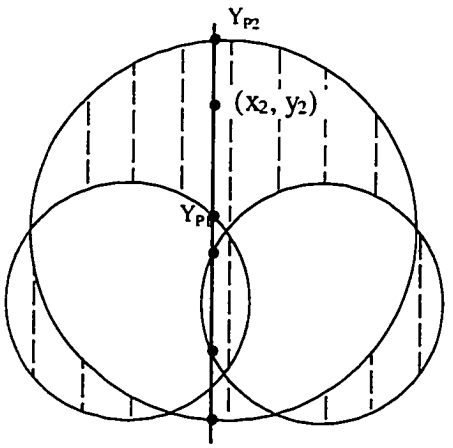

Figure 3.21 Constraint for Driven Crank Selection in Three Position Synthesis

These intersection points are taken in pairs (corresponding to the alternate region being infeasible) and y_2 is checked for its location between these pairs. If it does not lie in any of the infeasible regions then $G_{20} = 0$.

If it lies in the infeasible region the constraint is calculated as follows:

$$G_{20} = 2.0\sqrt{(y_2 - y_{p1})(y_{p2} - y_1)} \tag{3.32}$$

where y_{p1} and y_{p2} correspond to the infeasible region boundary points. The driven crank circle points lies in the feasible region when there are no intersection points. This type of constraint is specified to ensure that the constraint value vanishes at the boundary of feasible and infeasible segments and reaches a maximum at the center of the infeasible segment. The driving crank is selected from regions other than those eliminated by the Filemon construction. The synthesized linkages are also checked and rectified for circuit defects. As in two position synthesis the nine best linkages are stored for further optimization. In the case of synthesis from the center-point domain, the circle point of the driven crank is checked for infeasibility as defined by the branch theory. Thus the constraint remains the same whether the optimization is done from the circle-point or the center-point plane.

3.6.5 Four Position Automatic Synthesis

In four-position synthesis, some segments of the curve are infeasible for the selection of the driven crank. This will result in branch problem as described in subsection 3.5.3. Circle-points selected in these regions have no feasible area for the selection of the

driving circle-point. In other words, the difference of the Filemon angles are greater than π for these segments. If Filemon lines are ll' and mm' and the corresponding Filemon angles are ψ_l and ψ_m as shown in Fig. 3.19, the constraint G_{20} can be defined to eliminate such portions of the Burmester curve as expressed in Eq. 3.33.

$$G_{20} = k_1 \left(|\Psi_l - \Psi_m| - \pi \right) \tag{3.33}$$

where k_1 is used as a scaling factor to make the contribution of this term comparable to the other terms in the objective function evaluation. A negative value of the constraint means that the inequality constraint is satisfied and the magnitude is indicative of how close it is to the boundary. Order problem is also considered as a constraint as

$$\begin{aligned} G_{21} &= 2.0 \sqrt{(x_B - x_{min})(x_{max} - x_B)} && \text{(order problem)} \\ G_{21} &= 0.0 && \text{(no order problem)} \end{aligned} \tag{3.34}$$

where X_{min} and X_{max} correspond to the minimum and the maximum x coordinate of the segment bound by the image poles in which the driving circle-point lies.

Once the initial guesses are obtained, the linkages are optimized using the BFGS method in the x-y coordinates. For each iteration, the design variables are obtained arbitrarily in the x-y reference, and then forced back onto the Burmester curve. The iteration procedure is repeated until the optimum linkage is obtained. This is illustrated in Fig. 3.22.

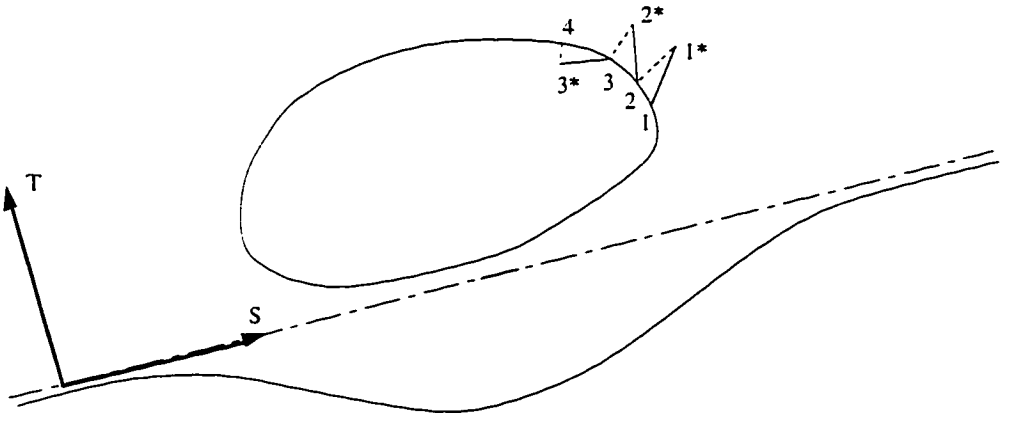

Figure 3.22 Stepped Optimization Along the Curve

CHAPTER IV

FOUR-BAR CIRCUIT RECTIFICATION AT SYNTHESIS LEVEL

A complete circuit rectification procedure for two, three, and four position motion generation of four-bar linkages at the synthesis level is described in this chapter. This is achieved by controlling the change of sign of one of the angles opposite to the shortest link. The procedure utilizes the algebraic method where special points are employed to eliminate the solutions with circuit defects as a function of the design positions. Complete rectification is accomplished at the mid-synthesis level by controlling the critical angles of the linkage that identify the existence of circuit defects. This accounts for the rectification of circuit defects at the synthesis stage. There are four sections in this chapter. Section 4.1 introduces a line construction to control the angle formed from input crank to the base link. This method is similar to Filemon construction. Elimination of circuit defects for two position motion generation using both Filemon construction and line construction is provided in Section 4.2. Section 4.3 gives the procedure to rectify circuit problems for three position motion generation where special consideration is rendered to locate infeasible regions for rocker-crank and double-rocker four-bars prior to any dyad selection. For four position motion generation, there exist certain sections on the Burmester curve that causes circuit defects for rocker-cranks and double-rockers. A method to detect these portions with the aid of newly defined special points on Burmester center-point curve is described in Section 4.4.

4.1 Line Construction

As shown in Fig. 2.1, a circuit defect in rocker-crank and double-rocker four-bar linkages exists when the angle of the driver link relative to the base link changes signs at one of the design positions. As an alternate to circuit rectification in rocker-cranks and double-rockers, the rotation angle ϕ [5] of the driving crank about the base link is under

[5] The sign convention for f is $-\pi < \phi \leq \pi$.

investigation and the sign of this angle must remain invariant at all design positions to avoid circuit defects.

The range of the input link is identified at the precision positions and the extreme positions are marked as the boundary lines l and m for the feasible (F) and infeasible (U) ranges for the location of the driven crank center point A* of the base link B*A*. This is shown in Fig. 4.1. If A* falls in the infeasible range U, then the angle ϕ of the driving crank will change sign at one of the design positions and a circuit defect exists in the linkage. On the other hand, if A* falls in the feasible range F, then the sign of the angle ϕ of the driving crank remains invariant at all the design positions and a circuit defect does not exist. The angle ϕ under investigation is formed between links A*B* and B*B of dyad A*B*B of the four-bar linkage shown in Fig. 4.2.

A *line construction* similar to the Filemon construction is applied to this dyad with link A*B* being the base link to eliminate infeasible regions for driving circle-point that can cause the angle ϕ to change signs in at least one of the design positions. As indicated in Fig. 4.3, A*B* is the base of the dyad and B^*B_i is the tracer of the dyad at the four

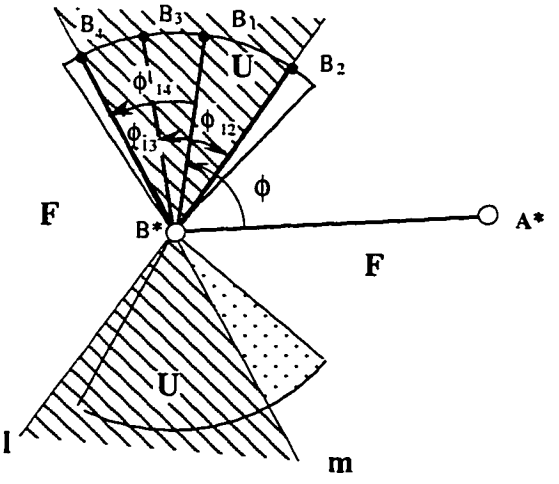

Figure 4.1 Feasible and Infeasible Areas for the Driven Crank Center-Point A*

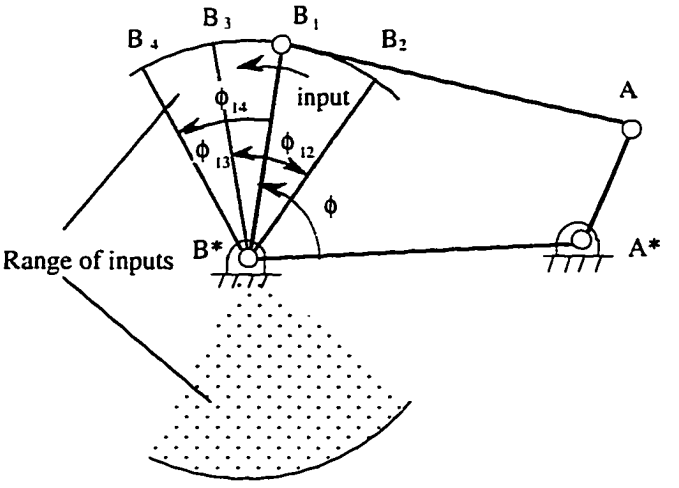

Figure 4.2 Circuits of a Four-Bar Linkage

positions for i = 1 to 4. The lines i_2, i_3, and i_4 form angles $-\phi_{12}$, $-\phi_{13}$, $-\phi_{14}$, respectively, with A*B*. Lines l and m form the limits of the feasible and infeasible regions for the location of the driving circle-point B where the angle between the lines l and m is the maximum range of the input crank rotation. In this case, the maximum range of the input link rotation is ϕ_{24} and hence the angle of the lines l and m are $-\phi_{12}$, $-\phi_{14}$, respectively, relative to the base link A*B*. In order for the link B*B to traverse the precision positions without a change of sign of the angle ϕ, B must be located in the feasible region marked F. Thus, the line construction eliminates the forbidden region for the selection of the circle point B. ϕ_{ij} denotes the range of the angle through which the driving crank, B*B, turns relative to the base link in order to reach position j from position i. The angle ϕ_i is calculated as follows:

$$\cos\phi_i = \frac{(x_{B*} - x_{A*})(x_{B_i} - x_{B*}) + (y_{B*} - y_{A*})(y_{B_i} - y_{B*})}{\sqrt{\left[(x_{B*} - x_{A*})^2 + (x_{B_i} - x_{B*})^2\right]\left[(y_{B*} - y_{A*})^2 + (y_{B_i} - y_{B*})^2\right]}}$$

$$\sin\phi_i = \frac{(x_{B*} - x_{A*})(y_{B_i} - y_{B*}) + (y_{B*} - y_{A*})(x_{B_i} - x_{B*})}{\sqrt{\left[(x_{B*} - x_{A*})^2 + (x_{B_i} - x_{B*})^2\right]\left[(y_{B*} - y_{A*})^2 + (y_{B_i} - y_{B*})^2\right]}}$$

$$\phi_i = 2.0 \tan^{-1}\left[\frac{\sin\phi_i}{1+\cos\phi_i}\right] \tag{4.1}$$

and

$$\phi_{ij} = \phi_j - \phi_i \tag{4.2}$$

where

$$-\pi < \phi_{ij} \leq \pi \qquad i = 1, 2, 3, 4 \quad \text{and} \quad j = 2, 3, 4$$

Therefore, a line construction method can be employed to eliminate circuit defects for rocker-crank and double-rocker four-bar linkages, which does not need to get the input crank range as the method used in Mirth and Chase (1995), and Bawab (1992).

4.2 Circuit Rectification for Two Positions

The procedure to eliminate circuit defects in four-bar linkages for two position motion generation is the same as that introduced in Section 3.3 except for the rocker-crank and double-rocker case.

Filemon construction is first applied to the driven crank circle-point to avoid circuit defects in crank-rocker and double-crank four-bars. This also eliminate branch problems for all types of four-bars. Once a driving circle-point is selected from Filemon feasible regions, the Grashof type of the four-bar linkage is classified, then line construction is used to detect a possible circuit problem for rocker-crank and double-rocker four-bars. If the driving circle-point is located in the infeasible areas of the line construction, the four-bar has circuit defects and needs to be redesigned. Otherwise, the rocker-crank and double-

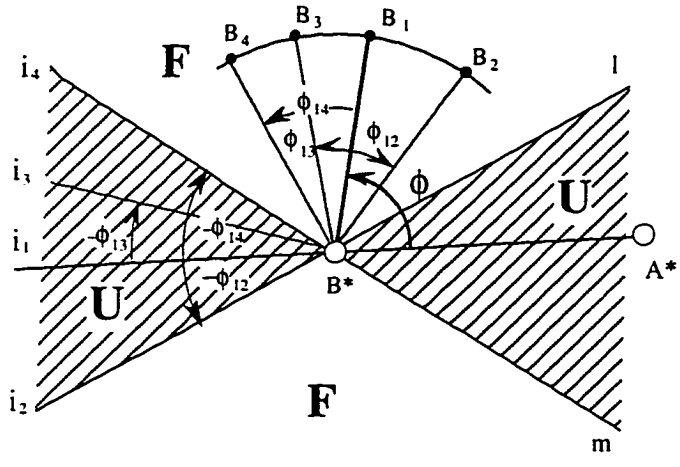

Figure 4.3 Line Construction

rocker four-bars are circuit defect free. To demonstrate its application, this new process has been programmed into RECSYN in place of the original one by Bawab (1992).

One example of a synthesized four-bar without the circuit defect rectification is shown in Figs. 4.4 to 4.7. The other example with circuit defect elimination procedure is showed in Figs. 4.8 to Fig 4.11. As described earlier, RECSYN has the capability to do both manual and automatic synthesis. However, manual synthesis is used here for better demonstration of the procedure. The rectified synthesis is done from the circle-point plane.

Figure 4.4 gives the specification of two design positions. In Fig 4.5, the circle-point of the driven dyad is selected anywhere in the plane, and the corresponding center-point is then selected randomly on the center-point line to form the driven dyad. The Filemon construction is applied to eliminate the regions of the circle-point plane with branch defects. A driving circle-point is selected from the feasible regions where branch defects are eliminated and the corresponding solution of the driving center-point is found to be a line that is sectioned into the different types and classes of four-bar linkages. Non-Grashof and Grashof crank-rocker and double-crank four-bars do not have circuit problems. However, rocker-cranks and double-rockers are not guaranteed to be circuit defects free. The driving center-point is then selected from the double-rocker portion to form the four bar linkage as illustrated in Fig. 4.6. But as demonstrated in Fig. 4.7, this linkage does not pass through the second position when animated because of the existence of a circuit defect.

The same design positions are used in the RECSYN where the aforesaid procedure for the elimination of the circuit defect is included. The selection for the driven dyad and the Filemon construction shown in Fig 4.6 of the first example are the same as the ones in Fig 4.10. Also, the same location of the driving circle-point is picked in this panel. However, the Grashof crank-rocker and double-crank sections of the previous solution locus of center-points are indicated as infeasible which means the existence of circuit defects on these portions. RECSYN keeps the users from choosing center-point out of these infeasible sections. In Fig 4.11, a driving center-point is selected close to the infeasible section to form a four-bar linkage.

4.3 Circuit Rectification for Three Positions

It is indicated in Section 3.4 that some regions of the circle-point plane for three position motion generation can result in the range of transmission angle greater than π. Similarly, in the center-point plane it can be verified that certain areas will cause the range of the angle ϕ formed from the crank to base link to exceed π. These regions that are the function of design positions are forbidden areas for the selection of the driving center-point in terms of circuit defect in rocker-cranks and double-rockers. A method to locate these infeasible regions is described in this section.

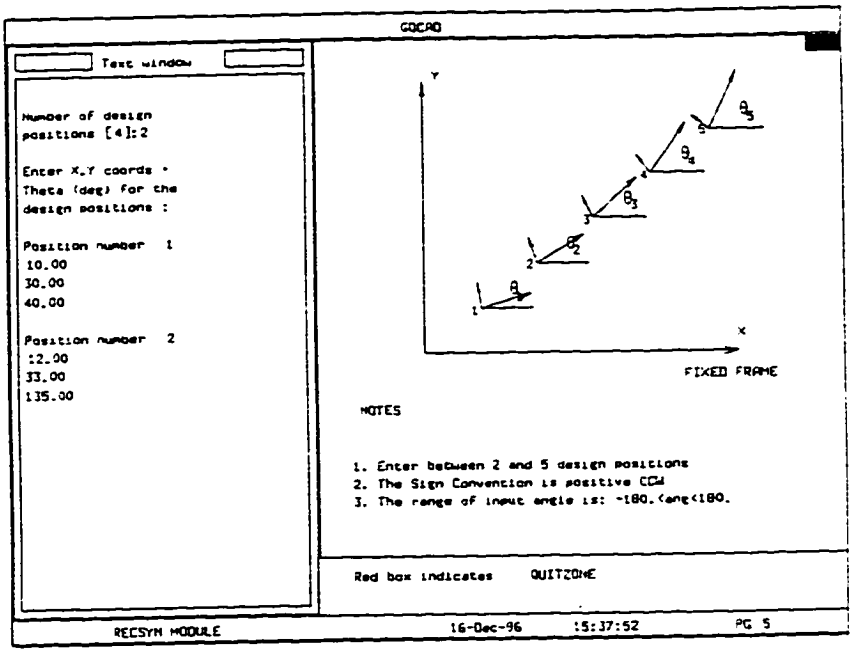

Figure 4.4 Two Position with Circuit Defect - Specification of Design Positions

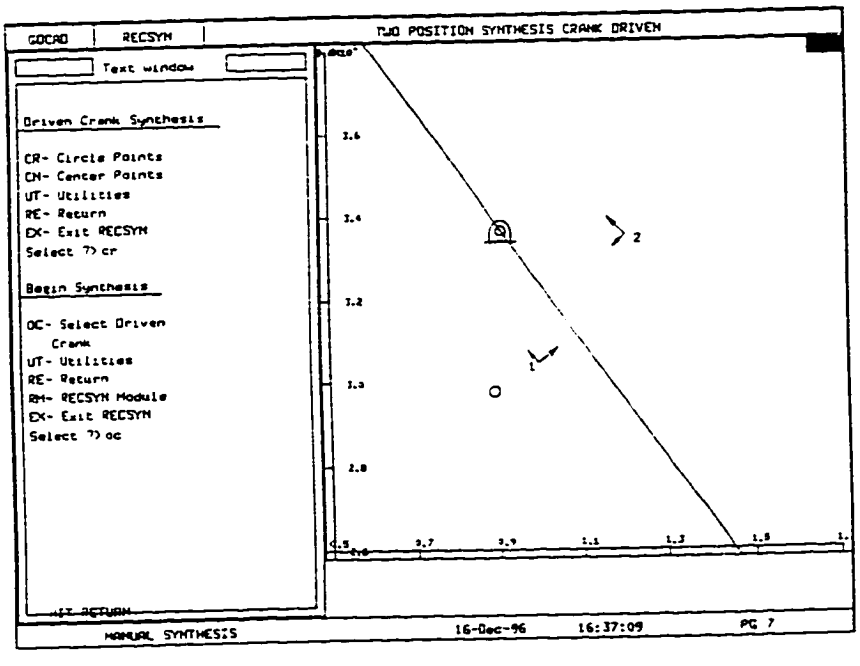

Figure 4.5 Two Position with Circuit Defect - Synthesis of Driven-Crank

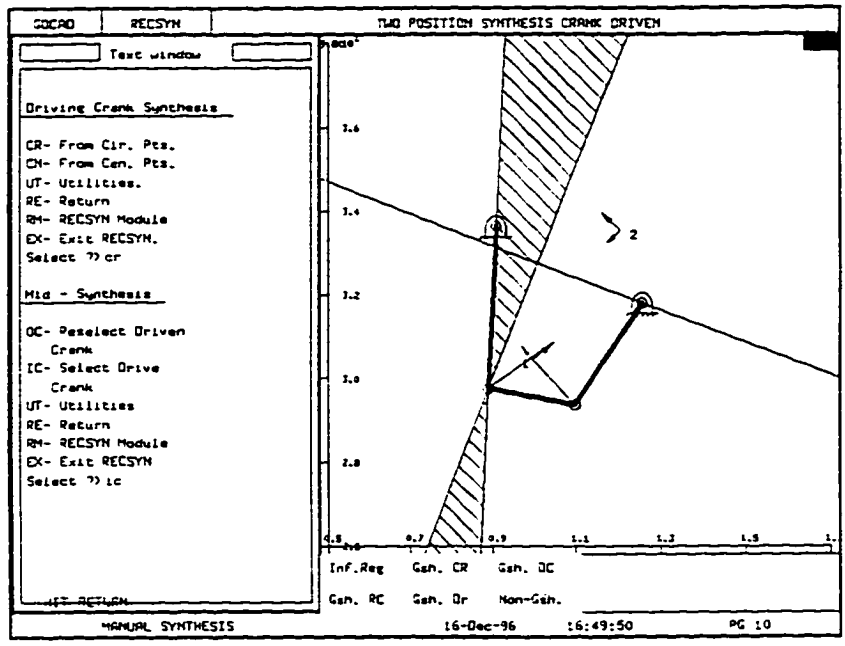

Figure 4.6 Two Position with Circuit Defect - Synthesis of Driving-Crank

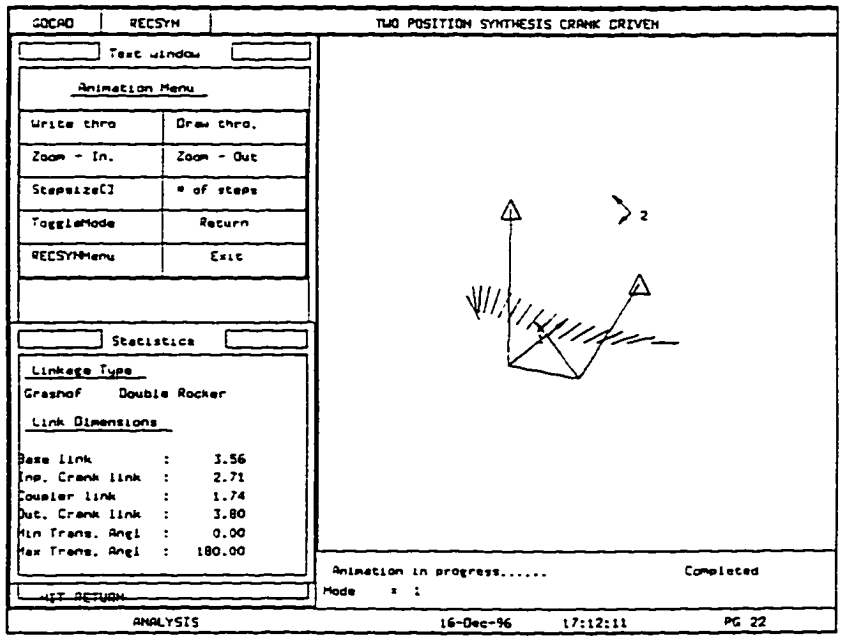

Figure 4.7 Two Position with Circuit Defect - Animation and Linkage Dimensions

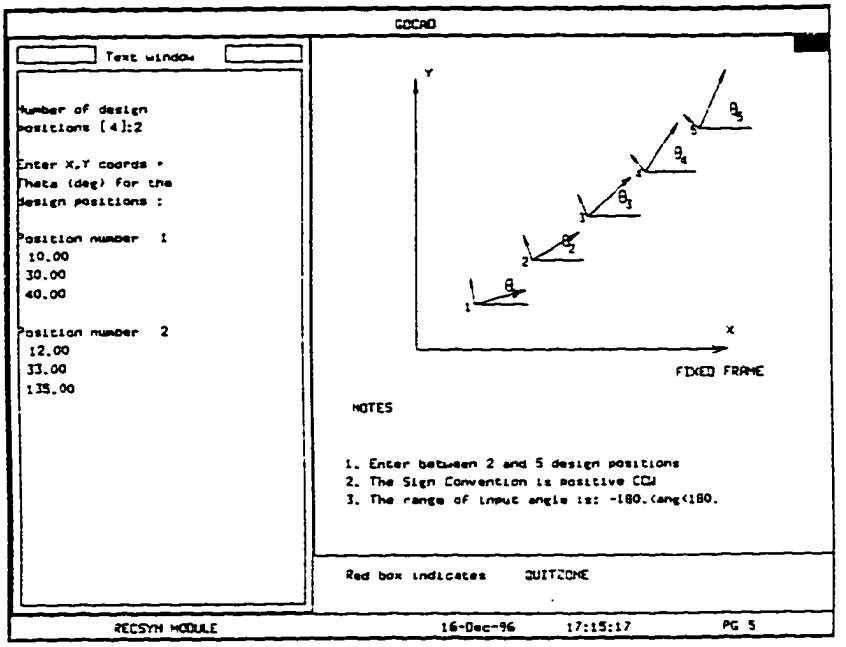

Figure 4.8 Two Position without Circuit Defect - Specification of Design Positions

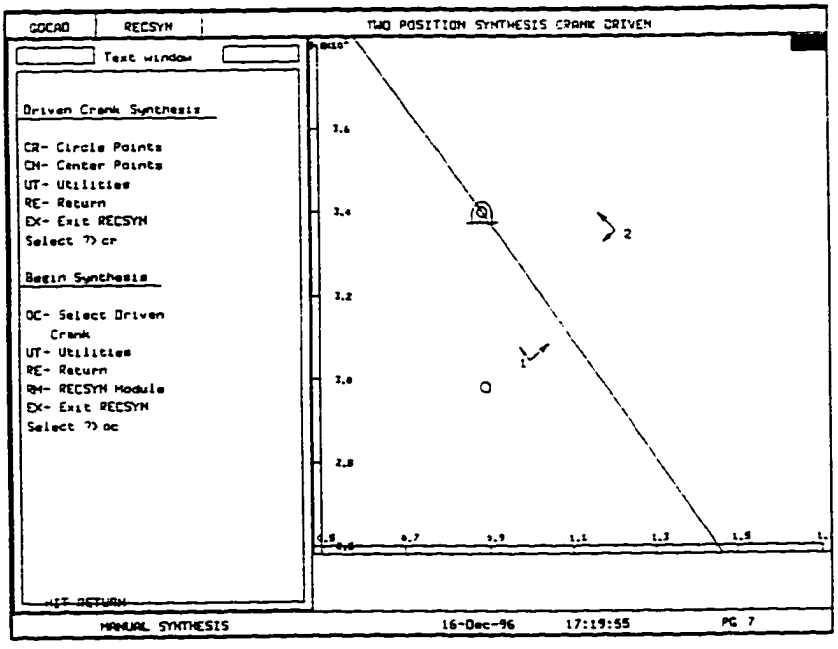

Figure 4.9 Two Position without Circuit Defect - Synthesis of Driven-Crank

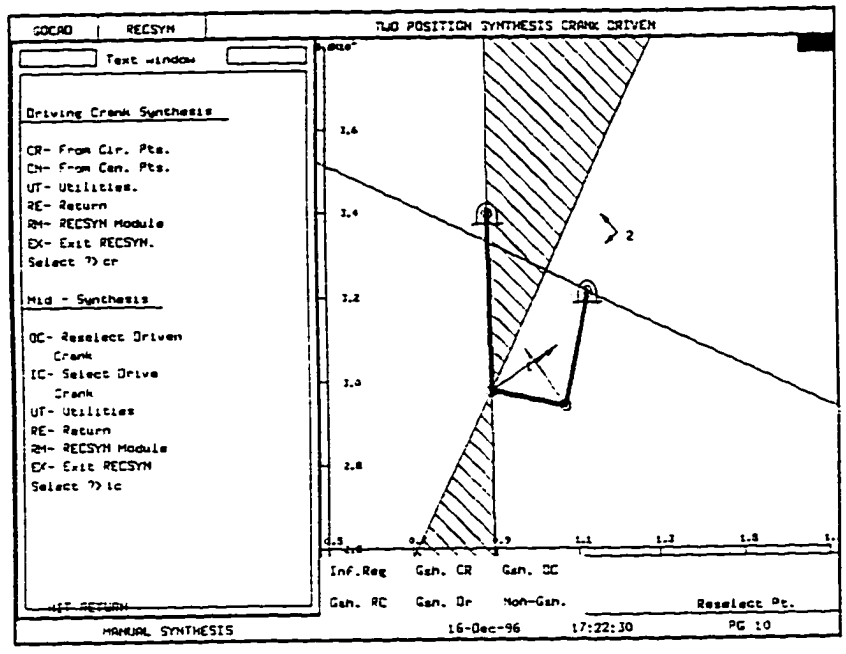

Figure 4.10 Two Position without Circuit Defect - Synthesis of Driving-Crank

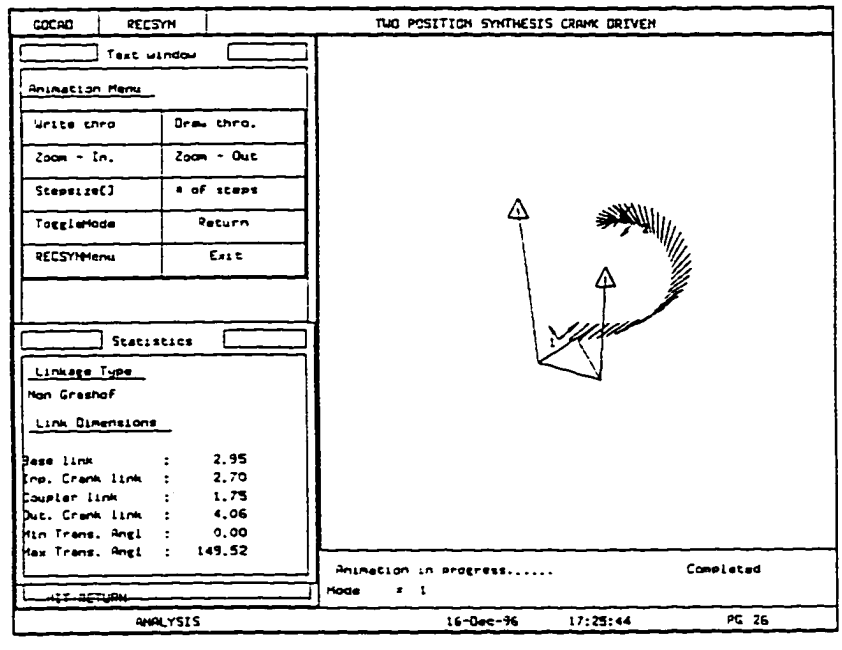

Figure 4.11 Two Position without Circuit Defect - Animation and Linkage Dimensions

Figure 4.12 provides the relationship between the angular range of ϕ_{ij} and pole pair P_{ik} and P_{jk}. Line $P_{ik}B^*$ bisects angle $B_kB^*B_i$; and line $P_{jk}B^*$ bisects angle $B_kB^*B_j$. Thus, the angle subtended at any center-point B^* by the pole pair $P_{ik}P_{jk}$ is $(\phi_{kj}/2 - \phi_{ki}/2)$ that equals to $\phi_{ij}/2$ measured from B^*P_{ik} to B^*P_{jk}, where ϕ_{ij} is the angular displacement of the crank relative to the frame and B^* is the center-point.

According to Fig. 4.13, a circle is drawn to pass through the poles $P_{ik}P_{jk}$. With the sign convention used such that $-\pi < \phi_{ij} < \pi$, the sign of ϕ_{ij} can be found at any point in the solution space. Since $\phi_{ik} = \phi_{ij} + \phi_{jk}$, it is necessary for the range of rotation to be of the same sign. For instance, if ϕ_{ij} and ϕ_{jk} are positive, then ϕ_{ik} must be positive to have a feasible point, i.e. a negative ϕ_{ik} means that $\phi_{ij} + \phi_{jk} > \pi$. This fact combined with the knowledge of sign of ϕ_{ij} provides a method to identify the infeasible regions. In the case of three design positions, three poles exist and the regions with change of sign of the angle ϕ of the crank relative to the frame are hatched as illustrated in Fig. 4.14. The procedure is simplified to the following:

- The three circles with diameter $P_{ij}P_{ik}$, $P_{ik}P_{jk}$ and $P_{ij}P_{jk}$ are drawn.
- The outer boundaries of all circles are feasible. Starting from these boundaries, alternate segments (hatched regions) are infeasible and the selection of the center point in these regions will have a change of sign of the angle ϕ of the crank relative to the frame causing a circuit defect in double-rocker or rocker-crank linkages.

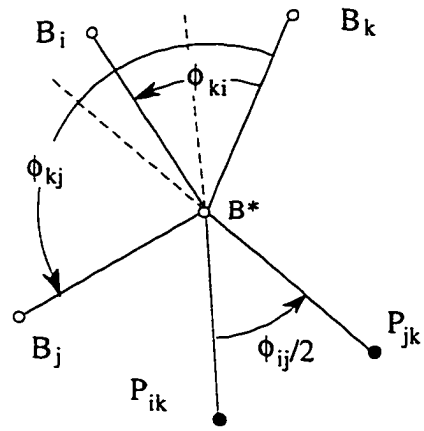

Figure 4.12 Angle Subtended by Poles $P_{ij}P_{jk}$

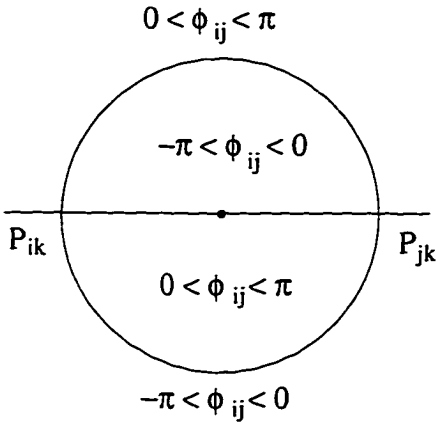

Figure 4.13 Layout of Sign of ϕ_{ij}

A complete procedure to rectify circuit defects for three position motion generation is summarized here. Initially, select a driven circle-point is selected from the feasible areas as described in Section 3.4. Once the circle point is picked, the center-point is obtained to form the driven crank. Filemon construction is applied to the circle-point and regions with branch defects eliminated for the selection of the driving circle-point and the results are mapped into the center-point regions. The remaining solution planes are then marked for the different types of Grashof linkages. The double-rocker and rocker-crank regions are further investigated for circuit defects since the regions with the other Grashof types are circuit defects free. Regions with circuit defects are identified by constructing the pole circles as shown in Fig. 4.14. The hatched areas are the regions where a sign change of the range of the angle ϕ of the crank relative to the frame occurs. Since this range is prohibited to change signs for the double-rocker and rocker-crank linkages, common regions of hatched areas and double-rocker (or rocker-crank) are highlighted to have circuit defects and are marked infeasible for the selection of the center point of the driving dyad. In each of the remaining regions of double-rocker and rocker-crank, a random center-point is selected to find its corresponding circle-point that forms the driving dyad. Equations. (4.1) and (4.2) are applied to the center point to find the infeasible regions of the line construction as illustrated in Fig. 4.3. The whole region is marked infeasible when the circle point B is located in the infeasible area of the line construction. The center point is selected from the remaining feasible areas and the circle point is obtained to complete the rectification procedure of the four-bar linkage.

One example to show a synthesized four-bar with a circuit defect is presented by Figs. 4.15 to Fig. 4.18. The synthesis is carried out in the circle-point plane with the manual mode of RECSYN. In Fig. 4.16, a circle-point of the driven dyad is selected from the feasible region where the branch defect does not occur and the corresponding center-point is obtained. Then the Filemon construction is applied and the feasible circle-point plane is divided into the different types and classes of four-bars. The coarse hatched regions are the Filemon infeasible regions in the circle-point plane. The different Grashof types and classes are identified using color indices and the correspondence between the colors and the linkage type is displayed at the bottom of the window. The driving circle-point is selected from the rocker-crank portion, and its corresponding center-point is obtained to form the four-bar linkage. These are shown in Fig. 4.17. But as demonstrated in Fig. 4.18, this linkage does not pass through the third position when animated because of the existence of a circuit defect.

The other example is presented in Figs. 4.19 to 4.22 which provides a designed four-bar for three position motion generation from RECSYN. In this example, the circuit rectification method is coded in. The same design positions as in the previous example are used and the selection of the driven dyad is also identical. A driving circle-point closing to the location of the earlier pick in Fig. 4.16 is selected from a non-Grashof areas, and center-point is generated to complete the design. Fig. 4.22 shows this linkage can pass all the design positions since the circuit defects are eliminated.

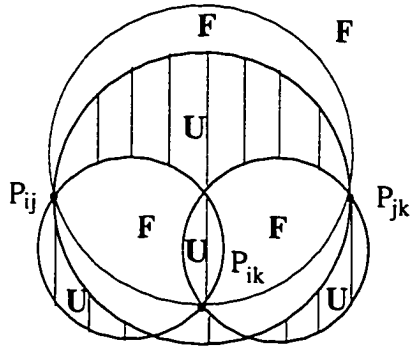

Figure 4.14 Feasible Regions for the Driving Center-Point of Rocker-Cranks and Double-Rocker

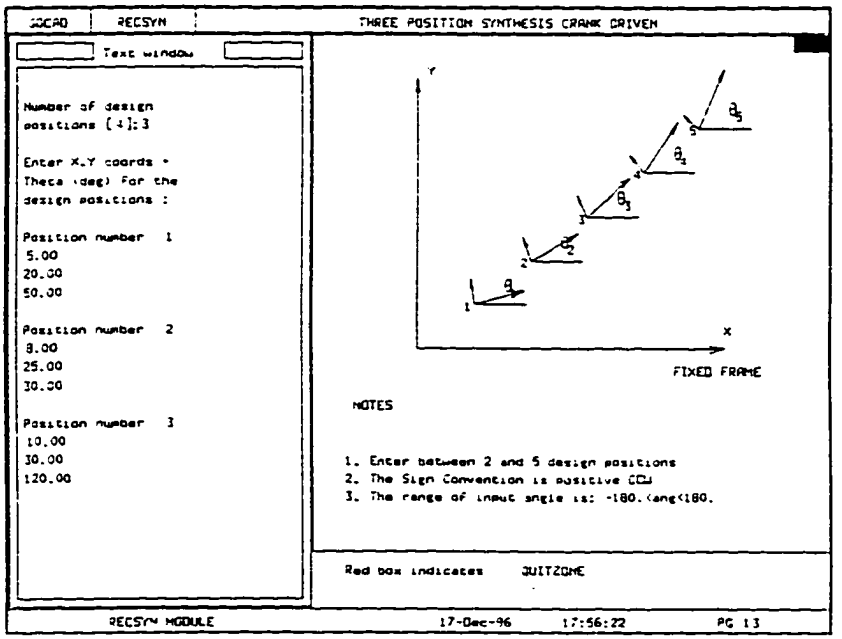

Figure 4.15 Three Position with Circuit Defect - Specification of Design Positions

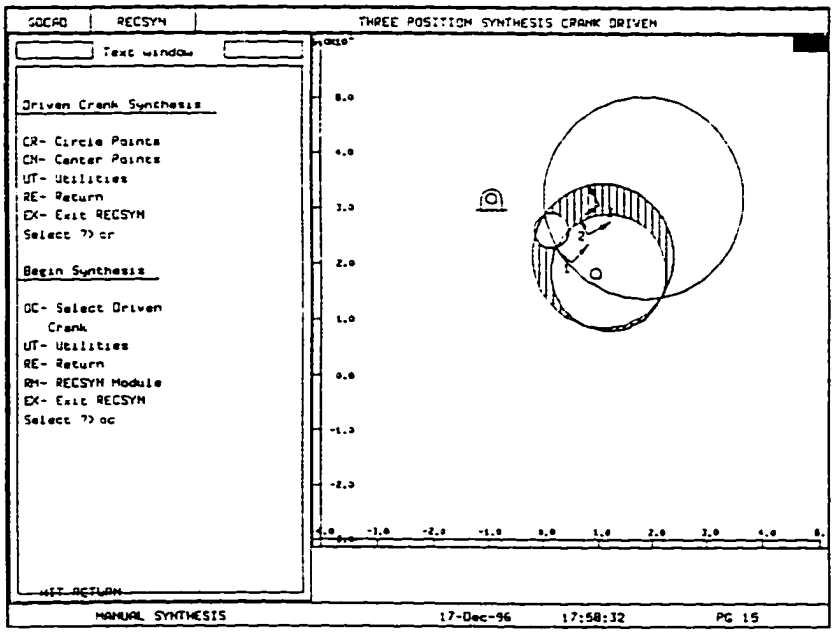

Figure 4.16 Three Position with Circuit Defect - Synthesis of Driven-Crank

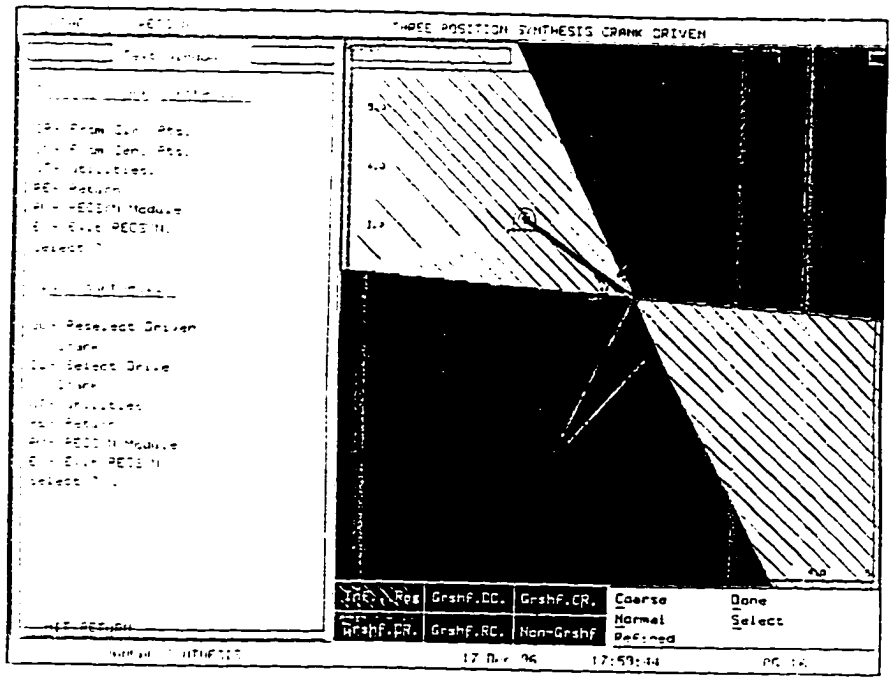

Figure 4.17 Three Position with Circuit Defect - Synthesis of Driving-Crank

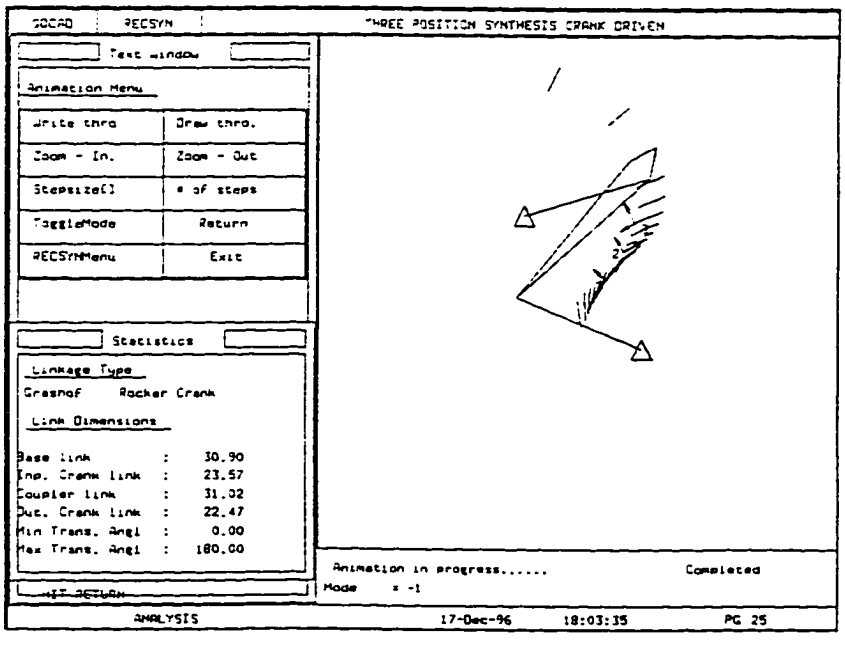

Figure 4.18 Three Position with Circuit Defect - Animation and Linkage Dimensions

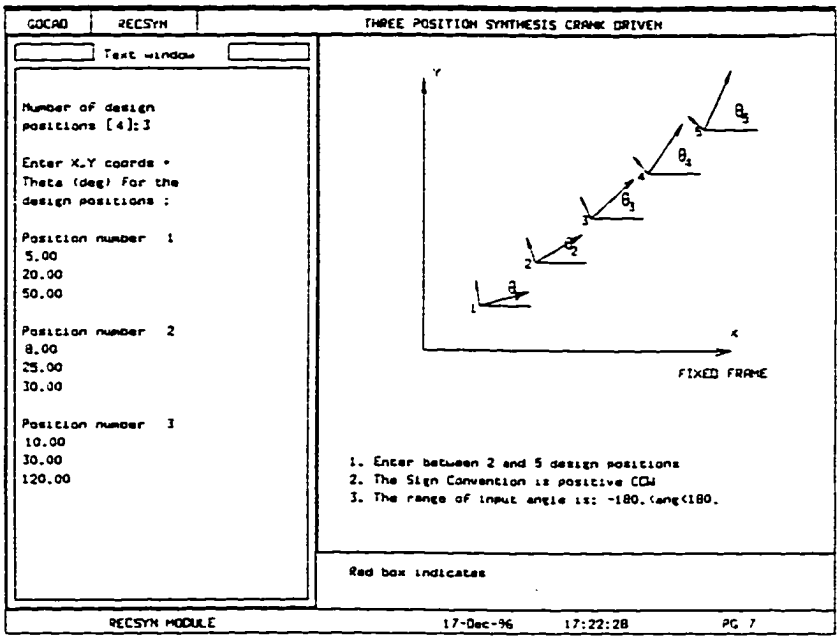

Figure 4.19 Three Position without Circuit Defect - Specification of Design Positions

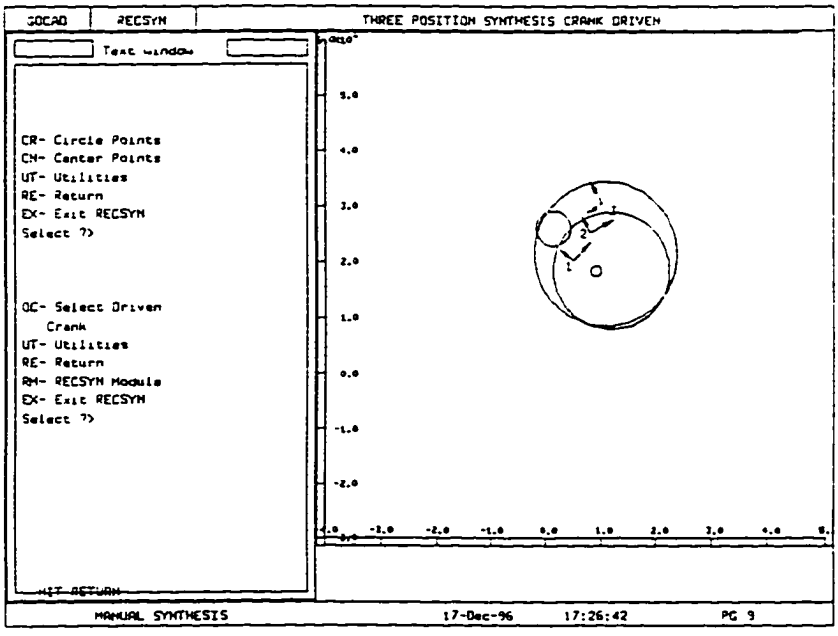

Figure 4.20 Three Position with Circuit Defect - Synthesis of Driven-Crank

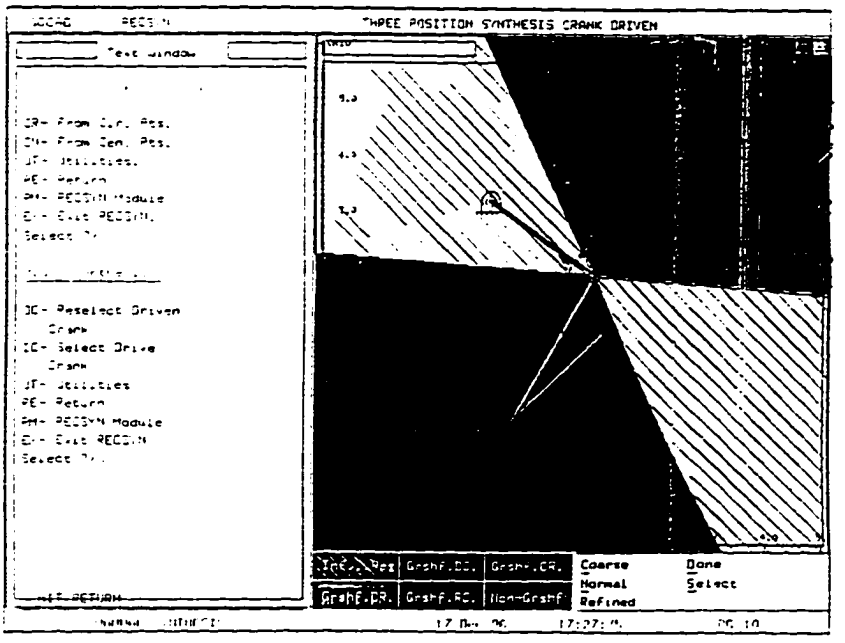

Figure 4.21 Three Position without Circuit Defect - Synthesis of Driving-Crank

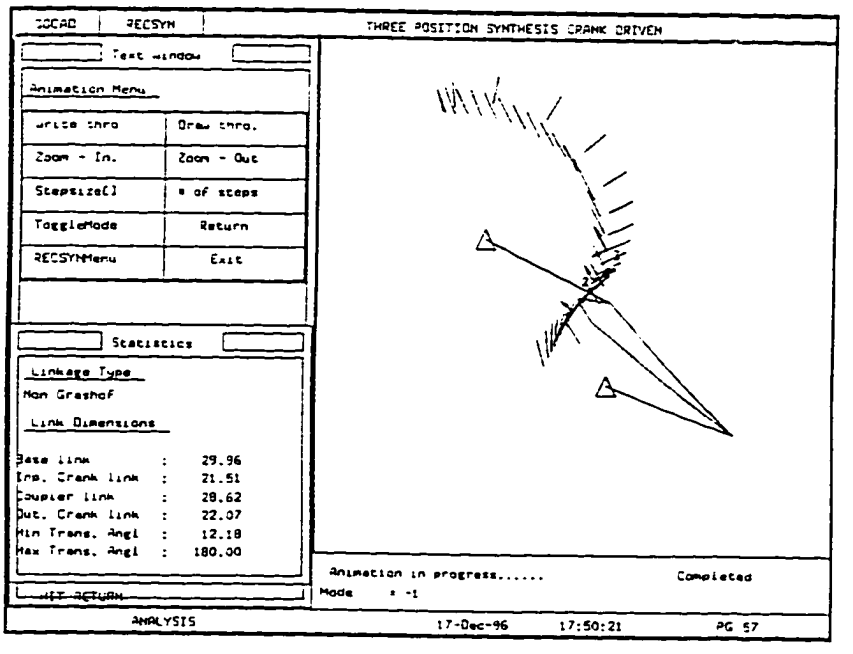

Figure 4.22 Three Position without Circuit Defect - Animation and Linkage Dimensions

4.4 Circuit Rectification for Four Positions

For the four design position motion generation, the solution is the circle-point and center-point Burmester curves. The special points discussed in Section 3.5 are applied to the circle point curve to eliminate segments of the curve with branch defects. These sections are functions of the design positions only. It is found that some portions on the center-point curve are guaranteed to change the sign of the range of the angle ϕ of the crank relative to the frame in at least one of the design positions. These sections that cause circuit defects for rocker-cranks and double-rockers can be identified with the aid of the poles and their corresponding special points as presented in the next subsection. It should be mentioned that these segments exist before any selection of center points made.

4.4.1 Special Points on Center-Point curve

As illustrated in Fig. 4.23, the Burmester center-point curve intersects the circle with diameter of pole pair $P_{ik}P_{jk}$ at the poles and three special points Z_{ij}, X_{ij} and Y_{ij}. These special points are the boundary of the segments for the change of the sign of ϕ_{ij}. The angle ϕ_{ij} is π at X_{ij} or Y_{ij} and is zero at Z_{ij} according to Fig. 4.13. Segments of the curve with the angle ϕ_{ij} greater than π are marked infeasible by the solid thick line, which means the existence of circuit defect if a center-point is selected from these sections for either a rocker-crank or a double-rocker four-bar. However, the identification of the feasible region becomes more confusing when all six poles are included. Therefore, it is easier to find the feasible region when dealing with the maximum range of motion of ϕ which must be less than π. Assume that the sequence of the positions is i j k l. Then the ranges of the angles of the crank relative to the base link are ϕ_{ij}, ϕ_{jk}, ϕ_{kl} and ϕ_{li}, which are bounded by $-\pi$ and π. If at least one of the range of ϕ's is of opposite direction, then the total range of rotation becomes less than π (Fig. 4.24a). If all the range of ϕ's are of the same sign, then the total range of rotation is greater than π (Fig. 4.24b).

These special points are used to implement the procedure algebraically. The order of rotation of the crank relative to the frame is bounded by the image poles in the circle-point planes. However, the Z's are the special points in the center-point plane corresponding to the image poles. Therefore the Z's bound segments of the curve on which the order of rotation of the crank relative to the frame is constant, i.e. a segment bounded by Z_{ij} Z_{ik} must have the sequence i k l j or i j l k. Figure 4.25 shows that ϕ_{ij} is π

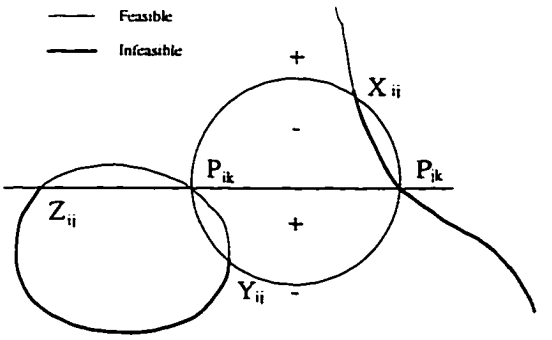

Figure 4.23 Feasible and Infeasible Sections on Center-Point Curve

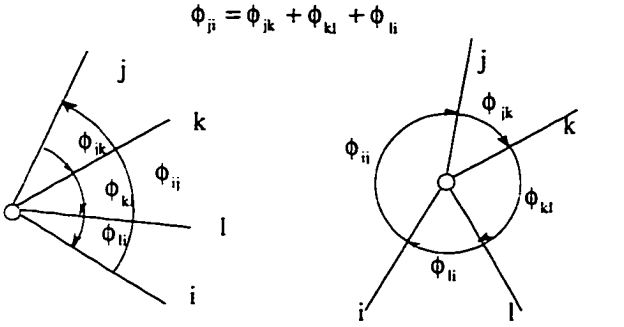

(a) Range Less Than π (b) Range Greater Than π

Figure 4.24 Rotational Range of the Crank Relative to the Base

at the special points X_{ij} or Y_{ij}. Thus, if positions i and j are adjacent in the order of crank rotation relative to the frame, X_{ij} or Y_{ij} marks the boundary of the feasible segment of the curve by a thinner line. On the other hand, if positions i and j are not adjacent, X_{ij} or Y_{ij} lie in the infeasible segment of the curve. The results are shown in Fig. 4.25.

4.4.2 Procedure of Circuit Rectification for Four Positions

The complete circuit rectification procedure for four position motion generation can be summarized as the following. The special points Q, T, and U are located on the Burmester circle-point to eliminate segments of the curve with branch defects. The circle point is selected in the feasible segment and the center-point is calculated to form the driven dyad. Filemon construction is then applied to the driven circle point and segments of the

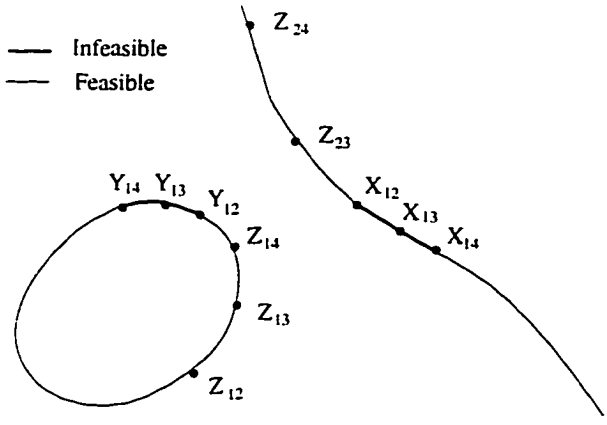

Figure 4.25 Circuit Identification in the Center-Point Burmester Curve

circle-point curve that fall in the infeasible section of the Filemon lines are marked infeasible for the selection of the driving circle point. The results are mapped into the center-point curve. In addition, section of the curves with order problem are eliminated with the aid of the image poles. Of the remaining feasible solutions, the curves are marked for the different types of Grashof linkages. In order to eliminate circuit defects in double-rocker and rocker-crank segments, the special points Z, X, and Y are applied to the center point curve, where Z corresponds to the image poles. This is illustrated in Fig. 4.26. The Z points bound the segments of the curve on which the order of rotation of the crank relative to the frame is constant. For instance, $Z_{12}Z_{13}$ must have a sequence 1 3 4 2 or 1 2 4 3. This concept is applied to the remaining segments of the curve to find the different sequences possible. The X and Y points mark the segments of the curve with invariant sign of the range of angle ϕ. If the subscripts of X or Y are adjacent in the order of rotation of the crank relative to the frame, than X or Y marks the boundary of the segments. The subscripts of the X or Y that are not adjacent mark the segment with a change of sign of the angular range and the neighboring segments have an invariant sign. In the example shown in Fig. 13, the segment of the curve between Z_{12} and Z_{13} has sequence 1 2 4 3. The segment between Z_{13} and Z_{23} has sequence 1 3 2 4, and the segment between $Z_{23}Z_{12}$ has sequence 1 2 3 4. Similarly, the segments between $Z_{14}Z_{24}$, $Z_{24}Z_{34}$, and $Z_{34}Z_{14}$ are 1 3 2 4, 1 2 4 3 , and 1 2 3 4, respectively. Since the X points fall in the sequence 1 2 3 4, X_{34} and X_{14} mark the boundary of the segments. The segment, where X_{24} is located, does not have the subscripts adjacent and is marked to have a change of sign of the range of angle ϕ

by a solid thick line. The remaining two segments are marked to have the sign of the angle of the crank relative to the frame invariant at the four precision points. Similarly, the Y points determine the segments of the second branch of the curve with invariant signs of the range of angle ϕ.

Since the angle of the driving crank relative to the frame is prohibited to change signs for the double-rocker and rocker-crank linkages, common segments of the curve marked double-rocker or rocker-crank and are in the solid thick segments (Fig. 4.26) have circuit defects and are marked infeasible for the selection of the center point driving dyad.

For the remaining feasible double-rocker and rocker-crank segments, a random point is selected to find its corresponding circle point that forms the driving dyad. Eqs. (4.1) and (4.2) are applied to the center-point to find the infeasible regions of the line construction as shown in Fig. 4.3. The segment is marked infeasible when the circle point of the driving dyad falls in the infeasible section of the line construction. Thus, the Burmester curves are rectified for the circuit, branch, and order defects for the selection of the driving dyad. The center-point and its corresponding circle-point are selected from the feasible segments of the curve to form the four-bar linkage. This whole procedure is

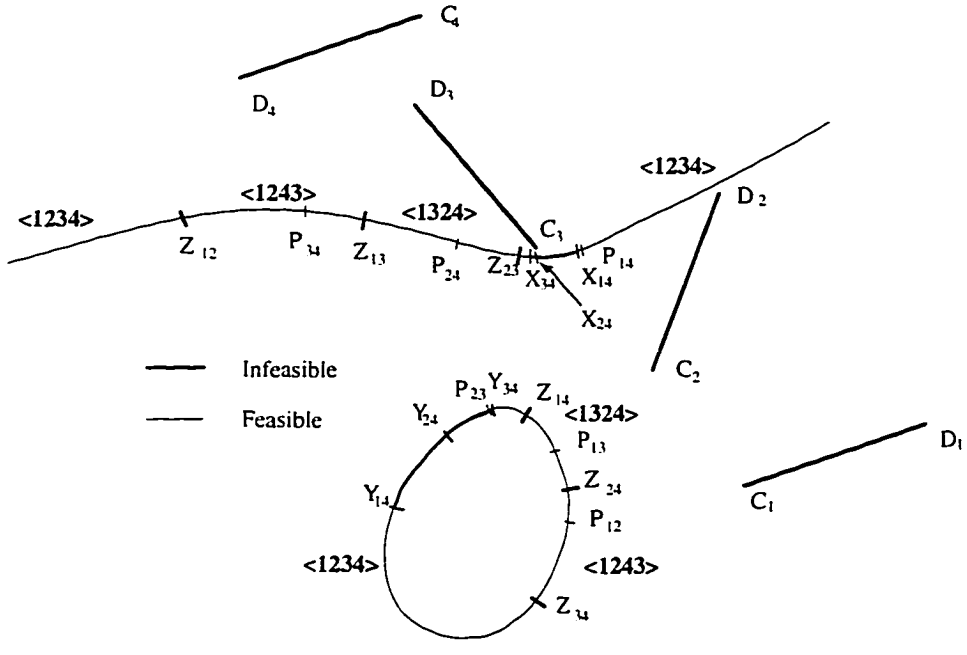

Figure 4.26 Feasible and Infeasible Segments of Driving Center-Point for Rocker-Cranks and Double-Rockers

programmed into RECSYN to eliminate circuit defects in four-bar linkages for four position motion generation with both manual and automatic synthesis.

4.4.3 Examples with RECSYN

In order to illustrate the circuit rectification for four design positions, two examples of synthesis are provided in the subsection. The manual mode is applied in both examples.

First, Figs. 4.27 to 4.30 show an example of four position synthesis with circuit defect. In Fig 4.28, the circle-point of the driven dyad is selected from the feasible region where the branch defect does not occur and the corresponding center-point is obtained. Then the Filemon construction is applied and the Burmester curves are sectioned into the different types and classes of four-bars. The regions with an order defect are then eliminated. The driving circle-point is selected from the feasible double-rocker section, and its corresponding center-point is obtained to form the four-bar linkage (Fig. 4.29). But as shown in Fig. 4.30, this linkage does not pass through the fourth position when animated because of the existence of a circuit defect.

In the other example given in Figs. 4.31 to 4.34, the same design positions are used in the new version of RECSYN where the procedure for the elimination of the circuit defect using aforedescribed method is included. The solution for the driven dyad is the same as the previous one as showed in Fig 4.32. In Fig 4.33, the Filemon construction is applied, and the Burmester curves are sectioned into the different types and classes of four-bars, and the sections with order defects are eliminated. However, the sections of double-rocker and rocker-crank indicated in Fig. 4.29 of the previous example are examined to have circuit defects and marked infeasible. Finally, the circle-point of the driving dyad is selected from the feasible regions which is close to the previous selection, and its corresponding center-point is obtained to form the four-bar linkage. The result is shown in Fig. 4.34 where the synthesized four-bar is animated to go through all the design position.

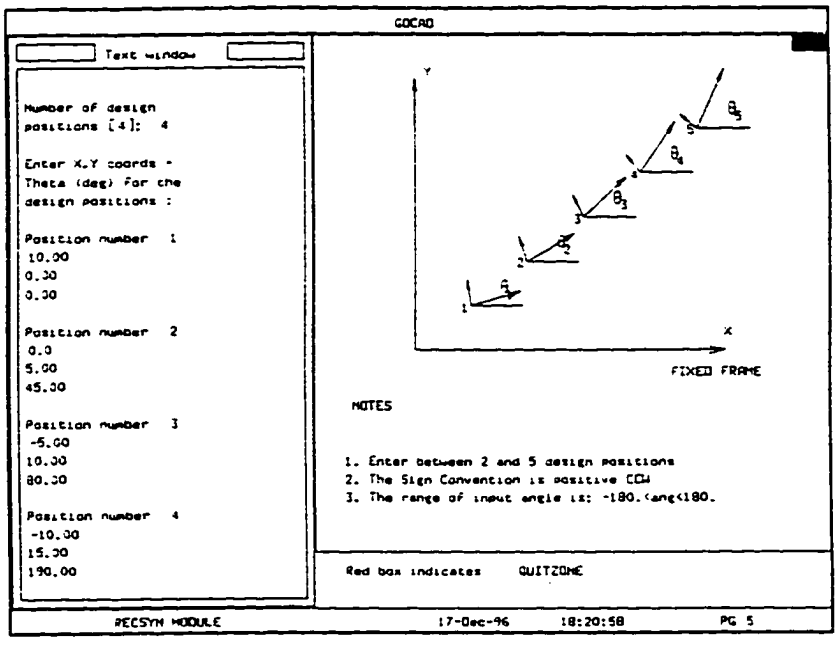

Figure 4.27 Four Position with Circuit Defect - Specification of Design Positions

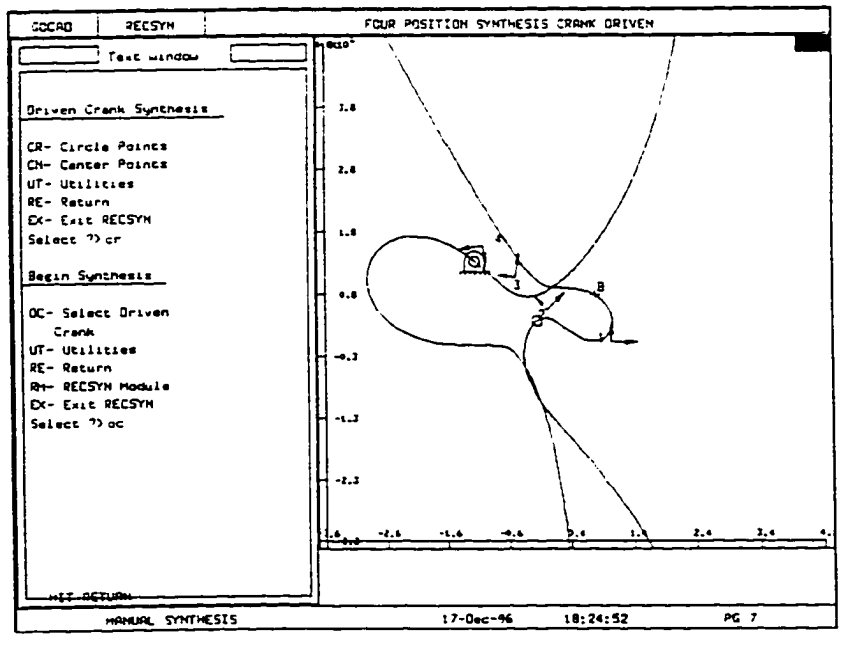

Figure 4.28 Four Position with Circuit Defect - Synthesis of Driven-Crank

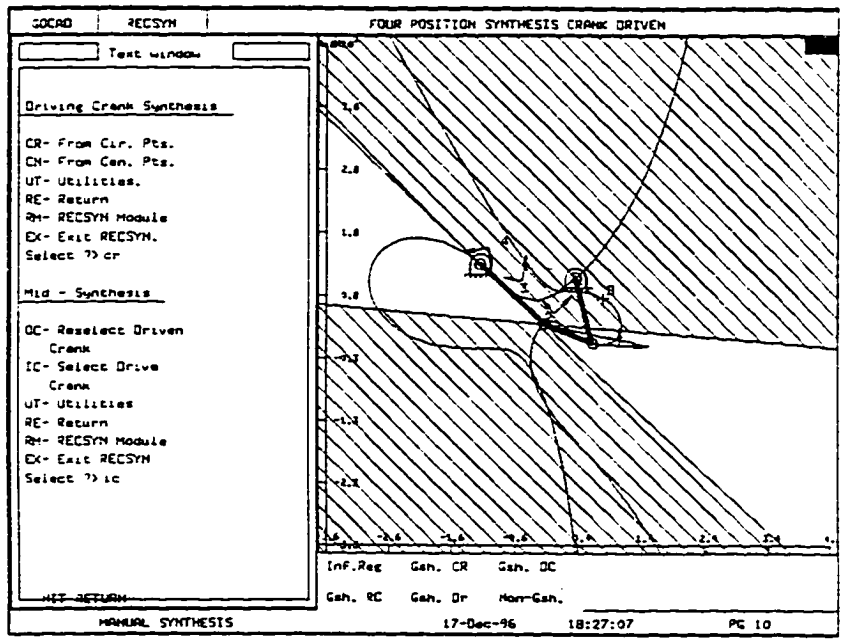

Figure 4.29 Four Position with Circuit Defect - Synthesis of Driving-Crank

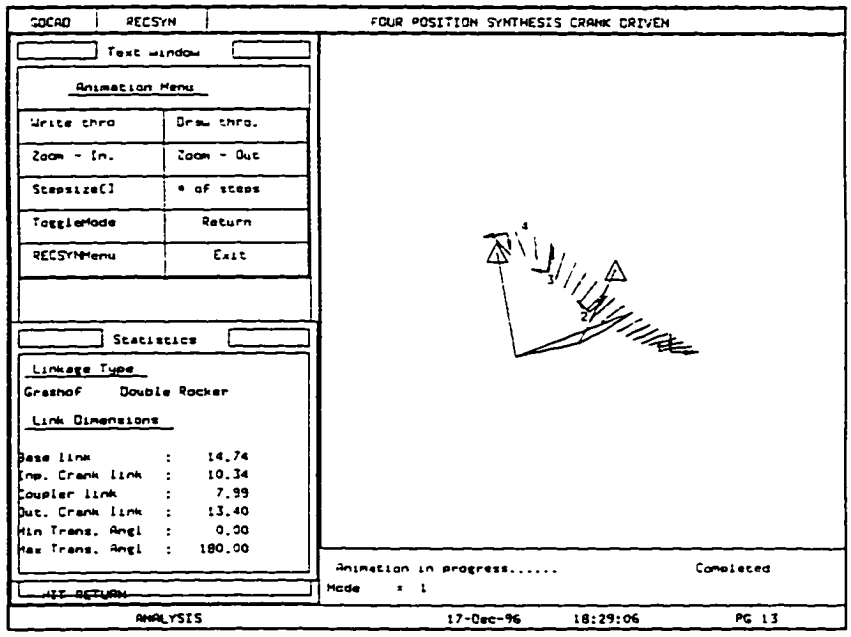

Figure 4.30 Four Position with Circuit Defect - Animation and Linkage Dimensions

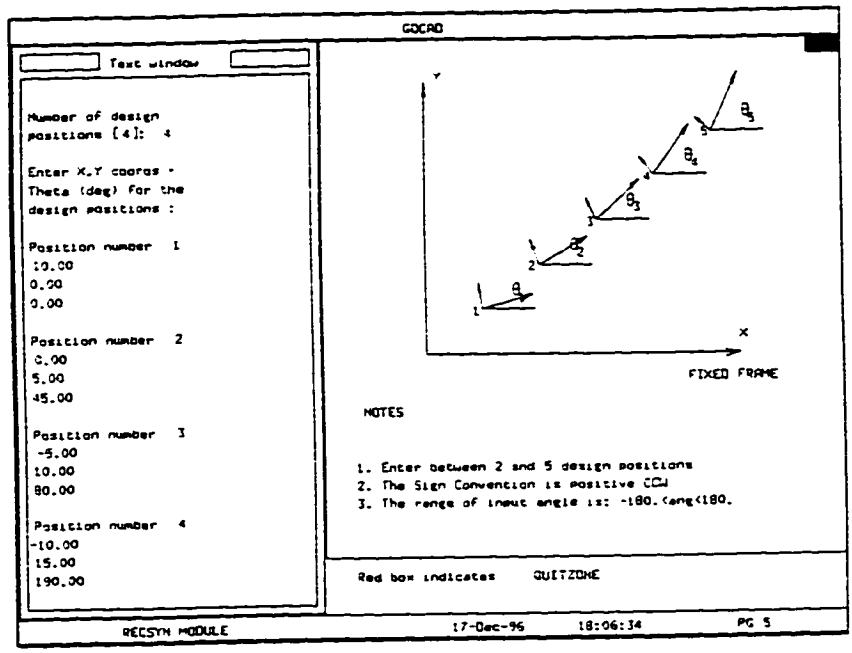

Figure 4.31 Four Position without Circuit Defect - Specification of Design Positions

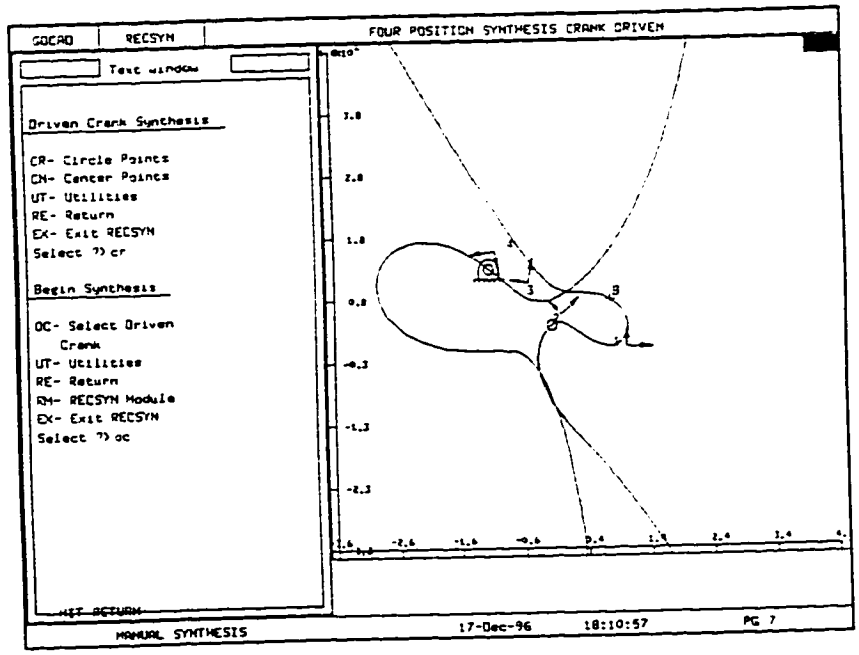

Figure 4.32 Four Position without Circuit Defect - Synthesis of Driven-Crank

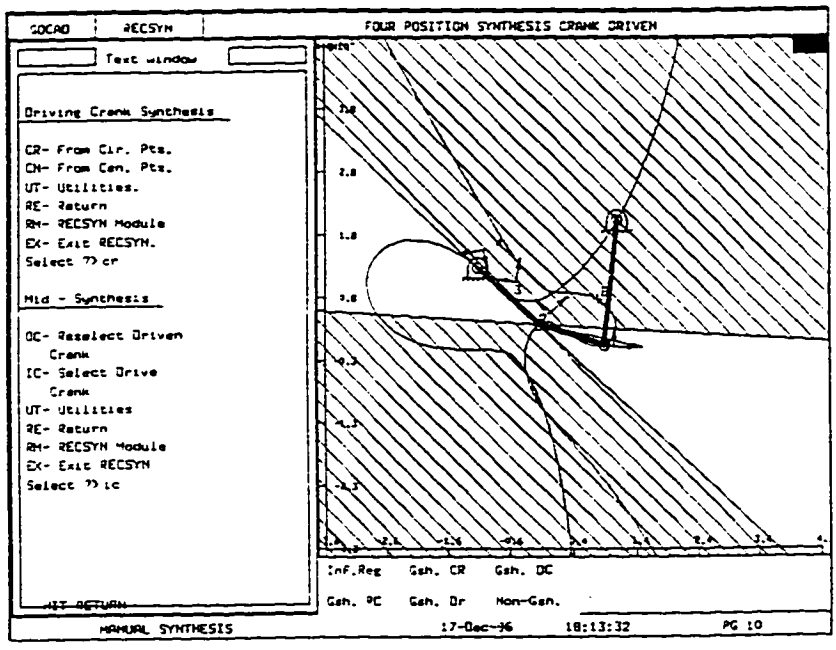

Figure 4.33 Four Position without Circuit Defect - Synthesis of Driving-Crank

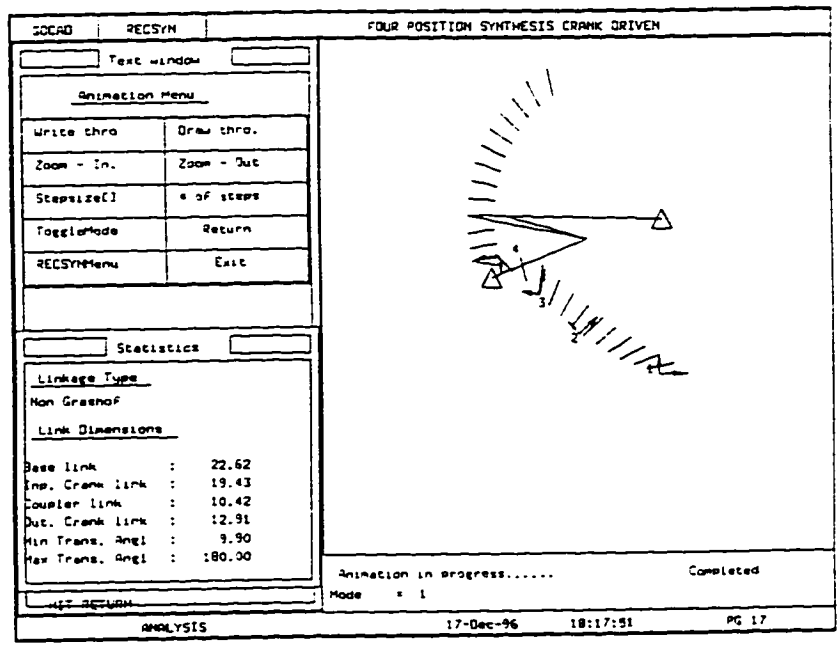

Figure 4.34 Four Position without Circuit Defect - Animation and Linkage Dimensions

CHAPTER V

RECTIFIED SYNTHESIS OF COUPLER-DRIVEN WATT I SIX-BAR LINKAGES

This chapter presents a complete procedure of the rectified synthesis of the Watt I six-bar linkage to pass through the pre-defined four design positions with the coupler being the driver. This is done by de-coupling the six-bar mechanism as a combination of a coupler-driven and crank-driven four-bar linkages with common links. The vector component mechanism modeling method is applied to these linkages where the dyad and triad synthesis approaches are adopted in conjunction with the algebraic method to find the solutions. The linkage with the coupler-driver is initially synthesized and rectified, then followed by the crank-driven four-bar linkage. The six-bar linkage is thus insured to assemble free of circuit, branch, and order defects. Section 5.1 reviews the rectified synthesis theory of coupler-driven four-bar which will be used in the subsequent sections. Triad synthesis theory is briefly introduced in Section 5.2. Section 5.3 discussed the transmission angles and vector representation for coupler-driven Watt I six-bar linkage. The rectified synthesis procedure of coupler-driven Watt I for four positions is developed in Section 5.4. Section 5.5 discusses the automatic synthesis that includes design variables, objective function, constraints, and optimization strategy. Finally, actual examples to design a coupler-driven Watt I using RECSYN is provided in Section 5.6.

5.1 Rectified Synthesis of Coupler Driven Four-Bar Linkages

The synthesis of a coupler-driven four-bar linkage for motion generation can not be done by directly using the theory for crank-driven four-bar because the rectification procedure varies based on the choice of input. This was solved by Bawab et al. (1992) who utilized the Robert's-Chebyshev theorem to transfer the problem from coupler-driven to crank-driven, then applied the traditional four-bar rectified synthesis theory. The major difference is that the transmission angle of a coupler-driven four-bar is different from that of a crank-driven four-bar as described in next subsection.

5.1.1 Transmission Angle

The transmission angle of a coupler-driven four-bar linkage can be determined through the mechanical advantage as given by Eq. 3.1. Fig. 5.2 shows a coupler-driven four-bar where coupler link c is the driver and link o is the output link. Assuming that the input and the output links are loaded by pure torque and there are no losses in the mechanism, the mechanical advantage MA can be represented as:

$$MA = \frac{\omega_c}{\omega_o} = \frac{\overline{I_{ro}I_{co}}}{\overline{I_{rc}I_{co}}} \tag{5.1}$$

where ω_c is the angular velocity of the coupler link, and ω_o is the angular velocity of the output link. I_{rc}, I_{ro}, and I_{co} are the instant centers between the ground link r and the input link c, the ground link r and the output link o, and the input link c and the output link o, respectively, as shown in Fig. 3.1. Toggle positions occur when the mechanical advantage becomes zero. For the toggle condition,

$$\overline{I_{ro}I_{co}} = 0 \quad \text{or} \quad \overline{I_{rc}I_{co}} = \infty \tag{5.2}$$

However, $\overline{I_{ro}I_{co}}$ is the length of the output link o and has a fixed dimension different from zero. On the other hand, $\overline{I_{rc}I_{co}}$ can become infinity when link i and link o become parallel. Therefore toggle position occurs when link i and link o are parallel, and the transmission angle (TA) is the angle $\overline{I_{ro}\, I_{rc}\, I_{ri}}$. The result is the same when link i is treated as the output link, and link o is taken as the intermediate link.

5.1.2 Branch and Circuit Defects

As defined in the literature, a branch defect occurs when the transmission angle changes sign when it passes through the design position. Therefore, the branch defects in coupler-driven four-bars occur when the two cranks become parallel. In order to avoid branch defect, the transmission angle formed between link i and o, i.e. angle $I_{ro}\, I_{rc}\, I_{ri}$, must keep the same sign. However, it is not possible to rectify the transmission angle sign because the position of the instant center I_{rc} is formed once the 2 dyads are obtained and therefore the theory is utilized as a verification to the validity of the angle rather than as a rectification.

This difficulty can recur to the properties of Robert's linkage (Fig. 5.2) as described in Bawab et al. (1992). Robert's-Chebyshev Theorem states that three different planar linkages can trace identical coupler curve. These three linkages are referred to as

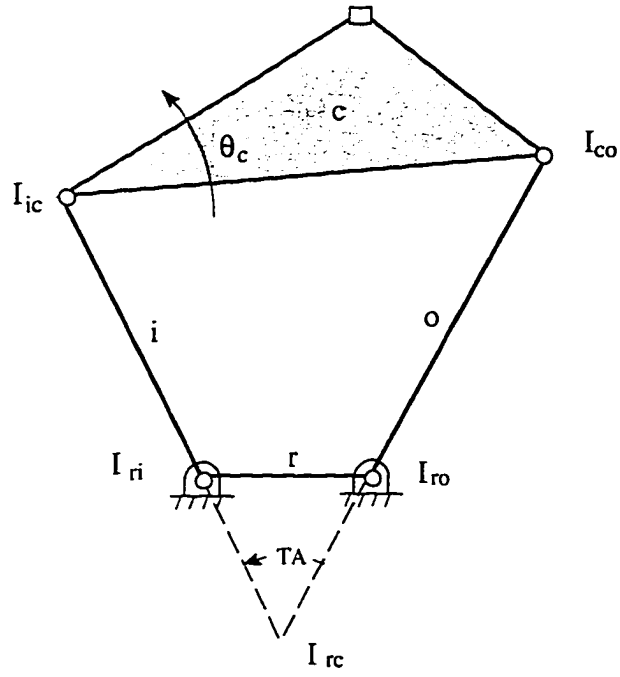

Figure 5.1 Transmission Angle of a Coupler Driven Four-bar

coupler curve cognate linkages. Robert's linkage is formed as a whole of these three cognate linkages.

In Fig. 5.2, three four-bar linkage cognates are formed such that their couplers could be pinned at the coupler point P, where triangles A*OB*, GFP, APB, PED, GOD, MFB and AEQ are similar, and the quadrilaterals A*APG, B*BPD, and OFPE are parallelograms. The three couplers do move at different speeds as the linkages move; however, their rotation angles are related to the link lengths and is detailed in Bawab et al. (1992).

For the coupler-driven four-bar linkage A*ABB*, $P(p_x, p_y, \theta)_i$, is the i^{th} design position. Since link ABP is the driver, the corresponding transmission angle (TA_i) ψ_i formed between the links r_2 and r_4 can be expressed by Eq. 5.3 (Bawab et al., 1992).

$$TA_i = \psi_i = \lambda_i - \alpha_i \tag{5.3}$$

where λ_i and α_i are the angles made by links $\overline{A^*A}$ and $\overline{B^*B}$ with respect to the X axis, respectively. It can be noted that the left cognate linkage A*GFO of coupler-driven linkage A*ABB* is crank-driven with $\overline{A^*G}$ as the driver and $P(p_x, p_y, \lambda)_i$, as the i^{th}

design position (Bawab et al., 1992). The angular displacement of link $\overline{A^*G}$ in linkage A*GFO is the same as the angular displacement of link $\overline{AB}$ (or $\overline{AP}$) of linkage A*ABB*. Also the angular displacement of links $\overline{FG}$ and $\overline{OG}$ of the cognate linkage are, respectively, equal to the angular displacement of links $\overline{A^*A}$ and $\overline{B^*B}$ of linkage A*ABB*. The transmission angle of the cognate linkage A*GFO is the angle formed between the output link $\overline{OF}$ and the coupler link $\overline{FG}$. Therefore, the angular displacement of the coupler-driven linkage A*ABB* from position i to 1 is the same as that of crank-driven cognate linkage A*GFO. Hence, the branch defect of the coupler-driven linkage A*ABB* can be inclusively rectified through crank-driven cognate linkage A*GFO.

The circuit defect in four-bar linkages occurs when a linkage cannot pass through the design positions unless it is resembled in a different configuration. In the synthesis of

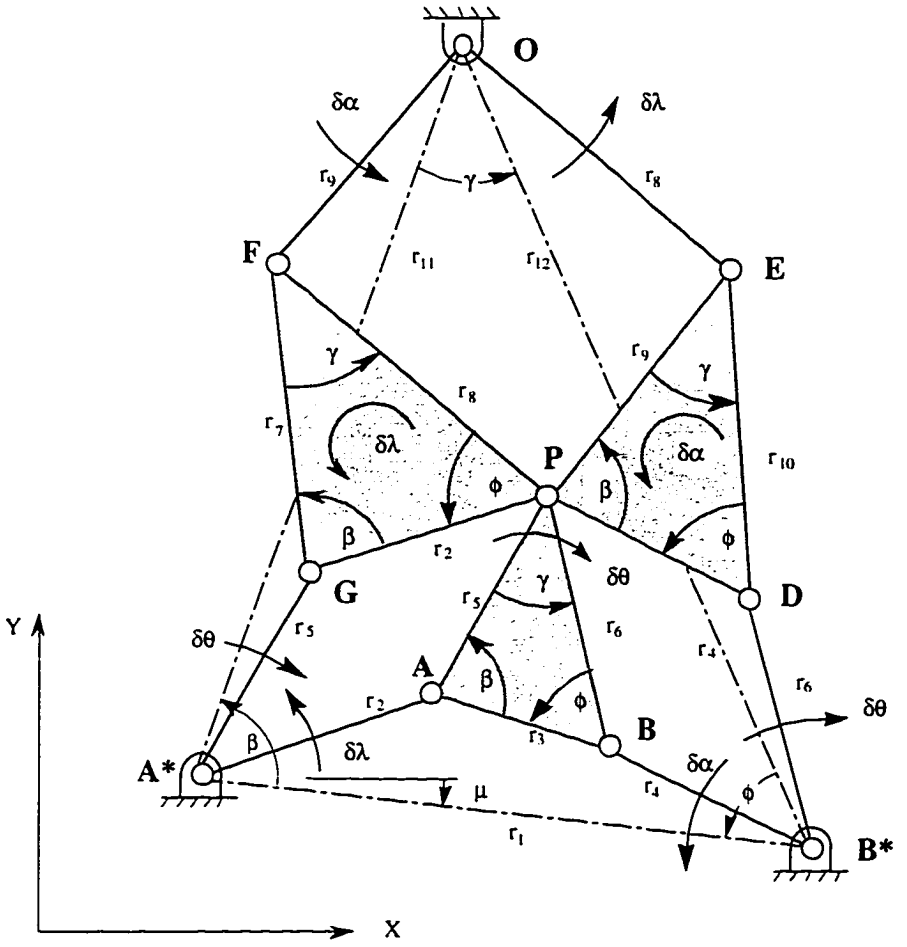

Figure 5.2 Robert's Cognate Linkage (Bawab, 1992)

coupler-driven four-bars, both circuit and branch defects are incorporated in the synthesis procedure. Referring to Fig 5.2, a coupler-driven four-bar linkage A*ABB* is converted to a crank-driven four-bar linkage A*GFO with the link $\overline{A^*G}$ being the input link. Thus, a coupler-driven crank-rocker is converted into a crank-driven double-rocker where the circuit defect is different from the branch defect, and the two types of defects are to be examined separately. A coupler-driven rocker-crank is converted to a crank-driven rocker-crank where the circuit defect and the branch defect are not the same and the two are examined separately. A coupler-driven Grashof double-rocker is converted into a crank-driven crank-rocker and coupler-driven double-crank is converted into a crank-driven double-crank, where the circuit-defect is the same as the branch-defect and the elimination of the branch defect would suffice. Finally, a coupler-driven non-Grashof four-bar linkage has only one-circuit and hence it is sufficient to eliminate the branch defect.

In summary, the coupler-driven four-bar linkage A*ABB* can be transformed into crank-driven four-bar linkage A*GFO by using Robert's linkage. A similar procedure can be repeated to form linkage B*DEO.

5.1.3 Coupler-Driven Four-Bar Synthesis

The synthesis procedure can be used for either the circle-point plane or the center-point plane in either manual or automatic mode. In the manual mode, the user needs to know more theory on the rectified synthesis and the sequence in which it must be applied compared to the automatic mode which is based on the optimization theory. The rectification procedure eliminates the circuit, the branch, and the order defects.

In the manual synthesis, the algebraic approach developed in Section 3.5 for determining dyads that assemble at the four design positions is applied to dyad PAA* of the coupler-driven four-bar of Fig. 5.2 where $P(P_X,P_Y, \theta)_i$ for i = 1 to 4 are the four design positions. The solution is a Burmester circle-point curve defined by Eq. 3.16, and the corresponding Burmester center-point curve is computed by Eq. 3.26.

Dyad PAA* in Fig. 5.3 is synthesized first. At this stage, the solution of point A and point A* is the whole circle-point and center-point curves. Hence, a circle-point can be selected anywhere on the curve and its corresponding center-point is computed to form dyad PAA*. However, the second dyad PBB* must be selected to form the coupler-driven four-bar A*ABB* without circuit and branch defects. Therefore, the curve must be rectified for the selection of the second dyad (dyad PBB*) to eliminate regions with defects. This can be achieved by using Robert's-Chebyshev Theorem.

When proceeding from the circle-point plane, with dyad PAA* already defined, Circle-point G of the left cognate linkage in Fig. 5.2 is obtained by applying Eq. (6) of

Bawab et al. (1992) at the four design positions. The angular positions of the rigid body PGF for crank-driven four-bar A*GFO can be determined since the coordinates of the two points G and P on it are known. The angular displacement λ_i can be calculated for i = 1 to 4 by applying Eq. (4) of Bawab et al. (1992).

Knowing the design positions $P(P_X, P_Y, \lambda)_i$ of the crank-driven cognate linkage, the circle-point and center-point Burmester curves are computed and rectified for branching by applying the method discussed in Chapter 3 and for circuit using the procedure provided in Section 4.4 with special points. However, it should be noted that the synthesis of the crank-driven four-bar A*GFO differs from the traditional one since the driving dyad PGA* is already defined. In order to rectify the Burmester curves for the coupler-driven four-bar with design positions $P(P_X, P_Y, \theta)_i$, i = 1 to 4 , the feasible curves for crank-driven four-bar have to be scanned.

To start the scanning, a driven circle-point is picked up from the far end of the feasible sections, and the corresponding center-point is computed. The Filemon construction is applied to this driven dyad. The circle point is marked feasible when the driving circle-point G falls in the feasible area of the Filemon lines, otherwise, it is marked as infeasible. Also, the type or class of this four-bar is identified. After scanning all the remaining sections, the segments of the curve of double-rocker and rocker-crank are further checked for circuit defect using line construction to one out of each segment, and

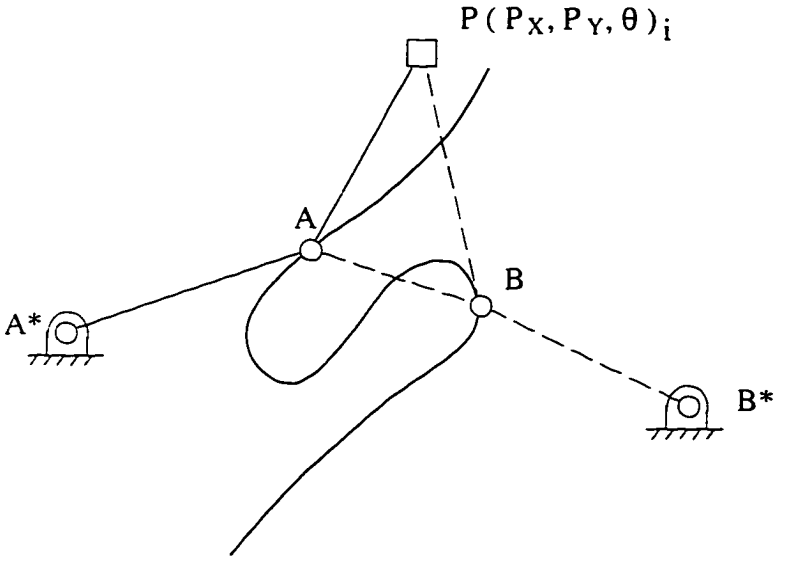

Figure 5.3 Scan of Circle-Point B along the Circle-Point Curve

eliminated when circuit defects are identified. These final segments of the circle-point curve and their corresponding center-point curve are free of circuit and branch defects.

The feasible rectified segments (of the driven dyad PFO) of the crank-driven four-bar are inverted into its cognate coupler-driven four-bar by applying Eqs. (1) and (3), and the proper transformation of the Grashof type is obtained according table 1 provided in Bawab et al. (1992). Note that the order defect was not considered in the process since the four-bar linkage to be rectified is driven by the coupler (rigid body) which passes through the design positions in the proper order by definition. Therefore, the user has the option of selecting the circle-point B and its corresponding center-point B* from the feasible segments of the curves where the Grashof types are labeled. This completes the manual synthesis.

The rectified synthesis of coupler-driven four-bar linkages can be performed automatically. Given the design positions $P(P_X,P_Y, \theta)_i$ of the coupler-driven four-bar linkage, the circle-point and center-point Burmester curves are computed using Eqs. (3.16) and (3.26). A double scan is applied to the circle-point curve. Initially, a scan is applied for the selection of circle-point A. For each selected point A, the corresponding center-point A* is computed and a scan for the selection of the circle-point B is proceeded. For each selected point B, the corresponding center-point B* is computed and the coupler-driven four-bar linkage is formed. The crank-driven cognate linkage A*GFO is found, then the objective function represented by Eq. (3.28) is computed for the cognate linkage[6] Linkages are then sorted in the ascending order of the objective function. The best nine coupler-driven linkages can be further optimized using the Davidon-Fletcher-Powel (DFP) method with penalty function approach (Eq. (3.27)). The one dimensional search is the Golden-Section method. The constraints are defined by Eqs. (3.29 to 3.33).

5.2 Triad Synthesis

A triad is represented by a chain of three links connected together. This is shown in Fig. 5.4. $P(p_X, p_Y)$ is the tracer precision point and θ is the angle of the tracer link relative to the X axis. $Q(q_X, q_Y)$ is the reference precision point and γ is the angle of the base link with respect to X axis. An algebraic method similar to that applied to the dyads is represented for the triads. It is developed by implementing the concept of triad synthesis by inversion (Chase, 1984) along with the algebraic method. The triad synthesis by inversion reduces a three link triad synthesis to a two link dyad synthesis. The result is

[6] The coupler-driven four-bar linkage and its cognate crank-driven four-bar linkage have the same objective function.

two Burmester circle-point and center-point curves on which point A and point A* fall, respectively. This is illustrated in Fig. 5.5.

The process of synthesizing a triad (Fig. 5.5) consists of viewing the motion of the intermediate link $\vec{W}$ and the tracer link $\vec{Z}$ with respect to the reference point Q and the angle γ of the base link at the four precision positions of the fixed reference. These precision points have known values and are described with respect to the fixed coordinate system X-Y. According to Fig. 5.6, the position of the reference point Q is prescribed as vector $\vec{R}_{Q_i}$, and vector $\vec{R}_{P_i}$ is denoted to the position of the tracer point P. The calculation is done with respect to the first position. Therefore, the solution depends on the range[7] of γ_i ($\delta\gamma_i$) and θ_i ($\delta\theta_i$) with respect to the first position γ_1 and θ_1, respectively, and not the actual angles γ_i and θ_i for i = 1 to 4. The relative axes X'-Y' are attached to the reference point Q such that the X' axis is parallel to X axis at precision position 1. Thus, the design position P is prescribed with respect to the relative reference X'-Y' as

$$\vec{R}'''_{P_i} = \vec{R}_{P_i} - \vec{R}_{Q_i} \qquad \text{for i = 1 to 4} \tag{5.4}$$

According to Eq. (5.4), the design position[8] P_i is prescribed with respect to the reference $(X'\text{-}Y')_i$ which is rotated by an angle $(\gamma_i - \gamma_1)$. This design position can be represented with respect to $(X', Y')_1$, by rotating $\vec{R}'''_i$ with an angle $-(\gamma_i - \gamma_1)$. Therefore the coordinates of the design positions with respect to the reference point and the base link angle at position 1 are

$$\vec{R}''_i = \left(\vec{R}_{P_i} - \vec{R}_{Q_i}\right) e^{-j(\gamma_i - \gamma_1)}$$

or

$$p''_{X_i} = \left(p_{X_i} - q_{X_i}\right)\cos(\gamma_i - \gamma_1) + \left(p_{Y_i} - q_{Y_i}\right)\sin(\gamma_i - \gamma_1)$$

$$p''_{Y_i} = -\left(p_{X_i} - q_{X_i}\right)\sin(\gamma_i - \gamma_1) + \left(p_{Y_i} - q_{Y_i}\right)\cos(\gamma_i - \gamma_1)$$

$$\text{i = 1 to 4} \tag{5.5}$$

---

[7] $\delta\gamma_i = \gamma_i - \gamma_1$ for i = 1 to 4

[8] The design position P is formed of the precision point (p_x, p_y) and the angle of the tracer link θ.

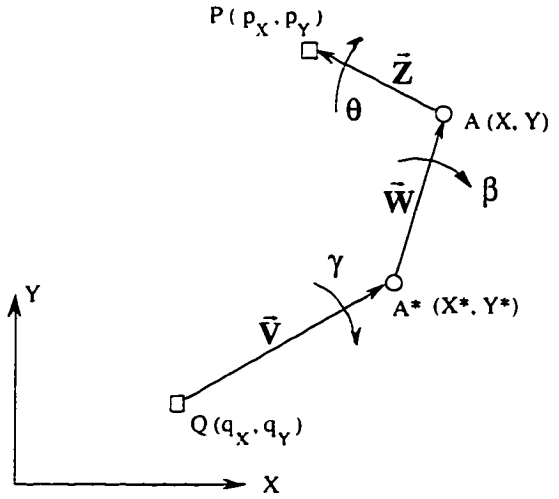

Figure 5.4 Triad Representation

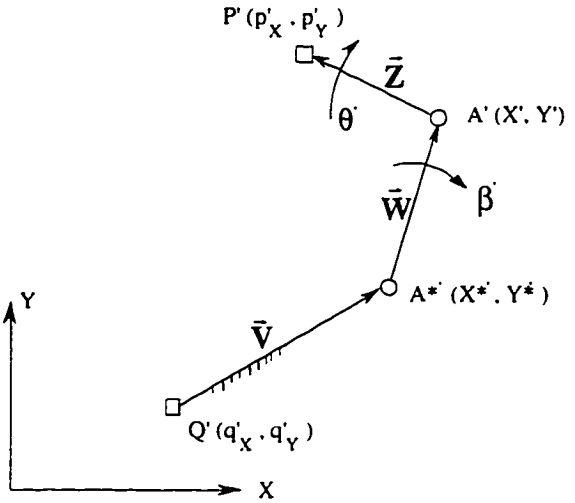

Figure 5.5 Triad Synthesis by Inversion

The design positions can be written with respect to the fixed reference at the first precision positions by translating Eq. (5.5) with $\vec{R}_{Q_1}$ to give:

$$p'_{X_i} = \left(p_{X_i} - q_{X_i}\right)\cos(\gamma_i - \gamma_1) + \left(p_{Y_i} - q_{Y_i}\right)\sin(\gamma_i - \gamma_1) + q_{X_1}$$

$$p'_{Y_i} = -\left(p_{X_i} - q_{X_i}\right)\sin(\gamma_i - \gamma_1) + \left(p_{Y_i} - q_{Y_i}\right)\cos(\gamma_i - \gamma_1) + q_{Y_1}$$

$$i = 1 \text{ to } 4 \qquad (5.6)$$

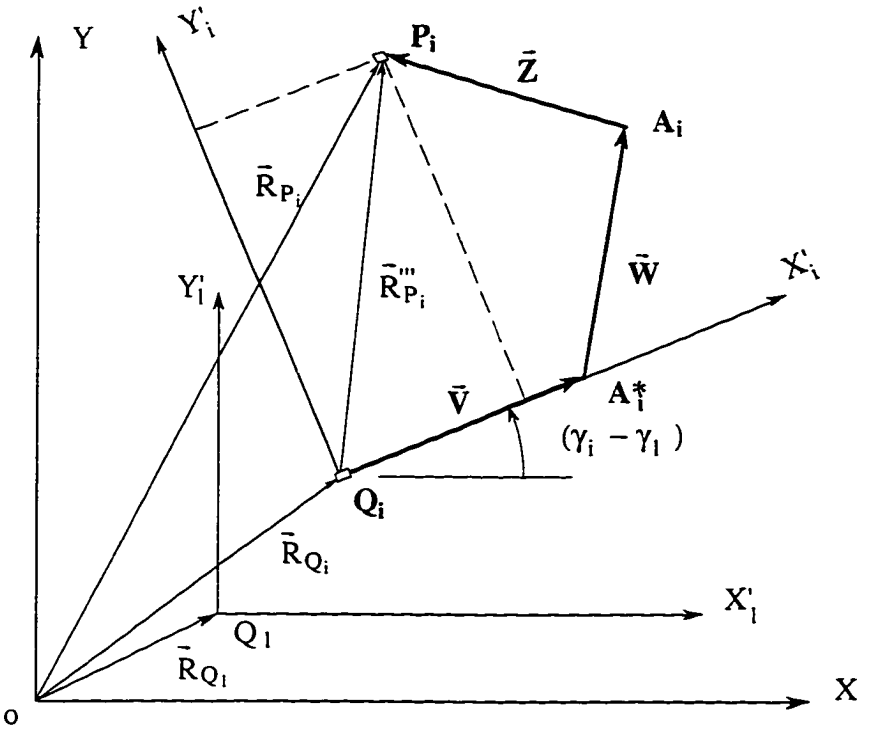

Figure 5.6 Design positions of triad synthesis by inversion

The angle of the tracer link (design position angle) can be written with respect to the X'-Y' reference as:

$$\theta'_i = \theta_i - \gamma_i \qquad \text{for} \quad i = 1 \text{ to } 4 \tag{5.7}$$

Equations (5.6) and (5.7) can be used to obtain the design positions of any triad with respect to its reference point and base link angle at position 1.

5.3 Transmission Angles and Vector Representation

The elimination of branch defects depends on identifying the transmission angles and keeping their signs invariant. The transmission angles of six-bar linkages can be determined by applying mechanical advantage equation; however, the expression of mechanical advantage becomes more complex since intermediate links exist between the input and output links. The mechanical advantage is presented by Eq. (5.8) for the coupler-driven (link 3) Watt I with link 4 being the output shown in Fig. 5.7.

$$MA = \frac{\omega_3}{\omega_4} = \frac{\omega_3}{\omega_6}\frac{\omega_6}{\omega_5}\frac{\omega_5}{\omega_4} = \frac{\overline{I_{16}I_{36}}}{\overline{I_{13}I_{36}}}\frac{\overline{I_{15}I_{56}}}{\overline{I_{16}I_{56}}}\frac{\overline{I_{14}I_{45}}}{\overline{I_{15}I_{45}}} = \frac{\overline{I_{14}I_{34}}}{\overline{I_{13}I_{34}}} \tag{5.8}$$

Toggle positions occur when

$$\overline{I_{16}I_{36}}\ \overline{I_{15}I_{56}}\ \overline{I_{14}I_{45}} = 0 \qquad \text{or}$$
$$\overline{I_{13}I_{36}}\ \overline{I_{16}I_{56}}\ \overline{I_{15}I_{45}} = \infty \tag{5.9}$$

The length $\overline{I_{15}\ I_{56}}$ or $\overline{I_{14}\ I_{45}}$ does not become zero unless length of link 5 or 4 is zero. This is impossible due to geometrical restrictions. $\overline{I_{16}\ I_{36}}$ can be equal to zero when the instant centers $I_{36}I_{56}I_{45}$ are aligned. Either $\overline{I_{15}\ I_{45}}$ or $\overline{I_{16}\ I_{56}}$ can not be infinite unless a specific configuration is given. $\overline{I_{13}\ I_{36}}$ can become infinite when link 2 and 4 are parallel. Therefore the transmission angles are defined as the angles $I_{14}I_{13}I_{12}$ and $I_{36}I_{56}I_{45}$ represented by ψ_1 and ψ_2, respectively. This is shown in Fig. 5.7.

Six-bar linkages can be represented by various combinations of vector chains, i.e. dyads, and triads, as long as the representations are self-efficient. The coupler-driven Watt I six-bar linkage shown in Fig. 5.7 is decomposed into a dyad ($\bar{W}_2$, $\bar{Z}_2$) and two triads, triad 1 ($\bar{V}_1$, $\bar{W}_1$, $\bar{Z}_1$) and triad 3 ($\bar{V}_3$, $\bar{W}_3$, $\bar{Z}_3$) in such a way that the transmission angles can be rectified[9]. The result is shown in Fig. 5.8.

5.4 Rectified Synthesis of Coupler Driven Watt I

The procedure of coupler-driven Watt I six-bar linkage rectified synthesis relies on the well established synthesis techniques for four bar linkages to avoid circuit defects, branch defects, and order defects as presented in the previous chapters of this work. Because of the complexity of the six-bar linkages compared to four-bar linkages, the synthesis is not done in an interactive mode; rather, it is completed automatically. Nine of the coupler-driven Watt I linkages with the best objective function are selected.

Initially, the tracer point design position $P(p_X, p_Y, \theta)_i$, for i = 1 to 4 for triad ($\bar{V}_1$, $\bar{W}_1$, $\bar{Z}_1$) or triad ($\bar{V}_3$, $\bar{W}_3$, $\bar{Z}_3$) is the only known. These triads cannot be inverted into dyads because more variables need to be known. Thus, the coordinates of the reference point $B^*(x_B^*, y_B^*)$ and the angle γ_i of the base link V_1 for position i = 1 to 4 are temporarily defined as initial guesses. Therefore, the triad 1 ($\bar{V}_1$, $\bar{W}_1$, $\bar{Z}_1$) can be synthesize.

Equations (5.6) and (5.7) is applied to find the design positions $P'(p'_X, p'_Y, \theta')_i$ for i = 1 to 4 with respect to the reference point B* and the base link angle γ at position 1.

---

[9] The transmission angles must be formed in the triads or dyads

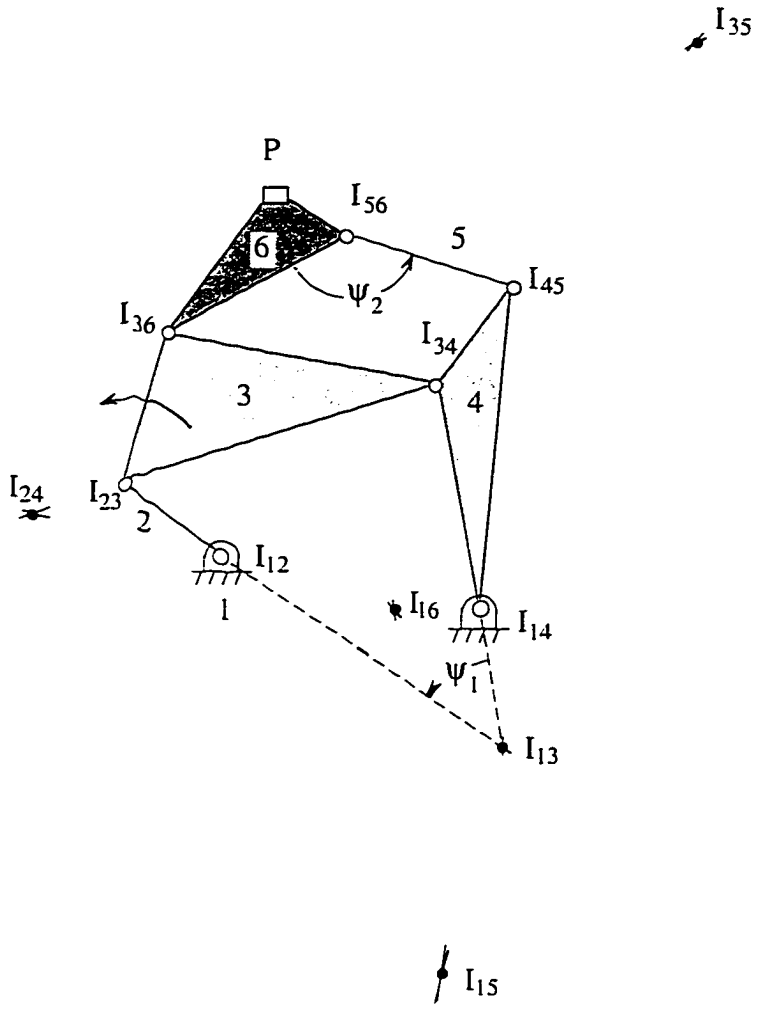

Figure 5.7 Transmission Angles of Coupler Driven Watt I

Thus, triad 1 is converted into a dyad. Eqs. (3.16) and (3.26) are applied to dyad ($\bar{W}_1$, $\bar{Z}_1$) to find the solutions of point C and point B which are the circle-point Burmester curve and center-point Burmester curve, respectively. The closest point of the circle-point Burmester curve to the centroid of the image poles is selected as point C, and the corresponding center-point B is obtained[10] using Eq. (7.6) of Bawab (1992). It is important to mention that the rectification is independent of the initial guess of the reference point $B^*(X_B^*, Y_B^*)$ and the angle γ_i of the base link V_1 for the triad 1 once the guess is make.

[10] The coordinates of points C and B are obtained with respect to position 1

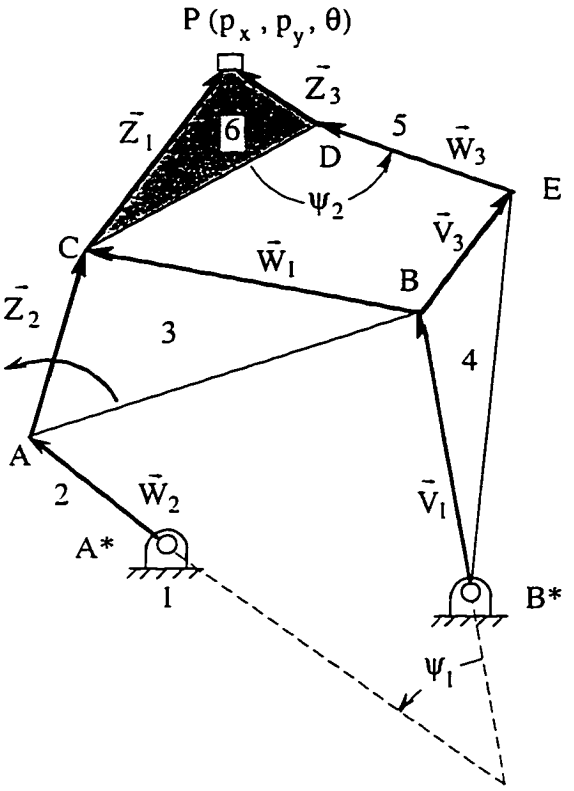

Figure 5.8 Vector Representation of Coupler Driven Watt I

Point C $(X_C, Y_C)_i$ and the angle β_{1i} of link W_i for i = 1 to 4 corresponding to the design positions (Fig. 5.9) are selected as the design positions of the coupler-driven four-bar A*ABB* with transmission angle ψ_1. This coupler-driven four-bar can be synthesized by applying the automatic synthesis process provided in Section 5.1. During the automatic synthesis, the objective function defined by Eq. (3.28) of the coupler-driven four-bar linkage A*ABB* is calculated. This objective function depends on the link length ratio and transmission angle ψ_1. Linkages with the best nine objective functions are collected as the initial selections of the loop A*ABB* of the Watt I mechanism.

In order to synthesis the crank-driven four-bar loop BCDE, triad 3 ($\bar{V}_3$, $\bar{W}_3$, $\bar{Z}_3$) needs to be synthesized first. For each of the solutions of four-bar loop A*ABB* stored, the coordinates of point $B(X_B, Y_B)_i$ can be found at the four positions. Also the angle γ_{3i} of the base link V_3 with respect to 1 is the same as that of the angle of the base link V_1 with respect to 1 because these two vectors belong to the same rigid body link 4. Therefore, for

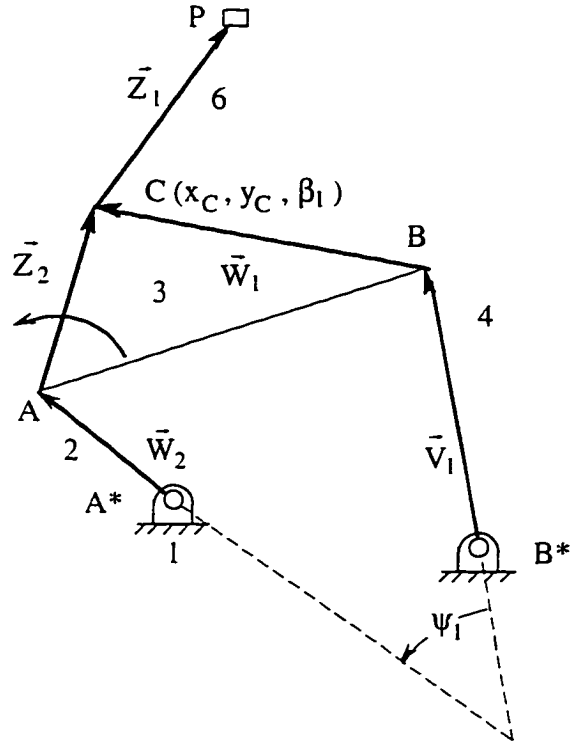

Figure 5.9 Coupler Driven Four-Bar Loop of Watt I

triad 3 ($\vec{V}_3$, $\vec{W}_3$, $\vec{Z}_3$) shown in Fig. 5.10, the tracer precision point $P(p_X, p_Y)_i$ and the angle θ_i of the tracer link Z_3, the reference precision point $B(x_B, y_B)_i$ and the angle γ_{1i} or γ_{3i} of the base link V_3 for i = 1 to 4 are all known. Eqs. (5.6) and (5.7) can then be applied to find the design positions of $P'(p'_X, p'_Y, \theta')_i$ for i = 1 to 4 with respect to the reference point B and the base link angle γ_3 at position 1. Eqs. (3.16) and (3.26) are then applied to the inverted triad 3 to find the solutions for points D and E which fall on the circle-point and center-point Burmester curves, respectively. In this case, the four-bar linkage already has the driving circle-point C and center-point B defined. Link W_1 acts as the input link. P'DE is the driven dyad and P'CB is the driving dyad. The synthesis process is slightly different from traditional one, which is described in detail as following.

The circle-point and center-point Burmester curves are computed and rectified for branching by applying the method discussed in Chapter 3 and for circuit using the procedure provided in Section 4.4 using special points. For each of the circle-point

scanned along the feasible segment, the Filemon construction is applied. If the circle-point C of the driving dyad falls in the feasible region of the Filemon lines, then this point is considered feasible. Otherwise, it is marked infeasible. A point search along the remaining feasible regions of the circle-point curve then proceeds. For each selected circle-point, the corresponding center-point is computed to form the driven dyad; the four-bar linkage is formed, and its type and class are indicated. Once the search is exhausted, the circle-point curve and its corresponding center-point curve are marked for the different types and classes of four-bar linkages. Double-rocker and rocker-crank sections are further checked for circuit defects, and those sections with circuit defects are eliminated to complete the rectification of the Burmester curves. This completes the rectified synthesis of four-bar loop BCDE shown in Fig. 5.10.

Circuit defects due to the superposition of the limits of one of the four-bar linkage on the other need to be explored to ensure that the synthesized Watt I is circuit defect free. Circuit defects may occur when the two overlap[11] cases of table 1 of Mirth and Chase (1995) happen, and that selection is considered infeasible if it is true. For each of the feasible points D and E selected in the second phase of the rectification, the objective function which is a function of the link-length ratio of the whole mechanism (Watt I) and the transmission angles ψ_1 and ψ_2 are computed. Nine Watt I linkages with the best objective functions are stored and displayed in RECSYN. The objective function, design variables, and constraints are provided in details in section 5.5.1.

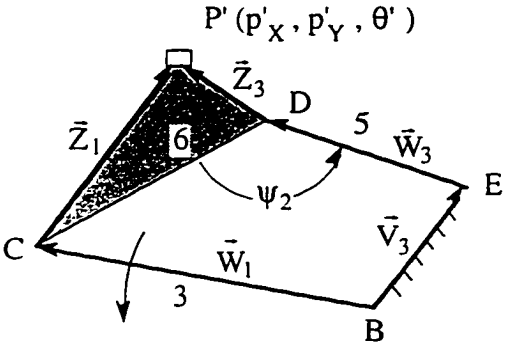

Figure 5.10 Synthesis of Triad 3 and Four-Bar BCDE

[11] This happens when the input ranges of link 3 for the two constitute four-bars conflict.

5.5 Automatic Synthesis

5.5.1 Objective Function and Constraints

Watt I linkages with the best nine objective function values are obtained as discussed in the previous section. The criteria for a good linkage is to have the link-length ratio of the linkage close to one, and the transmission angles as close as possible to 90 degrees. The objective function is defined as:

$$f(x,\mu) = Wf_1(x) + (1-W)\left(f_2(\mu)+f_3(\mu) \right) \qquad (5.10)$$

subject to constraints

$$G_j(x) \leq 0 \qquad j= 1,2,3,....m$$

where

$f(x,\mu)$	=	Objective Function
x	=	Design variables which correspond to the coordinates of the fixed, moving pivots
μ	=	The Minimum transmission angle μ_1 and the maximum transmission angle μ_2
W	=	Link-length to transmission angle weighting factor
$f_1(x)$	=	Link-length ratio function
$f_2(\mu)$	=	Transmission angle ratio ψ_1
$f_3(\mu)$	=	Transmission angle ratio ψ_2

The link length ratio function is given somewhat arbitrarily by:

$$f_1(x) = e^A$$

where

$$A = \frac{10\,(x_1^{max} - x_1)}{x_1}$$

x_1^{max}	=	Maximum link-length ratio of the desired linkage.
x_1	=	User desired limit for the link-length ratio.

The transmission angle function $f_2(x)$ of ψ_1 is given by:

$$f_2(x) = e^B$$

where

$$B = 10\,\text{Max}\left\{\left|\frac{\pi}{2}-\mu_1\right|,\ \left|\frac{\pi}{2}-\mu_2\right|\right\}$$

μ_1 and μ_2 are the limit for the transmission angle ψ_1

The transmission angle function $f_3(x)$ of ψ_2 is given by:

$$f_3(x) = e^C$$

where

$$C = 10 \text{ Max} \left\{ \left| \frac{\pi}{2} - \mu_3 \right|, \left| \frac{\pi}{2} - \mu_4 \right| \right\}$$

μ_3 and μ_4 are the limit for the transmission angle ψ_2

Basically, two sets of constraints are incorporated in the automatic synthesis procedure. The first set consists of boundary constraints which ensure that the pivots of the linkage lie within the specified constraint boundaries. The other type of constraints are based on the rectification to ensure that the linkage does not have circuit, branch or order defects. They are shown in Fig. 5.11. The constraints are set up so that negative values imply constraint satisfaction, while positive values mean violation.

The constraints G_1 to G_8 are defined for fixed constraints to ensure that the fixed pivots are within the user defined fixed boundary. The fixed boundary is specified by a

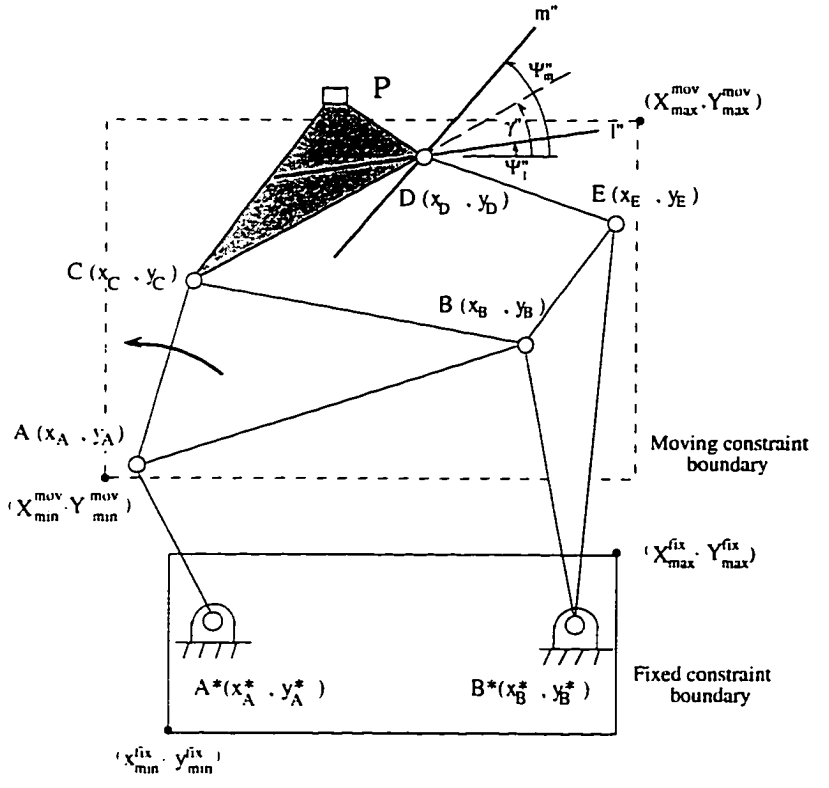

Figure 5.11 Constraints for Automatic Synthesis

minimum of x_{min}^{fix} and y_{min}^{fix} and a maximum of x_{max}^{fix} and y_{max}^{fix}. The fixed coordinates of the linkage are A* and B*. Thus, the constraints are represented by:

$$\begin{aligned} G_1 &= x_{min}^{fix} - x_A^* \\ G_2 &= x_1^* - x_{max}^{fix} \\ G_3 &= y_{min}^{fix} - y_A^* \\ G_4 &= y_A^* - y_{max}^{fix} \\ G_5 &= x_{min}^{fix} - x_B^* \\ G_6 &= x_B^* - x_{max}^{fix} \\ G_7 &= y_{min}^{fix} - y_B^* \\ G_8 &= y_B^* - y_{max}^{fix} \end{aligned} \tag{5.11}$$

Similarly, Constraints G_9 to G_{28} are defined to ensure that the moving pivots A, B, C, D, and E are within the user defined moving boundary. The moving boundary is specified by a minimum of x_{min}^{mov} and y_{min}^{mov} and a maximum of x_{max}^{mov} and y_{max}^{mov}. Thus, the constraints are represented by:

$$\begin{aligned} G_9 &= x_{min}^{mov} - x_A \\ G_{10} &= x_A - x_{max}^{mov} \\ G_{11} &= y_{min}^{mov} - y_A \\ G_{12} &= y_A - y_{max}^{mov} \\ G_{13} &= x_{min}^{mov} - x_B \\ G_{14} &= x_B - x_{max}^{mov} \\ G_{15} &= y_{min}^{mov} - y_B \\ G_{16} &= y_B - y_{max}^{mov} \\ G_{17} &= x_{min}^{mov} - x_C \\ G_{18} &= x_C - x_{max}^{mov} \\ G_{19} &= y_{min}^{mov} - y_C \\ G_{20} &= y_C - y_{max}^{mov} \end{aligned}$$

$$
\begin{aligned}
G_{21} &= x_{min}^{mov} - x_D \\
G_{22} &= x_D - x_{max}^{mov} \\
G_{23} &= y_{min}^{mov} - y_D \\
G_{24} &= y_D - y_{max}^{mov} \\
G_{25} &= x_{min}^{mov} - x_E \\
G_{26} &= x_E - x_{max}^{mov} \\
G_{27} &= y_{min}^{mov} - y_E \\
G_{28} &= y_E - y_{max}^{mov}
\end{aligned} \tag{5.12}
$$

In order to ensure that the coupler-driven four-bar loop A*ABB* is free of branch and circuit defects, constraints G_{29} to G_{32} are applied to the cognate linkage of loop A*ABB*. The driven circle-point of the cognate linkage should have a feasible areas after Filemon construction is applied. This can be represented by constraint G_{29}.

$$G_{29} = k_1 \left(|\Psi'_l - \Psi'_m| - \pi \right) \tag{5.13}$$

where angle Ψ'_l and Ψ'_m are the two limits of the Filemon construction with reference to the horizontal line, and k_2 is a scaling factor.

The branch defect constraints for the feasible selection of the driving circle point of the cognate linkage in term of branch defect are

$$
\begin{aligned}
G_{30} &= 0 && \text{feasible} \\
G_{30} &= \gamma' - \Psi'_l && \text{infeasible} \\
G_{31} &= 0 && \text{feasible} \\
G_{31} &= \Psi'_m - \gamma' && \text{infeasible}
\end{aligned} \tag{5.14}
$$

where γ' is the coupler angle of the cognate linkage with the horizontal.

Constraint G_{32} is applied to eliminate the circuit defect in loop A*ABB*.

$$
\begin{aligned}
G_{32} &= 0 && \text{no circuit defect} \\
G_{32} &= \infty && \text{with circuit defect}
\end{aligned} \tag{5.15}
$$

Constraints G_{33} to G_{37} are devoted to four-bar loop BCDE to eliminate branch, circuit, and order defects. For the Filemon construction at point D, let Ψ''_l and Ψ''_m be the corresponding Filemon angles. The feasible regions of the circle-point D on the segment of the Burmester curve where the branch defect is eliminated is given as:

$$G_{33} = k_2 \left(|\Psi''_l - \Psi''_m| - \pi \right) \tag{5.16}$$

where k_2 is a scaling factor. According to Fig. 5.11, the angle γ" which the coupler forms with the horizontal is represented by:

$$\gamma'' = \tan^{-1}\left[\frac{y_C - y_D}{x_C - x_D}\right] \tag{5.17}$$

Then the branch constraint for circle-point C of loop BCDE is

$$\begin{aligned} G_{34} &= 0 && \text{feasible} \\ G_{34} &= \gamma'' - \Psi''_1 && \text{infeasible} \\ G_{35} &= 0 && \text{feasible} \\ G_{35} &= \Psi''_m - \gamma'' && \text{infeasible} \end{aligned} \tag{5.18}$$

The constraint for the order defect of this loop is defined to be:

$$\begin{aligned} G_{36} &= 0 && \text{feasible} \\ G_{36} &= 2.0\sqrt{(x_B - x_{min})(x_{max} - x_B)} && \text{infeasible} \end{aligned} \tag{5.19}$$

where x_{min} and x_{max} correspond to the minimum and the maximum x coordinate of the segment bound by the image poles in which the driving circle-point lies.

The constraint for the circuit defect is treated as G_{37}

$$\begin{aligned} G_{37} &= 0 && \text{no circuit defect} \\ G_{37} &= \infty && \text{with circuit defect} \end{aligned} \tag{5.20}$$

Finally, constraint G_{38} deals with the circuit defect due to the interference of the two constitutive four-bar loops.

$$\begin{aligned} G_{38} &= 0 && \text{no circuit defect} \\ G_{38} &= \infty && \text{with circuit defect} \end{aligned} \tag{5.21}$$

5.5.2 Optimization

Optimization techniques are applied to the objective function to improve the solution of the linkages. The fixed boundary within which the center-points (fixed pivots) and the moving boundary where circle-points (moving pivots) must lie have a rectangular shape but can be generalized to a convex polygon shape.

The Broydon-Fletcher-Goldfarb-Shanno (BFGS) method with penalty function approach is used as the optimization technique with the Golden-Section method being the one dimensional search. The penalty function transforms a constrained problem into a sequence of unconstrained problems and a large penalty factor is assigned for the set of violated constraints and no penalty for the set of feasible constraints. The penalty function can be written as:

$$P(x, R) = f(x, \mu) + \lambda (R, G_J(x)) \tag{5.22}$$

where

$f(x, \mu)$ = objective function

R = set of penalty parameters

λ = penalty term

$G_J(x)$ = set of violated constraints ($G_j(x) > 0$)

5.6 Examples

In this section, a pin spotter sweep mechanism of a bowling machine is taken as an example problem to show the implementation of the aforementioned coupler-driven Watt I synthesis procedure in the program RECSYN. The original mechanism is a complex multiloop linkage with 13 links and two degrees of freedom as indicated in Fig. 5.12. A coupler-driven Watt I six-bar linkage will be designed to replace the original multiloop linkage.

The design positions for the sweep mechanism are shown in Fig. 5.13. Also the user may indicate the constraints for the center-points and circle-points. Fig. 5.14 indicates that the automatic synthesis is selected with a weight ratio of the link-length to the transmission angles of 0.5 and a maximum link-length ratio of 4.0. Fig. 5.15 shows the initial selection of the reference point B* and the angular displacement of the base link V_1 at the four positions. The rectified synthesis is performed automatically from here followed the procedure described in section 5.4 without optimization, and the nine solution linkages with the best objective functions are displayed in Fig. 5.16. Fig. 5.17 shows that one of the linkages passes through all the design positions.

Figure 5.18 displays nine solution linkages with the best objective functions being optimized Fig. 5.19 shows a solution that has a better sweep path than that without optimization.

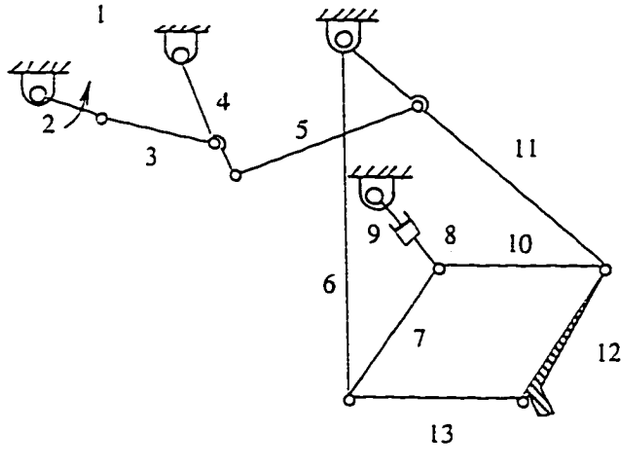

Figure 5.12 Pin Spotter Sweep Mechanism

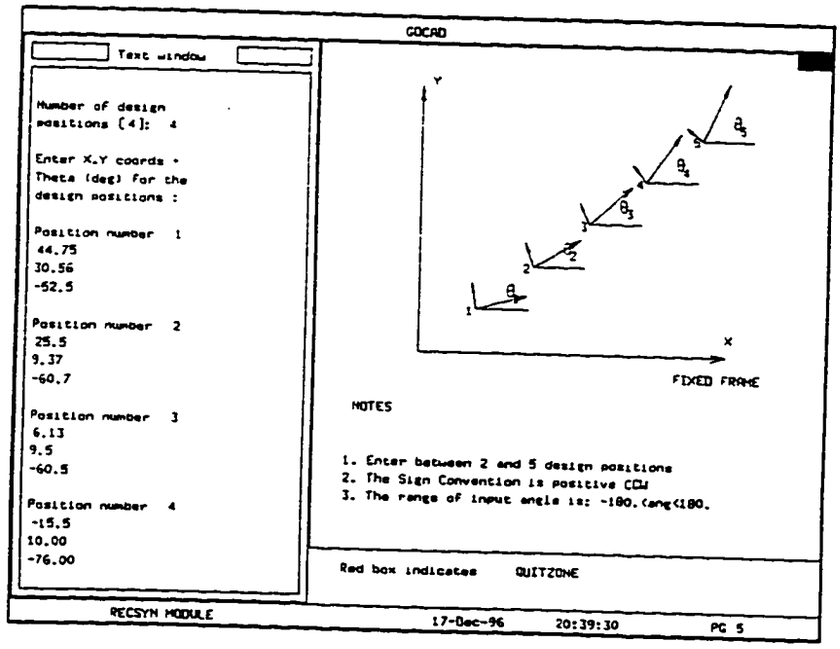

Figure 5.13 Four Design Positions of the Pin Sweep Mechanism

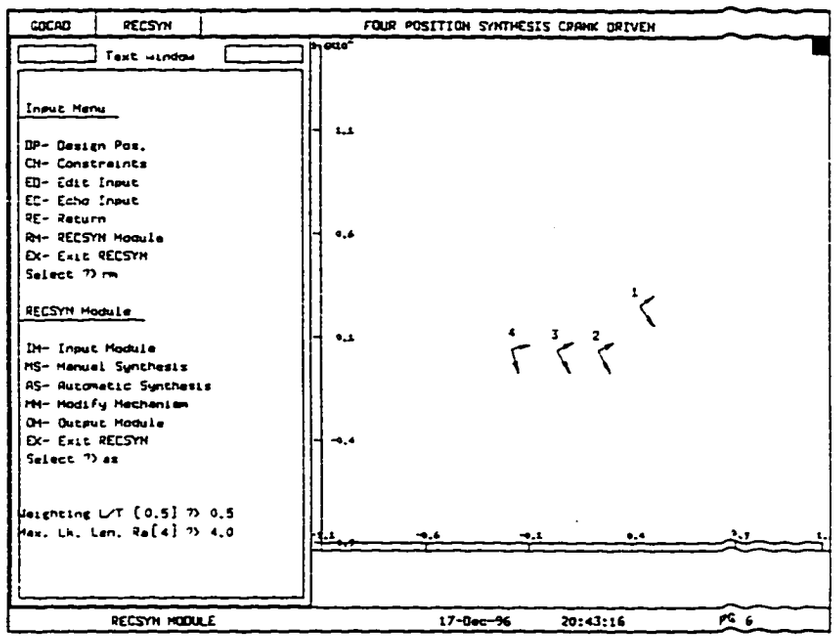

Figure 5.14 Weighting Factor and Maximum Link Ratio Selection

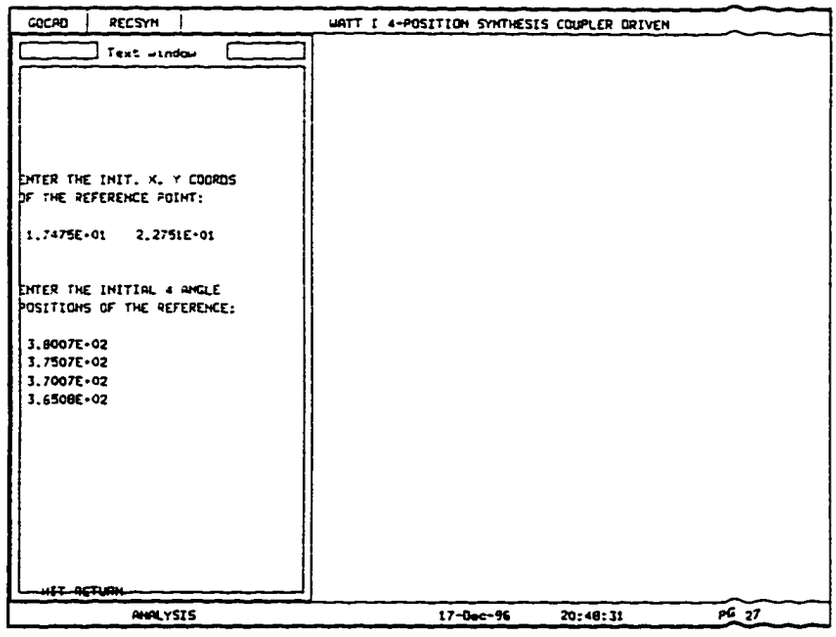

Figure 5.15 Initial Selection of the Reference Point and Angles With Respect to Four Positions for Triad One

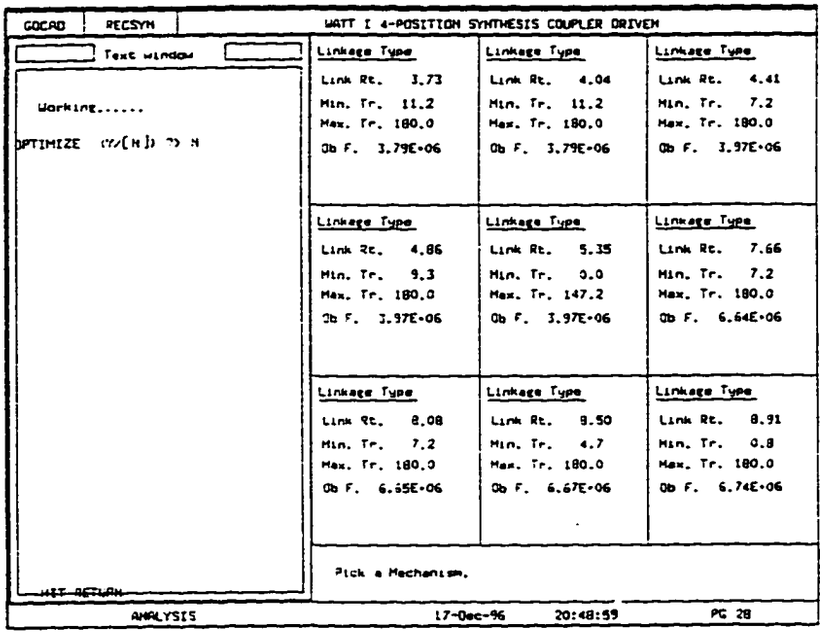

Figure 5.16 The Nine Best Solution Linkages Without Optimization

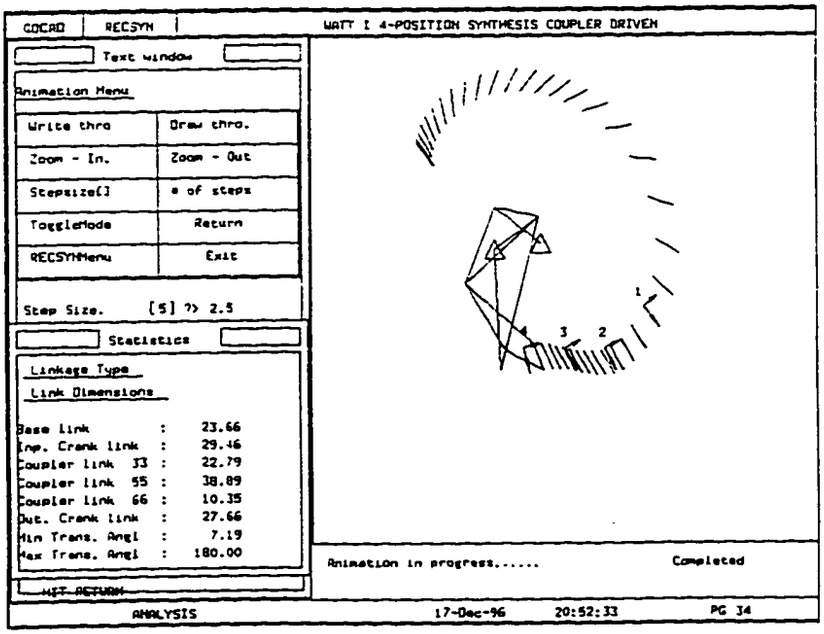

Figure 5.17 The Designed Linkage Passes Through the Four Design Positions

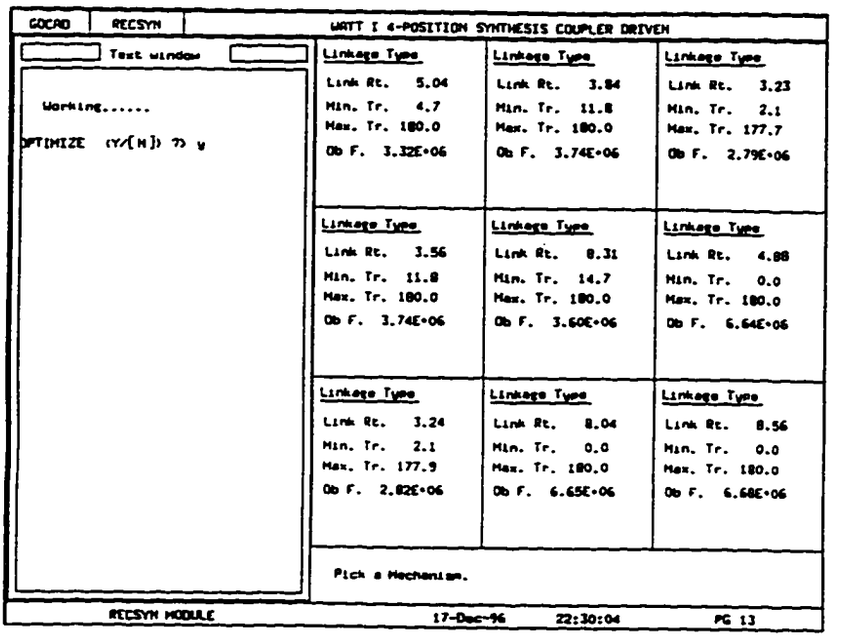

Figure 5.18 The Nine Best Solution Linkages After Optimization

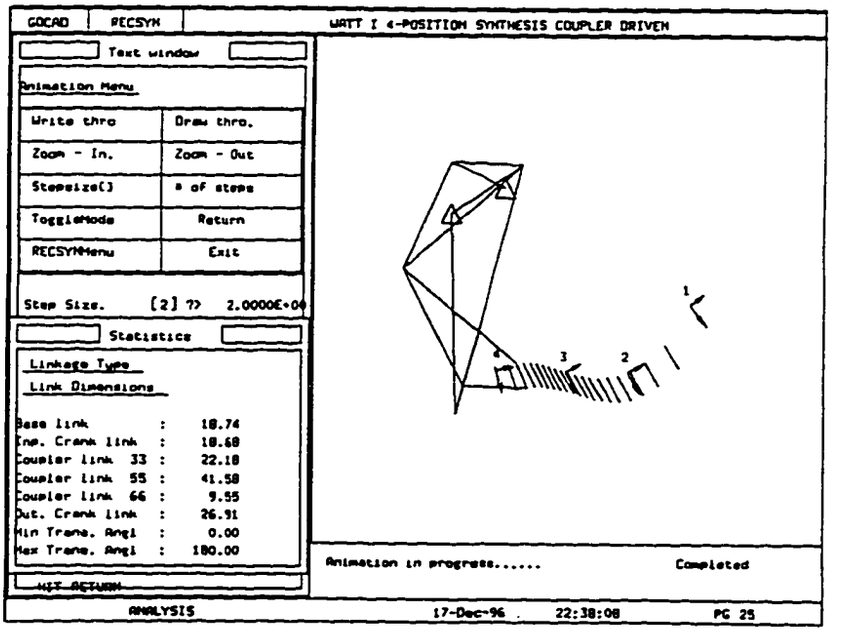

Figure 5.19 The Designed Linkage Passes Through the Four Design Positions With Better Path

CHAPTER VI

TOLERANCE SYNTHESIS OF FOUR-BAR LINKAGES FOR MOTION GENERATION

This chapter provides a methodology to determine the optimal link length tolerance and joint clearance distributions in four-bar linkages for two, three, and four position motion generation to satisfy a specified structural error for linkage manufacturing. A stochastic model incorporated with tolerances and clearances for four-bar motion generation is proposed. The tolerances and clearances are obtained as a result of solving an optimization problem with the objective function being the mechanical error and the structural error as constraint. Section 6.1 proposes a stochastic model for tolerance synthesis of four-bar motion generation. Statistical characteristics of the random variables in the model are also discussed in this section. Section 6.2 defines the mechanical error of four-bar motion generation as a function of statistical properties of random variables. Section 6.3 summarizes the tolerance synthesis as an optimization problem and presents several application examples of tolerance and clearance distributions.

6.1 Stochastic Model for Four-Bar Motion Generation

The very nature of the outputs of mechanisms with clearances and tolerances is probabilistic. Hence, it is practical that the tolerances of link lengths and clearances in hinges of four-bar motion generation linkages are determined as an optimization problem through an appropriately defined stochastic model.

6.1.1 Stochastic Model Setup for Four Position Motion Generation

A four-bar mechanism with nominal member size for motion generation is shown in Fig. 6.1. In motion generation, not only the coordinates but also the angular position of the coupler is under investigation. Figure 6.2 shows an exaggerated view of the relative position of the pin with respect to the race of a typical joint pair. The stochastic model for four-bar motion generation is introduced to have fifteen random variables as illustrated in Fig. 6.3. The first thirteenth random variables are the link lengths and the pin center position with respected to their local coordinate systems. The fourteenth and fifteenth

random variable, angles γ_1 and γ_2 in coupler link, are the manufacturing reference to obtain the output of motion generation. Another characteristic of the model in Fig. 6.3 is that the four bushes are allocated to the floating and fixed links and four pins to the cranks. A general form of the random variable vector array can be presented as

$$Z=\{z_1,z_2,...,z_5,...,z_m\}^T \tag{6.1}$$

Where m is the total number of random variables.

For the proposed four-bar stochastic model for motion generation, m is equal to 15, and the random variable vector can be written with meaningful items as,

$$Z=\{l_1,l_2,...,l_i,x_1,...,x_j,y_1,...,y_j,\gamma_1,\gamma_2\}^T \tag{6.2}$$

$$i=5 \quad \text{and} \quad j=4$$

where

l_i — the random link length, $\bar{l}_i-t_i \le l_i \le \bar{l}_i+t_i$, $\bar{l}_i$ is the nominal link length, t_i is the tolerance band on this link length

x_j and y_j — the coordinates of random location of pin centers in four clearance circles

γ_1 and γ_2 — the random angles on the coupler link controlling the coupler point angular position, $\bar{\gamma}_k-\Delta\gamma_k \le \gamma_k \le \bar{\gamma}_k+\Delta\gamma_k$, $\bar{\gamma}_k$ is the nominal coupler shape angle, $\Delta\gamma_k$ is the tolerance band on the angle with k=1 , 2.

6.1.2 Equivalent Linkage from the Stochastic Model

The four-bar linkage O_AABO_B shown with thicker lines in Fig 6.3 is defined as the equivalent linkage corresponding to the proposed stochastic model, which has random characteristics at different positions. The instantaneous coordinates of the four pin centers in equivalent linkage with respect to their local coordinated systems are $O_A(x_1, y_1)$, A (x_2, y_2), $B(x_3, y_3)$, and $O_B(x_4, y_4)$, respectively. The link lengths of the equivalent linkage O_AABO_B can be represented by the following formulas:

$$L_1 = \sqrt{(l_1 + x_4 - x_1)^2 + (y_4 - y_1)^2} \approx l_1 + x_4 - x_1$$
$$L_2 = l_2$$
$$L_3 = \sqrt{(l_3 + x_3 - x_2)^2 + (y_3 - y_2)^2} \approx l_3 + x_3 - x_2$$
$$L_4 = l_4$$
$$L_5 = \sqrt{(l_5 \cos\gamma_1 - x_2)^2 + (l_5 \sin\gamma_1 - y_2)^2}$$
$$L_6 = \sqrt{(l_3 + x_3 - l_5 \cos\gamma_1)^2 + (l_5 \sin\gamma_1 - y_3)^2} \qquad (6.3)$$

Because of $l_1 + x_4 - x_1 >> y_4 - y_1$ and $l_3 + x_3 - x_2 >> y_3 - y_2$, the random output $P(X_e, Y_e, \alpha_e)$ of the equivalent linkage $O_A ABO_B$ of the proposed stochastic model at any position with input angle ϕ_e can be given by

$$X_e = X_{O_A} + L_2 \cos(\phi_e + \theta_e) + L_5 \cos\delta_e \qquad (6.4)$$
$$Y_e = Y_{O_A} + L_2 \sin(\phi_e + \theta_e) + L_5 \sin\delta_e \qquad (6.5)$$
$$\alpha_e = \gamma_2 + \mu_e + \gamma_1 - \pi \qquad (6.6)$$

Where

$$\delta_e = \gamma_e + \theta_e + \eta_e - \varepsilon_e$$
$$\varepsilon_e = \tan^{-1}\left[\frac{L_2 \sin\phi_e}{L_1 - L_2 \cos\phi_e}\right]$$
$$\eta_e = \cos^{-1}\left[\frac{L_1^2 + L_2^2 + L_3^2 - L_4^2 - 2L_1 L_2 \cos\phi_e}{2L_3\sqrt{L_1^2 + L_2^2 - 2L_1 L_2 \cos\phi_e}}\right]$$
$$\mu_e = \omega_e + \theta_e + \eta_e - \varepsilon_e$$
$$\theta_e = \theta_0 - \Delta\phi_e$$
$$\phi_e = \phi_0 + \Delta\phi_e$$
$$\omega_e = \tan^{-1}\left[\frac{y_2 - y_3}{l_3 + x_3 - x_2}\right]$$
$$\Delta\phi_e = \tan^{-1}\left[\frac{y_1 - y_4}{l_1 + x_4 - x_1}\right]$$
$$\gamma_e = \cos^{-1}\left[\frac{L_3^2 + L_5^2 - L_6^2}{2L_3 L_5}\right]$$
$$X_{O_A} = X_{O_1} + x_1 \cos\theta_0 + y_1 \sin\theta_0$$
$$Y_{O_A} = Y_{O_1} - x_1 \sin\theta_0 + y_1 \cos\theta_0$$

During the assembly of the manufactured mechanism to a specific initial position, the variable θ_0, X_{O_1}, and Y_{O_1} may not be precisely adjusted to the ideal points and hence should be treated as random variables as well. However, limiting ourselves to the mechanism design and manufacturing, it is assumed that the manufactured linkage is able to be installed exactly at the specified points. Therefore, it is appropriate to consider these variables as deterministic here.

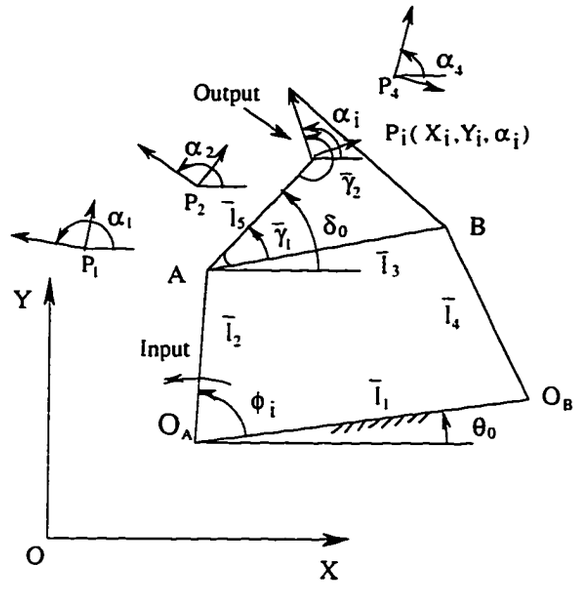

Figure 6.1 Four-bar Linkage for Motion Generation with Nominal Length

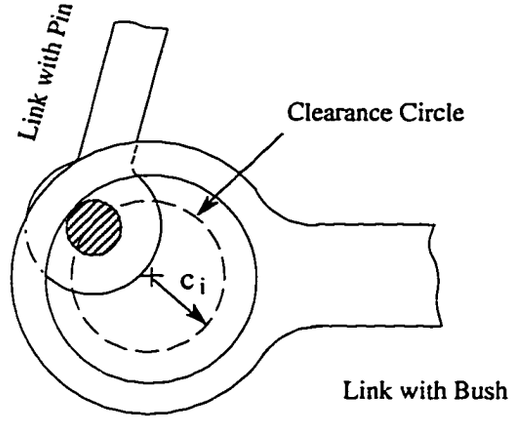

Figure 6.2 Exaggerated View Of a Typical Joint Pair

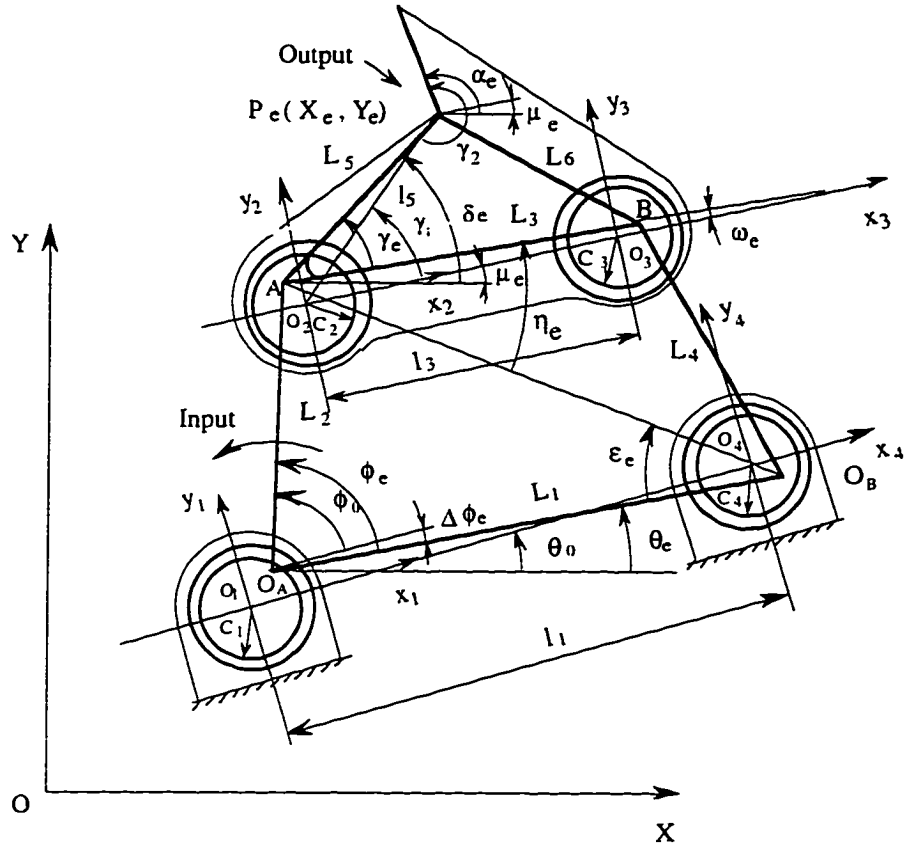

Figure 6.3 Stochastic Model for Four-Bar Motion Generation with Tolerances and Clearances

6.1.3 Statistical Characteristics of the Random Variables

It is seen that the output for motion generation is a function of random variables. To investigate the probability distribution of the output, the statistical characteristics of each individual random variable, such as the mean M and variance V, associated with the stochastic model should be obtained.

It is appropriate to treat the link lengths and angle on the coupler link as normally distributed since these are manufactured based on the nominal dimensions in the machine shop. A typical probability function for normal distribution is (Kapur and Lamberson, 1977)

$$f(z_m)=\frac{1}{\sqrt{2\pi V[z_m]}}\exp\left[-\frac{(z_i-M[z_m])^2}{2V[z_m]}\right] \tag{6.7}$$

Thus, for z_m in Eq. (6.1), m = 1 to 5, or l_i in Eq. (6.2), i=1 to 5

$$M[z_m]=\bar{l}_i \tag{6.8}$$

$$V[z_m]=\left(\frac{t_i}{3}\right)^2 \tag{6.9}$$

for z_m in Eq. (1), m =14, 15, or γ_k in Eq. (2), k =14, 15

$$M[z_m]=\bar{\gamma}_k \tag{6.10}$$

$$V[z_m]=\left(\frac{\Delta\gamma_k}{3}\right)^2 \tag{6.11}$$

The distribution of the random location of a pin center within the clearance circle is somewhat complicated due to the type of bearing and load variation used at the joint. However, it is fairly reasonable to assume that the pin center can be equally distributed anywhere inside the clearance circle (Dhande and Chakraborty 1973). If x_k and y_k are the coordinates of the pin center in its local coordinate system, the probability density is then given by,

$$f(x_j,y_j)=\begin{cases}\dfrac{1}{\pi c_j^2} & \text{if } x_j^2+y_j^2 \le c_j^2 \\ 0 & \text{if } x_j^2+y_j^2 > c_j^2\end{cases} \tag{6.12}$$

$$j = 1, 2, 3, 4$$

Hence the means and variances of the random location of pin centers are (Chakraborty 1975), m = 6, 7, ...12, 13, or j = 1, 2, 3, 4 are

$$\begin{aligned} M[z_m]&=M[x_j]=0 && m = 6, 7, 8, 9 \\ M[z_m]&=M[y_j]=0 && m = 10, 11, 12, 13 \end{aligned} \tag{6.13}$$

$$V[z_m] = V[x_j] = \frac{4c_j^2}{3\pi} \qquad m = 6, 7, 8, 9$$

$$V[z_m] = V[y_j] = \frac{4c_j^2}{3\pi} \qquad m = 10, 11, 12, 13 \tag{6.14}$$

The two random variables x_j and y_j are dependent but uncorrelated.

6.2 Mechanical Error of Four-bar Motion Generation

Unlike the function generation that has one output parameter which is the output angle, the output of motion generation consists of the tracer point position and coupler

angle. Hence, the output of motion generation is reflected by the output (X_e, Y_e, α_e) of the equivalent linkage in the stochastic model at different position. The statistical characteristics of the output function is studied in the following subsection.

6.2.1 Numerical Properties of the Output Function

Suppose the general form of one component of the output for four-bar motion generation is

$$G = G(z_m;\ m = 1, 2, ..., 15) \tag{6.15}$$

For the random variables z_m; m = 1, 2, ..., 15, the means and variances are given by Eqs. (6.8) and (6.9) when m = 1 to 5, Eqs. (6.13) and (6.14) when m = 6 to 13, and Eqs. (6.10) and (6.11) when m = 14 to 15. Thus, the probability distribution function F(G) of the output can be theoretically evaluated by

$$F(G) = \int_{-\infty}^{z_{15}} \int_{-\infty}^{z_{14}} \cdots \int_{-\infty}^{z_2} \int_{-\infty}^{z_1} f(z_m) \prod_{m=1}^{15} dz_m \qquad m = 1, 2, \ldots, 14, 15 \tag{6.16}$$

Since all the random variables are uncorrelated, the joint probability density function then becomes

$$f(z_m) = \prod_{m=1}^{15} f(z_m) \qquad m = 1, 2, \ldots, 14, 15 \tag{6.17}$$

Eq. (6.17) can be rewritten as

$$F(G) = \prod_{m=1}^{15} \int_{-\infty}^{z_m} f(z_m)\, dz_m \tag{6.18}$$

It is very difficult to use Eq. (6.18) in the synthesis of the mechanical error, because the integral limits z_m have to be expressed in terms of the output G using Eq. (6.15), which is extremely difficult, if not an impossible, task.

To obviate this difficulty, we will try to determine the mean and variance of output G. Eq. (6.15) can be expanded into a Taylor series about the mean value $M[z_m]$ of the random variables z_m as following

$$G \approx G(M[z_m]) + \sum_{m=1}^{15} \left(\frac{\partial G}{\partial z_m}\bigg|_{M[z_m]} \right) (z_m - M[z_m]) + R \qquad m = 1, 2, \ldots, 14, 15 \tag{6.19}$$

where, R represents the terms having order two or above. It is concluded that, in engineering practice, the higher order term R does not appreciably affect the results of

synthesis of mechanical error. This is due to the fact that the range of z_m's about their mean values are very small and the output curve is relatively smooth (Chakraborty 1975). Therefore, the linear expression of output G does not lead to any serious error and the term R can be dropped. As all the random variables are mutually independent and uncorrelated, the mean and variance of output G are given by:

$$M[G] = G(M[z_m]) \qquad m = 1, 2, \ldots, 14, 15 \qquad (6.20)$$

$$V[G] = \sum_{m=1}^{15} \left(\frac{\partial G}{\partial z_m}\bigg|_{M[z_m]} \right)^2 V[z_m] \qquad m = 1, 2, \ldots, 14, 15 \qquad (6.21)$$

It can be demonstrated that the function given in Eq. (6.19) is normally distributed.

To obtain the variance V[G] of Eq.(6.21), the partial derivatives of G with respect to the random variables z_m have to be examined from Eq. (6.15) and evaluated at their means $M[z_m]$. The results are presented in Appendix A.

6.2.2 Definition of the Mechanical Error for Motion Generation

If the deviation from the nominal output is analyzed with a 3σ (σ stands for the standard deviation of normal distribution) band of confidence level, a probability (reliability) of 0.9973 will attain (Beyer 1987). Dhande and Chakraborty (1973) and Garrett and Hall (1969) have demonstrated that it is sufficient to measure the mechanical error in function generator using 3σ band of confidence level in engineering practice. In the case of motion generation, 3σ band of confidence level can be applied to each component of the output to measure the mechanical error. Hence, the output error in x direction at position i, E_{X_i}, the mechanical error in y direction at position i, E_{Y_i}, and the angular mechanical error at position i, E_{α_i}, are given by Eqs. (6.22), (6.23) and (6.24), respectively.

$$E_{X_i} = 3V\left[X_{e_i}\right] = 3\sum_{m=1}^{15} \left(\frac{\partial X_{e_i}}{\partial z_m}\bigg|_{M[z_m]} \right)^2 V[z_m] \qquad (6.22)$$
$$m = 1, 2, \ldots, 14, 15$$

$$E_{Y_i} = 3V\left[Y_{e_i}\right] = 3\sum_{m=1}^{15} \left(\frac{\partial Y_{e_i}}{\partial z_m}\bigg|_{M[z_m]} \right)^2 V[z_m] \qquad (6.23)$$
$$m = 1, 2, \ldots, 14, 15$$

$$E_{\alpha_i} = 3\,V\left[\alpha_{e_i}\right] = 3\sum_{m=1}^{15}\left(\left.\frac{\partial \alpha_{e_i}}{\partial z_m}\right|_{M[z_m]}\right)^2 V[z_m] \qquad (6.24)$$

$$m = 1, 2, \ldots, 14, 15$$

6.3 Synthesis of Mechanical Error

The final performance of a linkage is appreciably affected by the inevitable manufacturing error. It is a challenging task for kinematicians to assign appropriate tolerances on link lengths and clearances in the joint for mechanisms. While stringent tolerances and clearances are desirable from the mechanism behavior standing point, unnecessary manufacturing cost may be involved. On the other hand, improper loose tolerances and clearances may result in assembly problem and inferior performance. Therefore, an ideal linkage design lies in reasonable tolerances and clearances allocation such that the output mechanical error is within specified structural error (E^s) limits and the tolerances and clearances allocated are as high as possible.

The synthesis of mechanical error for four-bar motion generation can be described as a problem of allocating the maximum permissible tolerance on every link length and controlling angle on the coupler link and clearance in every joint, while keeping the maximum output mechanical error within structural error (E^s) limits at each position. This can be achieved by formulating it as a constrained optimization problem consisting of two parts. The first part of prescribing the maximum permissible tolerance and clearance can be taken care of by the objective function, and the second part of limiting the total mechanical error within the specified structural error (E^s) limits can be incorporated in the constraints.

The form of the objective function is so chosen that its minimum corresponds to the maximum values of tolerances and clearances. In this paper, equal weight is given to tolerance and clearance to avoid computation difficulties. The objective function, Q, takes the following form:

$$Q = \sum_{m=1}^{15} \frac{1}{S_m} \qquad (6.25)$$

Where

$$S_m = V[z_m]$$

The constraints that ensure the resultant output error does not exceed the specified structural error (E^s) limits at design position i for motion generation with n (n = 2, 3, or 4) design positions and the S_m's do not take on negative values as given by Eqs. (6.26) through (6.29).

$$E_{X_i} - E^s_{X_i} \leq 0 \qquad i = 1, \ n \tag{6.26}$$

$$E_{Y_i} - E^s_{Y_i} \leq 0 \qquad i = 1, \ n \tag{6.27}$$

$$E_{\alpha_i} - E^s_{\alpha_i} \leq 0 \qquad i = 1, \ n \tag{6.28}$$

$$-S_m \leq 0 \qquad m = 1, 2, \ldots, 14, 15 \tag{6.29}$$

Therefore, there are totally (3n + 15) constraints for motion generation with n design positions. This optimization problem can be solved by any standard optimization design tool. In this work, ADS- Version 1.10, A Fortran Program for Automated Design Synthesis, will be employed (Vanderplaats, 1985). To link the ADS source code, a Fortran program is written and presented in Appendix B. This program also takes the dimensions of a four-bar linkage and the specified mechanical error limits.

6.4 Examples

To illustrate the tolerance synthesis procedures and validate the theory developed in the previous sections, examples of distributing link tolerances and joint clearances for four-bar two, three, and four position motion generation are demonstrated in this section.

Four-bar linkages are synthesized using RECSYN to precisely pass through two, three, and four design positions, respectively. The design positions for each case are given in Table 6.1. The synthesized linkages for through two, three, and four position motion generation in animation are separately shown by Figures 6.4, 6.5, and 6.6. The dimensions of these linkages are presented in Table 6.2.

Cases	Position No.	X Coord.	Y Coord	Angle (Degree)
Two Position	1	17.00	12.00	35.00
	2	15.00	13.00	70.00
Three Position	1	30.00	10.00	10.00
	2	28.00	12.00	35.00
	3	20.00	13.50	70.00
Four Position	1	30.00	10.00	10.00
	2	28.00	12.00	35.00
	3	20.00	13.50	70.00
	4	23.00	15.00	105.00

Table 6.1 The Exact Design Positions of Examples

	$\bar{l}_1$	$\bar{l}_2$	$\bar{l}_3$	$\bar{l}_4$	$\bar{l}_5$	θ_0	$\bar{\gamma}_1$	$\bar{\gamma}_2$
2-Position	0.898	0.983	0.987	1.047	1.612	26.323	10.77	212.98
3-Position	5.445	4.236	9.080	10.267	12.826	-113.55	7.14	188.41
4-Position	2.384	1.526	2.299	2.526	5.957	-131.80	82.95	164.59

Table 6.2 Dimensions of the Example Linkages

Two sets of uniform structural errors (SE) are separately applied to each design position for the three different motion generation cases in the examples. These structural errors are given in Table 6.3.

	E^s on X	E^s on Y	E^s on Angle
SE Set 1	0.03	0.03	0.5°
SE Set 2	0.05	0.05	1.0°

Table 6.3 Two Uniform Structural Error Cases

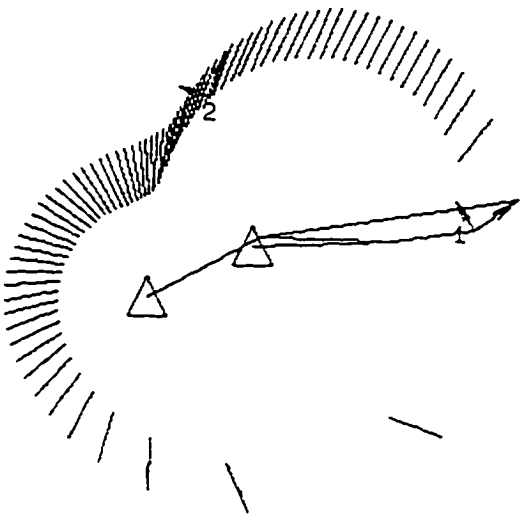

Figure 6.4 Example Linkage for Two Position Motion Generation

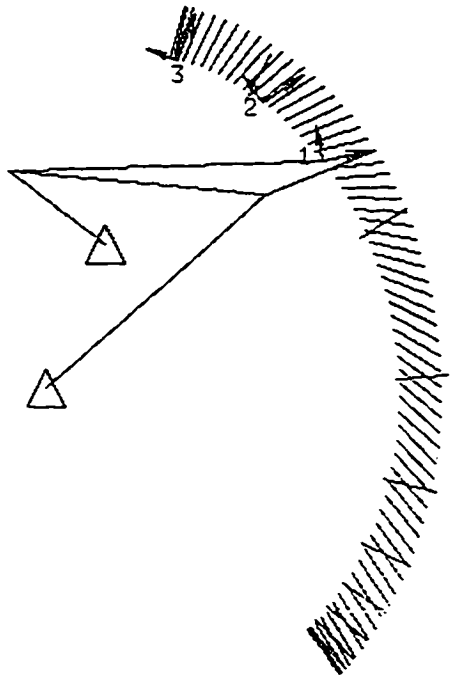

Figure 6.5 Example Linkage for Three Position Motion Generation

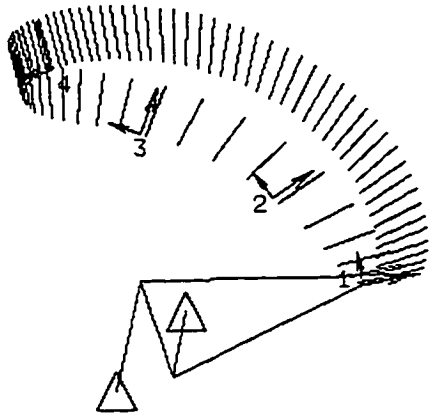

Figure 6.6 Example Linkage for Four Position Motion Generation

After reading the data file including the linkage dimensions and structural error specification, the program given in Appendix B will compute and output the tolerance and clearance distribution after an appropriate combination of optimization strategy, optimizer, and search method is issued. It is noticed that the optimal tolerance and clearance distribution is not unique for the same mechanism with identical structural error specification. The Fletcher-Reeves algorithm for unconstrained minimization using exterior penalty function method with polynomial interpolation/extrapolation without first finding bounds on the solution is selected as optimization strategy combination among different ones. The optimal tolerance and clearance distributions for the example linkages are provided in Table 6.4.

Design Position	Two Positions		Three Positions		Four Positions	
SE Case	Set 1	Set 2	Set 1	Set 2	Set 1	Set 2
t_1	1.744	1.454	2.119	3.147	2.734	3.825
t_2	1.930	1.441	2.123	3.521	2.737	3.396
t_3	1.487	1.642	2.126	3.077	2.501	2.662
t_4	1.499	1.653	2.115	3.174	2.810	2.858
t_5	3.179	3.743	3.504	3.533	3.382	3.400
c_1	0.848	0.969	1.047	1.523	1.658	1.682
c_2	0.816	0.878	1.083	1.448	1.682	1.635
c_3	0.767	0.846	1.082	1.623	1.438	1.462
c_4	0.784	0.935	1.029	1.462	1.713	1.756
$\Delta\gamma_1$	0.545°	0.410°	0.222°	0.226°	0.337°	0.344°
$\Delta\gamma_2$	0.596°	0.677°	0.188°	0.406°	0.377°	0.462°

Note: the units for tolerances on link length and joint clearances are 0.01.

Table 6.4 Tolerance and Clearance Distribution Results for Example Linkages

CHAPTER VII

CONCLUSIONS AND RECOMMENDATIONS

7.1 Research Summary

The fundamental rectified synthesis theories of crank and coupler-driven four-bar and crank-driven Watt I six-bar linkages for motion generation have been presented. The research is focused on the completion of circuit defect identification in double-rocker and rocker-crank four-bar linkages for motion generation at the synthesis stage, the rectified synthesis procedure of coupler-driven Watt I linkages for four position motion generation, and the tolerance synthesis in four-bar motion generation.

In combination with the existing circuit rectification theory for crank-rocker and double-cranks, a two step circuit rectification methodology for all Grashof four-bars is proposed. In the first step, solutions that are guaranteed to experience circuit defects are identified as a function of the design positions and eliminated at the synthesis level with the aid of the special points. In the second step to follow, a line construction procedure is developed to eliminate the remaining infeasible regions in the priori Grashof double-rocker and rocker-crank sections which are a function of the trial selection of the circle and center-points. The procedure is implemented graphically in an example to validate the theory. This method is programmed and incorporated into RECSYN to substitute the currently used brute force technique and examples demonstrating the application are given.

A complete procedure of the rectified synthesis of the Watt I six-bar linkage to pass through the pre-defined four design positions with the coupler being the driver. This is done by de-coupling the six-bar mechanism as a combination of a coupler-driven and crank-driven four-bar linkages with common links is presented. The vector component mechanism modeling method is applied to these linkages where the dyad and triad synthesis approaches are adopted in conjunction with the vector-algebraic method to find the solutions. The linkage with the coupler-driver is initially synthesized and rectified, then followed by the crank-driven four-bar linkage. The six-bar linkage is thus

insured to assemble free of circuit, branch, and order defects. Optimization techniques are used to render the best solution linkages according to the specified design criteria. The process is coded and added to RECSYN menu allowing a designer to synthesize coupler-driven Watt I linkages. The new circuit rectification theory is also applied in the program.

A methodology to determine the optimum link length tolerance and joint clearance distributions in four-bar linkages for motion generation with specified structural error in order to manufacture the linkages is proposed. A stochastic model incorporated with tolerances and clearances for four-bar motion generation is proposed. The statistical characteristics of the random variables in the model are discussed. The mechanical error of four-bar motion generation as a function of statistical properties of random variables is defined. The tolerances and clearances are obtained as a result of solving a optimization problem with the objective function of link length tolerances and joint clearances and structural error as constraint. A FORTRAN code is written based on the proposed theory and ADS is employed as an optimization design tool. With this program, optimum link length tolerance and joint clearance distribution can be computed when the user input the required linkage information and structural errors. Examples of assigning tolerance and clearance for four-bar motion generation are presented to demonstrate the application of the method.

7.2 Recommendations for Future Work

There are three floating links in a Watt I linkage. It is suggested that studies be conducted with each of the rest two floating links being driver rather that the coupler selected in this work. This will give the designers flexibility to mount the motor according to different working environment.

In general, the procedure of designing coupler-driven Watt I linkages works well; however, in some cases it is sensitive to the guess selection of the reference base point and the base link angle for the first triad. Slight changes of the base link angle selection can result in significant changes in the final solutions, while the reference base point location is less sensitive. A further investigation is recommended to be done on the sensitivity of initial guess to the solutions.

As for the tolerance synthesis in four-bar motion generation, a twelve random variable model excluding the link length from the output point and the input circle-point on the coupler as well as the two coupler angles is worth of studying since the measurements of the last three variables are easier to control compared to the joint clearances and the direct link lengths and therefore can be regarded as non-random. This

will reduce the computation process. The current tolerance synthesis program is suggested to be incorporated into RECSYN so that a user can make the online tolerance and clearance distribution once a four-bar linkage is design. It is advised to investigate the link length tolerance and joint clearance distributions in six-bar linkages for motion generation. The stochastic modeling approach may be applied in the study and more complex geometric relationship will be expected. In addition, it will be a complicated task to study the circuit, branch, and order defects for a linkage with tolerances and clearances.

RECSYN currently is capable of synthesizing linkages in the manual and the automatic modes. For the manual synthesis the user must have a basic understanding of the rectified synthesis theory. On the other hand, the user can synthesize a linkage without any knowledge of the synthesis theory, in the automatic mode. Automatic mode based optimization theory results in linkages with good characteristics, however the nine best solutions may not correspond to the user expectation. Therefore, it is desirable if more solutions following the nine best solutions can be available to the users.

In addition, the designer may want some part of the linkage to be pre-determined and then obtain a best solution. For example, in the case of four-bar synthesis a user may some location constrains on the driven dyad of the four-bar at the beginning. This will disqualify him or her from using the automatic modes. Thus, RECSYN would be more complete if options were available to link manual and automatic modes and create a semi-automatic mode.

It is noted that six-bar mechanisms can provide more compact and attractive solutions with less limitations on the design constraints and four-bars are sometimes incapable of generating the prescribed motion within the given constraints. Synthesis of six-bar linkages can also be studied for three and two design positions as they have a larger solution space and can replace the four-bars in applications where complex mechanisms are required. RECSYN has the capabilities to synthesize four-bar and Watt I six-bar linkages, and it is suggested to integrate the synthesis of all five types of six-bar linkages. Further utility of the software can be enhanced by incorporating options to synthesize for function and path angle generation. This in effect would provide the designer with a comprehensive linkage design tool.

It is also recommended that a print option be incorporated in the RECSYN module that would allow the user to obtain a hard copy of his design on paper. The current version of RECSYN is incapable of printing the graphical output. The versatility of the package would be enhanced with an option to save the file in a format that can be

imported into standard CAD software like AutoCAD, wherein the designer has the flexibility to make necessary changes.

Finally, with the availability of GUI (Graphic User Interface) the platform of RECSYN can be redesigned with pulldown menus and other user friendly environment. Also, a PC (Personal Computer) version of RECSYN is desirable and feasible with more powerful CPU (Central Processing Unit).

BIBLIOGRAPHY

Alizade, R.I., Novruzbekov, I.G. and Sandor, G.N., 1975, "Optimization of Four-Bar Function Generating Mechanisms Using Penalty Functions with Inequality and Equality Constraints", Mechanism and Machine Theory, Vol. 10, pp. 327-336.

Ang, A. H-S., and Tang, W.H., 1975, Probability Concepts in Engineering Planning and Design Vol. I - Basic Principles, Wiley, New York.

Bagci, C., 1974, "Precision Position Synthesis of Plane Mechanisms for Function Generation Via the Separation of Geometric Inversions", ASME Paper No. 74-DET-20.

Bagci, C. and Lee, In-Ping Jack., 1975, "Optimum synthesis of Plane Mechanisms for the Generation of Paths and Rigid-Body Positions via the Linear superposition Technique", ASME Journal of Engineering for Industry, Vol. 97, pp. 340-346.

Barker, C.R., 1983, "Complete Classification of Four-Bar Linkages", Proceedings, 8th OSU Applied Mechanisms Conference, St. Louis, Missouri.

Barker, C.R., Jeng, Y.R., 1985, "Range of the Six Fundamental Position Angles of a Planar Four-Bar Mechanism", Mechanism and Machine Theory, Vol. 20, pp. 329-344.

Baumgartong, J.R., and Werff, K. Van Der, 1985, "A Probabilistic Study Relating to Tolerancing and Path Generation Error," Mechanism and Machine Theory, Vol. 20, No. 1, pp. 71-76.

Beyer, W.H., 1987, CRC Standard Mathematical Tables, CRC Press, Boca Raton, Florida, pp. 553-560.

Bawab, S., 1992, "Computer-Aided Design and Analysis of Coupler-Driven Four-Bar and Crank Driven Watt I Linkages", Ph.D. Dissertation, Ohio State University.

Bawab, S. and Li, H, 1996, "A New Circuit Rectification Method in Four-Bar Linkages", accepted for ASME for ASME Journal of Mechanical Design.

Bawab, S. and Li, H, 1995, "Rectified Synthesis of Coupler-Driven Watt I Six-Bar Linkages for Four Position Motion Generation", Proceedings of the Fourth National Applied Mechanisms and Robotics Conference, AMR 95-015-01, Cincinnati, Ohio.

Bawab, S., Sabada, S., Srinivasan, U., Kinzel, G. L., and Waldron, K.J., 1996, "Automatic Synthesis of Crank Driven Four-Bar Mechanisms for Two, Three, or Four-Position Motion Generation", Accepted for ASME Journal of Mechanical Design.

Bawab, S. and Thiruvenkatachari, R, 1995, "Rectified Synthesis of Coupler-Driven Four-Bar Mechanisms for Three Position Motion Generation", Proceedings of the Fourth National Applied Mechanisms and Robotics Conference, AMR 95-012-01, Cincinnati, Ohio.

Bawab, S., Kinzel, G. L., and Waldron, K. J., 1992, "Rectified Synthesis of Coupler-Driven Four-Bar Mechanisms for Four-Position Motion Generation", Proceedings of the 22nd Biennial Mechanisms Conference, Scottsdale, Arizona, DE-Vol 46, pp. 147-155.

Beyer, R., 1963, The Kinematic Synthesis of Mechanisms, Translated by H. Keunzel, McGraw-Hill, New York, NY.

Burmester, L., 1888 Lehrbuch der Kinematic, A Felix Verlag, Leipzig, Germany, pp. 599-623.

Chakraborty, J., 1975, " Synthesis of Mechanical Error in Linkages," Mechanism and Machine Theory, Vol. 10, pp. 155-165.

Chase, T.R., 1984, "Burmester Theory for Four Precision Positions: An Extended Discourse with Application to the Dimensional Synthesis of Arbitrary Planar Linkages", Ph.D. Dissertation, University of Minnesota, Minneapolis.

Chase, T. R., Erdman, A.G., and Riley, D.R., 1987, "Triad Synthesis for up to Five Design Positions with Application to the Design of Arbitrary Planar Mechanisms", ASME Journal of Mechanisms, Transmissions, and Automation in Design, Vol. 109, No. 4, pp. 426-434.

Chase, T.R., and Fang, W.E., 1991, "Order Rectification for Complex Number Based Burmester Curves", ASME Journal of Mechanical Design, Vol. 113, No. 3, pp. 239-247.

Chase, T. R. and Mirth, J. A., 1993, "Circuits and Branches of a Single Degree of Freedom Planar Linkages," ASME Journal of Mechanical Design, Vol. 115, No. 2, pp. 223-230.

Chen, F.Y. and Chan, Ven-Lin, 1974, "Dimensional Synthesis of Mechanisms for Function-Generation Using Marquardt's Compromise", ASME *Journal of Engineering for Industry*, Vol 96, pp. 131-137.

Chiang, C.H., 1986a, "Design of Spherical and Planar Crank-Rockers and Double-Rockers as Function Generators - I", Mechanism and Machine Theory, Vol. 21, No. 4, pp. 287-296.

Chiang, C.H., 1986b, "Design of Spherical and Planar Crank-Rockers and Double-Rockers as Function Generators - II", Mechanism and Machine Theory, Vol. 21, No. 4, pp. 297-305.

Chuang, J. C., Strong, R.T., and Waldron, K.J., 1981, "Implementation of Solution Rectification Techniques in an Interactive linkage Synthesis Program", ASME Journal of Mechanical Design, Vol. 103, pp. 657-664.

Dhande, S.G., and Chakraborty, J., 1973, "Analysis and Synthesis of Mechanical Error in Linkages - A Stochastic Approach," ASME Journal of Engineering for Industry, Vol. 95, No. 3, pp. 672-676.

Dewey, G.H., and Soni., A.H., 1973, "Graphical Synthesis of Six-Link Stephenson Type III Function Generators", Proceedings of the Third Applied Mechanism Conference, Stillwater, Oklahoma, Nov. 1973, pp. 34.1-34.10.

Dou, X., and Ting, K.L., 1996, "Branch Identification of Geared Five-bar Chains", ASME Journal of Mechanical Design, Vol. 118, No. 3, pp. 384-389.

Erdman, A.G., 1985, "Computer-Aided Design of Mechanisms: 1984 and Beyond", Mechanism and Machine Theory, Vol. 20, pp. 245-249.

Erdman, A.G. and Sandor, G.N., 1984, Mechanism Design: Analysis and Synthesis, Volume 1, Prentice Hall, Inc., Englewood Cliffs, NJ.

Erdman, A.G., 1981, "Three and Four Precision Point Kinematic Synthesis of Planar Linkages", Mechanism and Machine Theory, Vol. 16, pp. 227-245.

Eschenbach, P.W., and Tesar, D., 1971, "Link-length Bounds on the Four-Bar Chain", ASME Journal of Engineering for Industry, Vol. 93, pp. 287-293.

Faik, S., and Erdman, A.G., 1991, "Sensitivity Distribution in the Synthesis Solution Space of Four-Bar Linkages", ASME Journal of Mechanical Design, Vol. 113, pp. 3-9.

Fenton, R.G., Cleghorn, W.L., and Fu, J.F., 1989, "Allocation of Dimensional Tolerances for Multiple Loop Planar Mechanisms," ASME Journal of Mechanisms, Transmissions, and Automation in Design, Vol. 111, pp. 465-470.

Filemon, E, 1971, "In Addition to the Burmester Theory", Proceedings of Third World Congress for Theory of Machines and Mechanisms, Kupari, Yugoslavia, Vol. D, pp. 63-78.
Filemon, E. 1972, "Useful Ranges of Centerpoint Curves for Design of Crank-and-Rocker Linkages", Mechanism and Machine Theory, Vol. 7, pp. 47-53.

Filemon, E, 1971, "In Addition to the Burmester Theory", Proceedings of Third World Congress for Theory of Machines and Mechanisms, Kupari, Yugoslavia, Vol. D, pp. 63-78.

Fox, R.L., and Willmert, K.D., 1967, "Optimum Design of Curve-Generating Linkages with Inequality Constraints", ASME Journal of Engineering for Industry, Series B, Vol. 89, No. 1, pp. 144-152.

Freudenstein, F., 1978, "Designing Crank-and-Rocker Links With Optimum Force Transmission", Product Engineering, Vol. 49, No. 1, pp. 45-47.

Freudenstein, F., and Chew, M.S., 1971, "Optimization of Crank-and-Rocker Linkages With Size and Transmission Constraints", ASME Journal of Mechanical Design, Vol. 101, pp. 51-57.

Freudenstein, F. and Primrose, E.J.F., 1972, "The Classical Transmission-Angle Problem", Proceedings, Conference on Mechanisms, Institution of Mechanical Engineers, London, pp. 105-110.

Freudenstein, F., and Sandor, G.N., 1961, "On the Burmester Points of a Plane", ASME Journal of Applied Mechanics, Series E, Vol. 28, No. 1, pp. 41-49.

Freudenstein, F., and Sandor, G.N., 1959, "Synthesis of Path-Generating Mechanisms by Means of a Programmed Digital Computer", ASME Journal of Engineering for Industry, Vol. 81B, No. 2, pp. 159-168.

Garrett, R.E., and Hall, A.S., 1969, "Effects of Tolerance and Clearance in Linkage Design," ASME Journal of Engineeering for Industry, Vol. 91, No.1, pp. 198-202.

Gibson, C. G., and Marsh, D., 1989, "On the Linkage Varieties of Watt 6-Bar Mechanisms - III Topology of the Real Varieties", Mechanism and Machine Theory, Vol. 24, No. 2, pp. 123-126.

Gupta, K.C., 1980, "Synthesis of Position, Path and Function Generating 4-Bar Mechanisms with Completely Rotatable Driving Links", Mechanism and Machine Theory, Vol. 15, No. 2, pp. 93-101.

Gupta, K.C., 1977, "Design of Four-bar Function Generators With Mini-Max Transmission Angle", ASME Journal of Engineering for Industry, Vol. 99, No. 2, pp. 360-365.

Gupta, K.C., and Kazerounian, S.M.K., 1983, "Synthesis of Fully Rotatable R-S-S-R Linkages", Mechanism and Machine Theory, Vol. 18, pp. 199-205.

Gupta, K.C., and Tinubu, S.O., 1983, "Synthesis of Bimodal Function Generating Mechanisms Without Branch Defect", ASME Journal of Mechanisms, Transmissions, and Automation in Design, Vol. 105, pp. 641-647.

Hall, A.S., Jr., 1961, Kinematics and Linkage Design, Prentice-Hall, Inc., Englewood Cliffs, NJ, pp. 143-147.

Harber, M.T., 1986, "Computer Aided Synthesis of Four-Bar Linkages for Three Prescribed Positions", M.S. Thesis, University of Minnesota.

Hartenberg, R.S., and Denavit, J., 1964, Kinematic Synthesis of Linkages, McGraw-Hill Book Company, New York, NY.

Hrones, J.A., and Nelson, G.L., 1951 Analysis of the Four-Bar Linkage, published jointly by the Technology Press of the Massachusetts Institute of Technology and Wiley, New York.

Hunt, K.H., 1978, Kinematic Geometry of Mechanisms, Oxford University Press, Oxford, Great Britain, pp. 222-245.

Kapur, K.C., and Lamberson, R.L., 1977, Reliability in Engineering Design, Wiley, New York.

Kaufman, R. E., 1973, "KINSYN Phase II: A Human Engineered Computer System for Kinematic Design and a New Least-Squared Synthesis Operator", Mechanism and Machine Theory, Vol. 8, pp. 469-478.

Kaufman, R.E., 1972, "Singular Solutions in Burmester Theory", ASME Paper No. 72-Mech-23.

Kaufman, R.E., 1971, "Synthesis of the Watt-I Six-Bar Linkage for Five Position Higher Coupler Motion Correlated With Input Crank Rotations", Proceedings of the Second Applied Mechanisms Conference, Stillwater, Oklahoma, pp. 281-285.

Kazerounian, S.M.K., and Gupta, K.C., 1982, "Synthesis of Position Generating Crank-Rocker or Drag-Link Mechanisms", Mechanism and Machine Theory, Vol. 17, No. 4, pp. 243-247.

Keller, R.E., 1965, "Sketching Rules for the Curves of Burmester Mechanism Synthesis", ASME Journal of Engineering for Industry, Vol. 87, pp. 155-160.

Kemler, E.N., and Howe, R.J., 1951, Machine Design, No. 23.

Khare, A.K., and Dave, R.K., 1980, "Synthesis of Double-Rocker Mechanisms With Optimum Transmission Characteristics", Mechanism and Machine Theory, Vol. 15, pp. 77-80.

Knappe, L.f., 1960, "Mechanism Tolerances," Machine Design, Vol 32, No. 12, pp. 152-158.

Kramer, S.N. and Sandor, G.N., 1975, "Selective Precision Synthesis - A General Method of Optimization for Planar Mechanisms", ASME Journal of Engineering for Industry, pp. 689-701.

Krishnamurty, S. and Turcic, D.A., 1992, "Branching Determination in Non-Dyadic Planar Multiloop Mechanisms", ASME Journal of Mechanical Design, Vol. 114, No. 2, pp. 245-250.

Krishnamurty, S. and Turcic, D.A., 1988, "A General Method of Determining and Eliminating Branching in Planar Multiloop Mechanisms", ASME Journal of Mechanisms, Transmissions and Automation in Design, Vol. 110, pp. 414-422.

Kwong, C.W., Wiederrich, J.L., and Gupta, K.C., 1981, "Design and Evaluation of Drag-Link Driven Cams", ASME Journal of Mechanical Design, Vol. 103, No. 3, pp. 592-601.

Larson, H.J., 1982, Introduction to Probability Theory and Statistical Inference, 3rd Edition, Wiley, New York, pp. 286-299.

Levitskii, N.I., Sarkissyan, Y.L. and Gekchian, G.S., 1972, "Optimum Synthesis of Four-Bar Function-Generating Mechanisms", Mechanism and Machine Theory, Vol. 7, pp. 387-398.

Mabie, Hamilton H. and Reinholtz, Charles F., 1987, Mechanisms and Dynamics of Machinery, John Wiley & Sons, Inc., New York, NY, pp. 545 -579.

Mallik, A K., and Dhande, S. G., 1987, "Analysis and Synthesis of Mechanical Error in Path-Generating Linkages Using a Stochastic Approach," Mechanism and Machine Theory, Vol. 22, No. 2, pp. 115-123.

McLarnan, C.W., 1963, "Synthesis of Six-Link Plane Mechanisms by Numerical Analysis", ASME Journal of Engineering for Industry, Vol. 85, pp. 5-11.

Mirth, J.A., 1994, "General order criteria for the precision position synthesis of single-degree of freedom planar linkages.", ASME Proceedings of the 23rd Binennial Mechanisms Conference, Minneapolis, MN, DE-Vol. 70, pp. 245-252.

Mirth, J. A., and Chase, T. R., 1995, "Circuits Rectification for Four Precision Position Synthesis of Four-Bar and Watt Six-Bar Linkages", ASME Journal of Mechanical Design, Vol. 117, No. 4, pp. 612-619.

Norton, T.W., Midha, A. and Howell, L.L., 1992, "Graphical Synthesis for Limit Positions of Four-bar Mechanism using Triangle Inequality Concept," ASME Proceedings of the 22rd Binennial Mechanisms Conference, Scottsdale, Arizona, DE-Vol. 46, pp. 377

Patwardhan, A.G., and Soni, A.H., 1977, "A Two-Stage Graphical Solution for Rigid Body Guidance With Watt's Six-Link Mechanism", Proceedings of the Fifth Applied Mechanisms Conference , Oklahoma City, Oklahoma, pp. 4.1-4.9.

Prasad, K.N. and Bagci, C., 1974, "Minimum Error Synthesis of Multiloop Plane Mechanisms for Rigid-Body Guidance", ASME Journal of Engineering for Industry, Vol. 96, pp. 107-116.

Radcliffe, C.W., 1980, "Synthesis of Sliders for Plane Rigid Body Guidance", ASME Paper No. 80-DET-109.

Rao, A.V.M., Erdman, A.G., Sandor, G.N., 1971, "Synthesis of Multiloop, Dual-Purpose Planar Mechanisms Utilizing Burmester Theory", Proceedings of the Second Applied Mechanisms Conference, Stillwater, Oklahoma, Oct. 1971, pp. 7.1-7.23.

Rao, S.S., and Reddy, C.R., 1979, "Mechanism Design by Chance Constrained Programming Technique," Mechanism and Machine Theory, Vol. 14, No. 2, pp. 413-424.

Rhyu, J.H., and Kwak, B.M., 1988, "Optimal Stochastic Design of Four-Bar Mechanisms for Tolerance and Clearance," ASME Journal of Mechanisms, Trnasmissions, and Automation in Design, Vol. 110, 1988, pp. 255-262.

Rose, R.S. and Sandor, G.N., 1973, "Direct Analytic Synthesis of Four-Bar Function Generators with Optimal Structural Error", ASME Journal of Engineering for Industry, Vol. 95, pp. 563-567.

Rubin, C.A., 1995, The Student Edition of Working Model-Version 2.0, Knowledge Revolution, Addison-Wesley Publishing Company, Reading, MA.

Sandor, G.N., and Erdman, A.G., 1984, Advanced Mechanism Design: Analysis and Synthesis: Volume 2, Prentice-Hall, Inc., Englewood Cliffs, NJ.

Sandor, G.N., 1959, "A General Complex-Number Method of Plane Kinematic Synthesis", Ph.D. Dissertation, Columbia University, New York, University Microfilms, Library of Congress Card No. Mic 59-2596, Ann Arbor, MI.

Sharfi, O. M.A., and Smith, M.R., 1983, "A Simple method for the Allocation of Appropriate Tolerances and Clearances in Linkage Mechanisms", Mechanism and Machine Theory, Vol. 18, No. 2, pp.123-129.

Sheth, P.N., and Uicker, J.J. Jr., 1971, " IMP (Integrated Mechanism Program): A Computer-Aided Design Analysis System for Mechanisms and Linkages", ASME Journal of Engineering for Industry, Vol. 93, pp. 102-112.

Shoup, T.E., and Pelan, B.J., 1971, "Design of Four-Bar Mechanisms for Optimum Transmission Angle and Optimum Structural Error", Proceedings of the Second OSU Applied Mechanisms Conference, Stillwater, Oklahoma, pp. 4.1-4.9.

Sivertsen, O., and Myklebust, A., 1980, "MECSYN: An Interactive Computer Graphics System for Mechanism Synthesis by Algebraic Means", ASME Paper No. 80-DET-68.

Sparks, J.W., Walters, W.T., and Tesar, D., 1968, "Multiply Separated Position Synthesis - Parts I and II", ASME Paper No. 68-Mech-66.

Srinivasan, U, Sabada, S., Kinzel, G., and Waldron, K., 1988, "Computer-Aided Design of Four-Bar Linkages for Two, Three, and Four Position Rigid Body Guidance Using Optimization Techniques", Recsyn Documentation, The Ohio State University.

Strong, R.T., and Waldron, K.J., 1979 "Joint Displacements in Linkage Synthesis Solutions", ASME Journal of Mechanical Design, Vol. 101, pp. 477-487.

Suh, C.H., and Radcliffe, C.W., 1978, Kinematics and Mechanisms Design, Wiley, New York, NY.

Sutherland, G.H. and Roth, B., 1975, "An Improved Least-Squares Method for Designing Function-Generating Mechanisms", ASME Journal of Engineering for Industry, Vol. 97, pp. 303-306.

Thiruvenkatachari, R., 1996, "Rectified Synthesis of Coupler Driven Four-Bar Mechanisms for Two and Three Position Motion Generation", Master Thesis, Old Dominion University.

Ting, K.L., 1994, "Mobility Criteria of Geared Five-Bar Linkage", Mechanism and Machine Theory, Vol. 29, No. 2, pp. 251-264.

Ting, K.L., and Long Y., 1996, "Performance Quality and Tolerance Sensitivity of Mechanism," ASME Journal of Mechanical Design, Vol. 118, pp. 114-150.

Ting, K.L., and Liu, Y.W., 1991, "Rotatability Laws for N-Bar Kinematic Chain and Their Proof", ASME Journal of Mechanical Design, Vol. 113, No. 1, pp. 32-39.

Tinubu, S. O., and Gupta, K. C., 1984, "Optimal Synthesis of Function Generators Without the Branch Defect", ASME Journal of Mechanisms, Transmissions, and Automation in Design, Vol. 106, No. 3, pp. 348-354.

Tao, D. C., 1964, Applied Linkage Synthesis, Addison-Wesley, Reading, MA.

Tsai, L.W., 1983a, "Design of Drag-Link Mechanisms With Optimum Transmission Angle", ASME Journal of Mechanisms, Transmissions, and Automation in Design, Vol. 105, pp. 254-258.

Tsai, L.W., 1983b, "Design of Drag-Link Mechanisms With Minimax Transmission Angle Deviation", ASME Journal of Mechanisms, Transmissions, and Automation in Design, Vol. 105, pp. 686-691.

Tuttle, S.b., 1963, "Error Analysis," Machine Design, Vol 35, No. 12, pp 155-157.

Vanderplaats, G.N., 1985, "ADS - A FORTRAN Program for Automated Design Synthesis - Version 1.10", Final Report, NASA, Washington, DC.

Vanderplaats, G.N., 1984, Numerical Optimization Techniques for Engineering Design With Applications, McGraw-Hill, New York, NY.

Vanderplaats, G.N., 1984, "An Efficient Feasible Directions Algorithm for Design Synthesis," AIAA Journal, Vol. 22, No. 11, pp. 1633-1640.

Venkataraman, S.C., Kinzel, G.L., and Waldron, K.J., 1992, "Optimal Synthesis of Four-bar Linkages for Four-Position Rigid-Body Guidance With Selective Tolerance Specifications," ASME DE-Vol 46, pp. 651- 659.

Waldron, K.J., 1978, "Location of Burmester Synthesis With Fully Rotatable Cranks", Mechanism and Machine Theory, Vol. 13, pp. 125-137.

Waldron, K.J., 1977, "Graphical Solution of the Branch and Order Problems of Linkage Synthesis for Multiply Separated Positions", ASME Journal of Engineering for Industry, Vol. 99, pp. 591-597.

Waldron, K.J. 1976, "Elimination of the Branch Problem in Graphical Burmester Mechanism Synthesis for Four Finitely Separated Positions", ASME Journal of Engineering for Industry, Vol. 98, pp. 176-182.

Waldron, K.J. 1975a, "Graphical Burmester Design of Four-Bar Linkages for a Specified Position Order and With all Positions Reachable Without Disconnection", Proceedings, The 4th OSU Applied Mechanisms Conference, Chicago, Illinois.

Waldron, K. J., 1975b, "The Order Problem of Burmester Linkage Synthesis", ASME Journal of Engineering for Industry, Vol. 97, pp. 1405, 1406.

Waldron, K.J., 1974a, "Range of Joint Rotation in Planar Four-Bar Synthesis for Finitely Separated Positions: Part I - The Multiple Branch Problem", ASME Paper No. 74-DET-108.

Waldron, K.J., 1974b, "Range of Joint Rotation in Planar Four-Bar Synthesis for Finitely Separated Positions: Part II - Elimination of Unwanted Grashof Configurations", ASME Paper No. 74-DET-109.

Waldron, K.J., and Kumar, A., 1977, "Numerical Burmester Synthesis on a Pocket Calculator", Proceedings of the Fifth OSU Applied Mechanisms Conference, Oklahoma City, OK, Paper No. 9.

Waldron, K. J., and Stephenson, E. N., Jr., 1979, "Elimination of Branch, Grashof, and Order Defects in Path-Angle Generation and Function Generation Synthesis", ASME Journal of Mechanical Design, Vol. 101, No. 3, pp. 428-437.

Waldron, K. J., and Strong, R. T., 1978a, "Improved Solutions of the Branch and Order Problems of Burmester Linkage Synthesis", Mechanism and Machine Theory, Vol. 13, pp. 199-207.

Waldron, K. J. and Strong, R.T., 1978b, "Improved Precision Position Mechanism Synthesis", Final Report on NSF Grant No. ENG 75-20889.

Watanabe, K., and Funabashi, H., 1984a, "Kinematic Analysis of Stephenson's Six-Link Mechanisms (1st Report, Discrimination of Composition Loops)", Bulletin of JSME, Vol. 27, No. 234, pp. 2863-2870.

Watanabe, K., and Funabashi, H., 1984b, "Kinematic Analysis of Stephenson's Six-Link Mechanisms (2nd Report, Index of Motion Transmission Characteristics)", Bulletin of JSME, Vol. 27, No. 234, pp. 2871-2878.

Watanabe, K., Huang, Z. and Kawai, Y, 1987, "A Displacement Analysis of Complex Six-Link Mechanisms of the Stephenson Type", JSME International Journal, Vol. 30, No. 261, pp. 507-514.

White, R. J., 1987, "Solution Rectification for a Stephenson III Motion Generator", M.S. Thesis, University of Minnesota.

Wilson, C. E., and Sadler, J. P., 1993, Kinematics and Dynamics of Machinery, Harper-Collins College Publishers, New York, NY, pp. 1-13.

Yan, Hong-Sen, and Long-Iong Wu, 1989, "On the Dead-Center Positions of Planar Linkage Mechanisms", ASME Journal of Mechanisms, Transmissions and Automation in Design, Vol. 111, pp. 40-46.

APPENDIX A

PARTIAL DERIVATIVES

This section provides the partial derivatives of the outputs from the equavalent linkage in Fig. 6.3 with respect to the fifteen random variables evaluated at the means of the the fifteen random variables.

The outputs are given in Equations (6.4) to (6.6) and renumbered here as

$$X_e = X_{O_A} + L_2\cos(\phi_e + \theta_e) + L_5\cos\delta_e \tag{A.1}$$

$$Y_e = Y_{O_A} + L_2\sin(\phi_e + \theta_e) + L_5\sin\delta_e \tag{A.2}$$

$$\alpha_e = \gamma_2 + \mu_e + \gamma_1 - \pi \tag{A.3}$$

where

$$L_1 = \sqrt{(l_1 + x_4 - x_1)^2 + (y_4 - y_1)^2} \approx l_1 + x_4 - x_1$$

$$L_2 = l_2$$

$$L_3 = \sqrt{(l_3 + x_3 - x_2)^2 + (y_3 - y_2)^2} \approx l_3 + x_3 - x_2$$

$$L_4 = l_4$$

$$L_5 = \sqrt{(l_5\cos\gamma_1 - x_2)^2 + (l_5\sin\gamma_1 - y_2)^2}$$

$$L_6 = \sqrt{(l_3 + x_3 - l_5\cos\gamma_1)^2 + (l_5\sin\gamma_1 - y_3)^2}$$

$$\delta_e = \gamma_e + \theta_e + \eta_e - \varepsilon_e$$

$$\varepsilon_e = \tan^{-1}\left[\frac{L_2\sin\phi_e}{L_1 - L_2\cos\phi_e}\right]$$

$$\eta_e = \cos^{-1}\left[\frac{L_1^2 + L_2^2 + L_3^2 - L_4^2 - 2L_1L_2\cos\phi_e}{2L_3\sqrt{L_1^2 + L_2^2 - 2L_1L_2\cos\phi_e}}\right]$$

$$\mu_e = \omega_e + \theta_e + \eta_e - \varepsilon_e$$

$$\theta_e = \theta_0 - \Delta\phi_e$$

$$\phi_e = \phi_0 + \Delta\phi_e$$

$$\omega_e = \tan^{-1}\left[\frac{y_2 - y_3}{l_3 + x_3 - x_2}\right]$$

$$\Delta\phi_e = \tan^{-1}\left[\frac{y_1 - y_4}{l_1 + x_4 - x_1}\right]$$

$$\gamma_e = \cos^{-1}\left[\frac{L_3^2 + L_5^2 - L_6^2}{2L_3L_5}\right]$$

$$X_{O_A} = X_{O_1} + x_1\cos\theta_0 + y_1\sin\theta_0$$

$$Y_{O_A} = Y_{O_1} - x_1\sin\theta_0 + y_1\cos\theta_0$$

The fifteen random variables are

$$Z = \left\{l_1, l_2, ..., l_i, x_1, ..., x_j, y_1, ..., y_j, \gamma_1, \gamma_2\right\}^T \qquad (A.4)$$

$$i = 5 \quad \text{and} \quad j = 4$$

where

l_i the random link length, $\bar{l}_i - t_i \le l_i \le \bar{l}_i + t_i$, $\bar{l}_i$ is the nominal link length, t_i is the tolerance band on this link length

x_j and y_j the coordinates of random location of pin centers in four clearance circles

γ_1 and γ_2 The random angles on the coupler link controlling the coupler point angular position, $\bar{\gamma}_k - \Delta\gamma_k \le \gamma_k \le \bar{\gamma}_k + \Delta\gamma_k$, $\bar{\gamma}_k$ is the nominal coupler shape angle, $\Delta\gamma_k$ is the tolerance band on the angle with k=1 , 2.

In order to simplify the expresion of the derivatives, the following substitites are used,

$$s_1 = \bar{l}_1^2 + \bar{l}_2^2 - 2\bar{l}_1\bar{l}_2\cos\phi_0$$

$$s_2 = \frac{\bar{l}_1^2 + \bar{l}_2^2 + \bar{l}_3^2 - \bar{l}_4^2 - 2\bar{l}_1\bar{l}_2\cos\phi_0}{2\bar{l}_3(\bar{l}_1^2 + \bar{l}_2^2 - 2\bar{l}_1\bar{l}_2\cos\phi_0)}$$

$$s_3 = -\frac{1}{\sqrt{1 - s_2^2}}$$

$$s_4 = -\frac{1}{\sqrt{1 - \cos^2\bar{\gamma}_1}}$$

$$\bar{\delta} = \bar{\gamma}_1 + \theta_0 + \cos^{-1}(s_1) + \tan^{-1}\left(\frac{l_2\sin\phi_0}{l_1 - l_2\cos\phi_0}\right)$$

Then, the partial derivatives evaluated at the means of the fifteen random variables can be expressed as

$$\left.\frac{\partial X_e}{\partial I_1}\right|_{M[z_m]} = -\bar{I}_5 \sin\bar{\delta}\left(\frac{s_3(s_1-\bar{I}_3^2+\bar{I}_4^2)(\bar{I}_1-\bar{I}_2\cos\phi_0)+2\bar{I}_2\bar{I}_3\sqrt{s_1}\sin\phi_0}{2\bar{I}_3 s_1\sqrt{s_1}}\right)$$

$$\left.\frac{\partial Y_e}{\partial I_1}\right|_{M[z_m]} = \bar{I}_5 \cos\bar{\delta}\left(\frac{s_3(s_1-\bar{I}_3^2+\bar{I}_4^2)(\bar{I}_1-\bar{I}_2\cos\phi_0)+2\bar{I}_2\bar{I}_3\sqrt{s_1}\sin\phi_0}{2\bar{I}_3 s_1\sqrt{s_1}}\right)$$

$$\left.\frac{\partial \alpha_e}{\partial I_1}\right|_{M[z_m]} = \frac{s_3(s_1-\bar{I}_3^2+\bar{I}_4^2)(\bar{I}_1-\bar{I}_2\cos\phi_0)+2\bar{I}_2\bar{I}_3\sqrt{s_1}\sin\phi_0}{2\bar{I}_3 s_1\sqrt{s_1}}$$

$$\left.\frac{\partial X_e}{\partial I_2}\right|_{M[z_m]} = \cos(\theta_0+\phi_0) - \bar{I}_5 \sin\bar{\delta}\left(\frac{s_3(s_1-\bar{I}_3^2+\bar{I}_4^2)(\bar{I}_2-\bar{I}_1\cos\phi_0)-2\bar{I}_2\bar{I}_3\sqrt{s_1}\sin\phi_0}{2\bar{I}_3 s_1\sqrt{s_1}}\right)$$

$$\left.\frac{\partial Y_e}{\partial I_2}\right|_{M[z_m]} = \sin(\theta_0+\phi_0) + \bar{I}_5 \sin\bar{\delta}\left(\frac{s_3(s_1-\bar{I}_3^2+\bar{I}_4^2)(\bar{I}_2-\bar{I}_1\cos\phi_0)-2\bar{I}_2\bar{I}_3\sqrt{s_1}\sin\phi_0}{2\bar{I}_3 s_1\sqrt{s_1}}\right)$$

$$\left.\frac{\partial \alpha_e}{\partial I_2}\right|_{M[z_m]} = \frac{s_3(s_1-\bar{I}_3^2+\bar{I}_4^2)(\bar{I}_2-\bar{I}_1\cos\phi_0)-2\bar{I}_2\bar{I}_3\sqrt{s_1}\sin\phi_0}{2\bar{I}_3 s_1\sqrt{s_1}}$$

$$\left.\frac{\partial X_e}{\partial I_3}\right|_{M[z_m]} = -\bar{I}_5 \frac{s_3(\bar{I}_3^2+\bar{I}_4^2-s_1)}{2\bar{I}_3^2\sqrt{s_1}}\sin\bar{\delta}$$

$$\left.\frac{\partial Y_e}{\partial I_3}\right|_{M[z_m]} = \bar{I}_5 \frac{s_3(\bar{I}_3^2+\bar{I}_4^2-s_1)}{2\bar{I}_3^2\sqrt{s_1}}\cos\bar{\delta}$$

$$\left.\frac{\partial \alpha_e}{\partial I_3}\right|_{M[z_m]} = \frac{s_3(\bar{I}_3^2+\bar{I}_4^2-s_1)}{2\bar{I}_3^2\sqrt{s_1}}$$

$$\left.\frac{\partial X_e}{\partial I_4}\right|_{M[z_m]} = \frac{s_3\bar{I}_4\bar{I}_5}{\bar{I}_3\sqrt{s_1}}\sin\bar{\delta}$$

$$\left.\frac{\partial Y_e}{\partial I_4}\right|_{M[z_m]} = -\frac{s_3\bar{I}_4\bar{I}_5}{\bar{I}_3\sqrt{s_1}}\cos\bar{\delta}$$

$$\left.\frac{\partial \alpha_e}{\partial l_4}\right|_{M[z_m]} = -\frac{s_3 \bar{l}_4}{\bar{l}_3\sqrt{s_1}}$$

$$\left.\frac{\partial X_e}{\partial l_5}\right|_{M[z_m]} = \cos\bar{\delta}$$

$$\left.\frac{\partial Y_e}{\partial l_5}\right|_{M[z_m]} = \sin\bar{\delta}$$

$$\left.\frac{\partial \alpha_e}{\partial l_5}\right|_{M[z_m]} = 0$$

$$\left.\frac{\partial X_e}{\partial x_1}\right|_{M[z_m]} = \cos\theta_0 + \bar{l}_5 \sin\bar{\delta}\left(\frac{s_3(s_1 - \bar{l}_3^2 + \bar{l}_4^2)(\bar{l}_1 - \bar{l}_2\cos\phi_0) + 2\bar{l}_2\bar{l}_3\sqrt{s_1}\sin\phi_0}{2\bar{l}_3 s_1\sqrt{s_1}}\right)$$

$$\left.\frac{\partial Y_e}{\partial x_1}\right|_{M[z_m]} = -\sin\theta_0 - \bar{l}_5 \cos\bar{\delta}\left(\frac{s_3(s_1 - \bar{l}_3^2 + \bar{l}_4^2)(\bar{l}_1 - \bar{l}_2\cos\phi_0) + 2\bar{l}_2\bar{l}_3\sqrt{s_1}\sin\phi_0}{2\bar{l}_3 s_1\sqrt{s_1}}\right)$$

$$\left.\frac{\partial \alpha_e}{\partial x_1}\right|_{M[z_m]} = -\frac{s_3(s_1 - \bar{l}_3^2 + \bar{l}_4^2)(\bar{l}_1 - \bar{l}_2\cos\phi_0) + 2\bar{l}_2\bar{l}_3\sqrt{s_1}\sin\phi_0}{2\bar{l}_3 s_1\sqrt{s_1}}$$

$$\left.\frac{\partial X_e}{\partial x_2}\right|_{M[z_m]} = -\cos\bar{\gamma}_1\cos\bar{\delta} + \bar{l}_5 \sin\bar{\delta}\left(\frac{s_3(\bar{l}_3^2 + \bar{l}_4^2 - s_1)}{2\bar{l}_3^2\sqrt{s_1}} + \frac{s_4 \sin^2\bar{\gamma}_1}{\bar{l}_5}\right)$$

$$\left.\frac{\partial Y_e}{\partial x_2}\right|_{M[z_m]} = -\cos\bar{\gamma}_1\sin\bar{\delta} - \bar{l}_5 \sin\bar{\delta}\left(\frac{s_3(\bar{l}_3^2 + \bar{l}_4^2 - s_1)}{2\bar{l}_3^2\sqrt{s_1}} + \frac{s_4 \sin^2\bar{\gamma}_1}{\bar{l}_5}\right)$$

$$\left.\frac{\partial \alpha_e}{\partial x_2}\right|_{M[z_m]} = -\frac{s_3(\bar{l}_3^2 + \bar{l}_4^2 - s_1)}{2\bar{l}_3^2\sqrt{s_1}}$$

$$\left.\frac{\partial X_e}{\partial x_3}\right|_{M[z_m]} = -\bar{l}_5\frac{s_3(\bar{l}_3^2 + \bar{l}_4^2 - s_1)}{2\bar{l}_3^2\sqrt{s_1}}\sin\bar{\delta}$$

$$\left.\frac{\partial Y_e}{\partial x_3}\right|_{M[z_m]} = \bar{l}_5\frac{s_3(\bar{l}_3^2 + \bar{l}_4^2 - s_1)}{2\bar{l}_3^2\sqrt{s_1}}\cos\bar{\delta}$$

$$\left.\frac{\partial \alpha_e}{\partial x_3}\right|_{M[z_m]} = \frac{s_3(\bar{l}_3^2 + \bar{l}_4^2 - s_1)}{2\bar{l}_3^2\sqrt{s_1}}$$

$$\left.\frac{\partial X_e}{\partial x_4}\right|_{M[z_m]} = -\bar{l}_5 \sin\bar{\delta}\left(\frac{s_3(s_1 - \bar{l}_3^2 + \bar{l}_4^2)(\bar{l}_1 - \bar{l}_2\cos\phi_0) + 2\bar{l}_2\bar{l}_3\sqrt{s_1}\sin\phi_0}{2\bar{l}_3 s_1\sqrt{s_1}}\right)$$

$$\left.\frac{\partial Y_e}{\partial x_4}\right|_{M[z_m]} = \bar{l}_5 \cos\bar{\delta}\left(\frac{s_3(s_1 - \bar{l}_3^2 + \bar{l}_4^2)(\bar{l}_1 - \bar{l}_2\cos\phi_0) + 2\bar{l}_2\bar{l}_3\sqrt{s_1}\sin\phi_0}{2\bar{l}_3 s_1\sqrt{s_1}}\right)$$

$$\left.\frac{\partial \alpha_e}{\partial x_4}\right|_{M[z_m]} = \frac{s_3(s_1 - \bar{l}_3^2 + \bar{l}_4^2)(\bar{l}_1 - \bar{l}_2\cos\phi_0) + 2\bar{l}_2\bar{l}_3\sqrt{s_1}\sin\phi_0}{2\bar{l}_3 s_1\sqrt{s_1}}$$

$$\left.\frac{\partial X_e}{\partial y_1}\right|_{M[z_m]} = \sin\theta_0 - \bar{l}_5 \sin\bar{\delta}\left(\frac{s_3(\sqrt{s_1} - \bar{l}_3^2 + \bar{l}_4^2 - s_1)\bar{l}_2\sin\phi_0}{2\bar{l}_3 s_1} - \frac{\bar{l}_2(\bar{l}_1\cos\phi_0 - \bar{l}_2) + s_1}{\bar{l}_1 s_1}\right)$$

$$\left.\frac{\partial \alpha_e}{\partial y_1}\right|_{M[z_m]} = \frac{s_3(\sqrt{s_1} - \bar{l}_3^2 + \bar{l}_4^2 - s_1)\bar{l}_2\sin\phi_0}{2\bar{l}_3 s_1} - \frac{\bar{l}_2(\bar{l}_1\cos\phi_0 - \bar{l}_2) + s_1}{\bar{l}_1 s_1}$$

$$\left.\frac{\partial X_e}{\partial y_2}\right|_{M[z_m]} = -\sin\bar{\gamma}_1\cos\bar{\delta} - \bar{l}_5\sin\bar{\delta}\left(\frac{s_4(\bar{l}_3\cos\bar{\gamma}_1 - \bar{l}_5)\sin\bar{\gamma}_1}{\bar{l}_3\bar{l}_5}\right)$$

$$\left.\frac{\partial Y_e}{\partial y_2}\right|_{M[z_m]} = -\sin\bar{\gamma}_1\sin\bar{\delta} + \bar{l}_5\cos\bar{\delta}\left(\frac{s_4(\bar{l}_3\cos\bar{\gamma}_1 - \bar{l}_5)\sin\bar{\gamma}_1}{\bar{l}_3\bar{l}_5}\right)$$

$$\left.\frac{\partial \alpha_e}{\partial y_2}\right|_{M[z_m]} = \frac{1}{\bar{l}_3}$$

$$\left.\frac{\partial X_e}{\partial y_3}\right|_{M[z_m]} = -\frac{\bar{l}_5 s_4\sin\bar{\gamma}_1\sin\bar{\delta}}{\bar{l}_3}$$

$$\left.\frac{\partial Y_e}{\partial y_3}\right|_{M[z_m]} = \frac{\bar{l}_5 s_4\sin\bar{\gamma}_1\cos\bar{\delta}}{\bar{l}_3}$$

$$\left.\frac{\partial \alpha_e}{\partial y_3}\right|_{M[z_m]} = -\frac{1}{\bar{l}_3}$$

$$\left.\frac{\partial X_e}{\partial y_4}\right|_{M[z_m]} = \bar{l}_5 \sin\bar{\delta}\left(\frac{s_3(\sqrt{s_1} - \bar{l}_3^2 + \bar{l}_4^2 - s_1)\bar{l}_2 \sin\phi_0}{2\bar{l}_3 s_1} - \frac{\bar{l}_2(\bar{l}_1 \cos\phi_0 - \bar{l}_2) + s_1}{\bar{l}_1 s_1}\right)$$

$$\left.\frac{\partial Y_e}{\partial y_4}\right|_{M[z_m]} = -\bar{l}_5 \cos\bar{\delta}\left(\frac{s_3(\sqrt{s_1} - \bar{l}_3^2 + \bar{l}_4^2 - s_1)\bar{l}_2 \sin\phi_0}{2\bar{l}_3 s_1} - \frac{\bar{l}_2(\bar{l}_1 \cos\phi_0 - \bar{l}_2) + s_1}{\bar{l}_1 s_1}\right)$$

$$\left.\frac{\partial \alpha_e}{\partial y_4}\right|_{M[z_m]} = \frac{\bar{l}_2(\bar{l}_1 \cos\phi_0 - \bar{l}_2) + s_1}{\bar{l}_1 s_1} - \frac{s_3(\sqrt{s_1} - \bar{l}_3^2 + \bar{l}_4^2 - s_1)\bar{l}_2 \sin\phi_0}{2\bar{l}_3 s_1}$$

$$\left.\frac{\partial X_e}{\partial \gamma_1}\right|_{M[z_m]} = -\bar{l}_5 \sin\bar{\delta}$$

$$\left.\frac{\partial Y_e}{\partial \gamma_1}\right|_{M[z_m]} = \bar{l}_5 \cos\bar{\delta}$$

$$\left.\frac{\partial \alpha_e}{\partial \gamma_1}\right|_{M[z_m]} = 1$$

$$\left.\frac{\partial X_e}{\partial \gamma_2}\right|_{M[z_m]} = 0$$

$$\left.\frac{\partial Y_e}{\partial \gamma_2}\right|_{M[z_m]} = 0$$

$$\left.\frac{\partial \alpha_e}{\partial \gamma_2}\right|_{M[z_m]} = 1$$

APPENDIX B

FORTRAN PROGRAM FOR TOLERANCE SYNTHESIS

```
C     ****************************************************************
      PROGRAM TOLSYN
C     ****************************************************************
C
C     A PROGRAM USED TO SYNTHESIS THE TOLERANCE AND
C      CLEARANCE OF 4-BAR
C     MOTION GENERATION
      CALL TOLMAIN
      STOP
      END
C     ****************************************************************
      SUBROUTINE COEFF(COEF1,COEF2,COEF3,COEF4,COEF5,COEF6,
     &           COEF7,COEF8,COEF9,COEF10,COEF11,TOLX,TOLY,TOLALP)
C     ****************************************************************
C
C     THIS SUBROUTINE CALCULATE THE DERIVATIVES OUTPUT W.R.T.
C     THE RANDOM VARIABLES AND THE COEFFICIENTS FOR DESIGN
C     CONSTRAINTS
C     LOCAL VARIABLES
C
C     K      -IN  LOOP VARIABLE K=6
C     NDP    -IN  NUMBER OF DESIGN POSITIONS
C     PI     -RL  PI CONSTANT
C     X      -RL  ARY-USD-DIM(6) X COORDS OF THE LINKAGE PIN LOCATN
C     Y      -RL  ARY-USD-DIM(6) Y COORDS OF THE LINKAGE PIN LOCATN
C     ANGINP -RL  ARY-USD-DIM(5) INPUT ANGLE WRT X AXIS IN DEGREE
C     THETA0 -RL  BASE LINK ANGLE
C     TOLX   -RL  ARY-USD-DIM(NDP) X DESIGN POSITION LIMIT VALUE
C     TOLY   -RL  ARY-USD-DIM(NDP) Y DESIGN POSITION LIMIT VALUE
C     TOLAOP -RL  ARY-USD-DIM(NDP) ANGULAR DESIGN POSI LIMIT C
C     VALUE
C     L1     -RL  BASE LINK LENGTH
C     L2     -RL  INPUT LINK LENGTH
C     L3     -RL  COUPLER LINK LENGTH

C     L4     -RL  OUTPUT LINK LENGTH
C     L5     -RL  LINK LENGTH FROM INPUT CIRCLE PT TO OUTPUT POINT
C
      REAL L1, L2, L3, L4, L5
      DIMENSION PHI0(4), X(6),Y(6), ANGINP(5)
      DIMENSION COEF1(12),COEF2(12),COEF3(12),COEF4(12),COEF5(12),
     &COEF6(12),COEF7(12),COEF8(12),COEF9(12),COEF10(12),COEF11(12)
      DIMENSION S1(4),S2(4),S4(4),S5(4), COF1(4),COF2(4),
     &          ETEE(4),GUMANE(4),EPSE(4),DTE(4)
      DIMENSION ETEL1(4), ETEL2(4), ETEL3(4), ETEL4(4),ETEY4(4),
```

```
     &          ETEX1(4),ETEX2(4),ETEX3(4),ETEX4(4),ETEY1(4)
      DIMENSION EPSL1(4), EPSL2(4),EPSX1(4),EPSX4(4),
     &          EPSY1(4),EPSY4(4),GUMAX2(4),GUMAY2(4),GUMAY3(4),
     &          GUMAM1(4),THETY1(4),THETY4(4)
      DIMENSION XEL1(4),XEL2(4),XEL3(4),XEL4(4),XEL5(4),
     &          XEX1(4),XEX2(4),XEX3(4),XEX4(4),XEY1(4),XEY2(4),
     &          XEY3(4),XEY4(4),XEGUM1(4)
      DIMENSION YEL1(4),YEL2(4),YEL3(4),YEL4(4),YEL5(4),
     &          YEX1(4),YEX2(4),YEX3(4),YEX4(4),YEY1(4),YEY2(4),
     &          YEY3(4),YEY4(4),YEGUM1(4)
      DIMENSION ALPHL1(4),ALPHL2(4),ALPHL3(4),ALPHL4(4),
     &          ALPHL5(4),ALPHX1(4),ALPHX2(4),ALPHX3(4),ALPHX4(4),
     &          ALPHY1(4),ALPHY2(4),ALPHY3(4),ALPHY4(4)
      DIMENSION TOLX(4),TOLY(4),TOLALP(4)
C
      COMMON /DEPCOM/ NDP
      OPEN(UNIT=4,FILE='INPUT.DAT')
      READ(4,*)NDP, (X(K),Y(K), K=1,6),(ANGINP(J), J=1,NDP),
     &  (TOLX(I),TOLY(I),TOLALP(I),I=1,NDP)
      PI=4.0*ATAN(1.0)
      DTR=PI/180.

      L1 = SQRT ((X(4)-X(1))**2 + (Y(4)-Y(1))**2)
      L2 = SQRT ((X(2)-X(1))**2 + (Y(2)-Y(1))**2)
      L3 = SQRT ((X(3)-X(2))**2 + (Y(3)-Y(2))**2)
      L4 = SQRT ((X(4)-X(3))**2 + (Y(4)-Y(3))**2)
      L5 = SQRT ((X(6)-X(2))**2 + (Y(6)-Y(2))**2)
      THETA0 = ATAN2 (Y(4) - Y(1), X(4) - X(1))
      GUMAN1 = ATAN2 (Y(6) - Y(2), X(6) - X(2))
     +         -ATAN2 (Y(3) - Y(2), X(3) - X(2))
      GUMAN2 = ATAN2 (Y(5) - Y(6), X(5) - X(6))
     +         -ATAN2 (Y(2) - Y(6), X(2) - X(6))

      WRITE(*,*)'L1 = ', L1
      WRITE(*,*)'L2 = ', L2
      WRITE(*,*)'L3 = ', L3
      WRITE(*,*)'L4 = ', L4
      WRITE(*,*)'L5 = ', L5
      WRITE(*,*) 'GUMAN1 = ', GUMAN1
      WRITE(*,*) 'GUMAN2 = ', GUMAN2
C
      DO 100 I=1,NDP
      PHI0(I) = ANGINP(I) -THETA0
C
      S2(I) = L1*L1 + L2*L2 - 2.*L1*L2*COS( PHI0(I))
```

```
      S1(I) = (S2(I) + L3*L3 -L4*L4)/(2.*L3*SQRT(S2(I)))
      S4(I) = (L3*L3 + L5*L5 -(L3-L5*COS(GUMAN1))*(L3 - L5*COS(GUMAN1))
     &     -L5*L5*SIN(GUMAN1)*SIN(GUMAN1))/(2.*L3*L5)
      S5(I) = (L1-L2*COS(PHI0(I)))*(L1-L2*COS(PHI0(I))) +
     $        L2*L2*SIN(PHI0(I))*SIN(PHI0(I))
      COF1(I) = -1./SQRT(1.-S1(I)*S1(I))
      COF2(I) = -1./SQRT(1.-S4(I)*S4(I))
C
      THETAE = THETA0
      ETEE(I) = ACOS(S1(I))
      GUMANE(I) = ACOS(S4(I))
      EPSE(I) = ATAN((L2*SIN(PHI0(I)))/(L1-L2*COS(PHI0(I))))
      IF (EPSE(I).LE.0.) THEN
      EPSE(I) = PI + EPSE(I)
      ENDIF
      DTE(I) = GUMANE(I) + THETAE + ETEE(I) - EPSE(I)
C
C     DERIVATIVE OF XE,YE,ALPHAE, W.R.T. L1
      ETEL1(I) = (COF1(I)*(SQRT(S2(I))-(S2(I) + L3*L3 -L4*L4)/
     &       (2.*SQRT(S2(I))))*(L1-L2*COS(PHI0(I))))/(L3*S2(I))
      EPSL1(I) = -L2*SIN(PHI0(I))/S5(I)
      XEL1(I) = -L5*SIN(DTE(I)) *( ETEL1(I) - EPSL1(I))
      YEL1(I) = L5*COS(DTE(I)) *( ETEL1(I) - EPSL1(I))
      ALPHL1(I) = ETEL1(I) - EPSL1(I)
C     DERIVATIVE OF XE,YE,ALPHAE, W.R.T. L2
      ETEL2(I) = (COF1(I)*(SQRT(S2(I))-(S2(I) + L3*L3 -L4*L4)/
     &        (2.*SQRT(S2(I))))*(L2-L1*COS(PHI0(I))))/(L3*S2(I))
      EPSL2(I) = L1*SIN(PHI0(I))/S5(I)
      XEL2(I) = COS(THETA0+PHI0(I))-L5*SIN(DTE(I))*(ETEL2(I)-EPSL2(I))
      YEL2(I) = SIN(THETA0+PHI0(I))+L5*COS(DTE(I))*(ETEL2(I)-EPSL2(I))
      ALPHL2(I) =ETEL2(I)-EPSL2(I)
C     DERIVATIVE OF XE,YE,ALPHAE, W.R.T. L3
      ETEL3(I) = COF1(I)*(L3*L3+L4*L4-S2(I))/(2.*SQRT(S2(I))*L3*L3)
      XEL3(I) = -L5*SIN(DTE(I))*ETEL3(I)
      YEL3(I) = L5*COS(DTE(I))*ETEL3(I)
      ALPHL3(I) = ETEL3(I)
C     DERIVATIVE OF XE,YE,ALPHAE, W.R.T. L4
      ETEL4(I) = -COF1(I)*L4/(L3*SQRT(S2(I)))
      XEL4(I) = -L5*SIN(DTE(I))*ETEL4(I)
      YEL4(I) = L5*COS(DTE(I))*ETEL4(I)
      ALPHL4(I) = ETEL4(I)
C     DERIVATIVE OF XE,YE,ALPHAE, W.R.T. L5
      XEL5(I) = COS(DTE(I))
      YEL5(I) = SIN(DTE(I))
      ALPHL5(I) = 0.
```

```
C     DERIVATIVE OF XE,YE,ALPHAE, W.R.T. X1
      ETEX1(I)= -ETEL1(I)
      EPSX1(I)= -EPSL1(I)
      XEX1(I) = COS(THETA0) - L5*SIN(DTE(I))*(ETEX1(I)-EPSX1(I))
      YEX1(I) = -SIN(THETA0) + L5*COS(DTE(I))*(ETEX1(I)-EPSX1(I))
      ALPHX1(I) =ETEX1(I)-EPSX1(I)
C     DERIVATIVE OF XE,YE,ALPHAE, W.R.T. X2
      GUMAX2(I)= -COF2(I)*SIN(GUMAN1)*SIN(GUMAN1)/L5
      ETEX2(I)= -ETEL3(I)
      XEX2(I)=-COS(GUMAN1)*COS(DTE(I))-L5*SIN(DTE(I))
     &        *(ETEX2(I)+GUMAX2(I))
      YEX2(I)=-COS(GUMAN1)*SIN(DTE(I))+L5*COS(DTE(I))
     &        *(ETEX2(I)+GUMAX2(I))
      ALPHX2(I) = ETEX2(I)
C     DERIVATIVE OF XE,YE,ALPHAE, W.R.T. X3
      ETEX3(I)= ETEL3(I)
      XEX3(I)= -L5*SIN(DTE(I))*ETEX3(I)
      YEX3(I)= L5*COS(DTE(I))*ETEX3(I)
      ALPHX3(I) = ETEX3(I)
C     DERIVATIVE OF XE ,YE,ALPHAE,W.R.T. X4
      ETEX4(I)= ETEL1(I)
      EPSX4(I)=EPSL1(I)
      XEX4(I)= -L5*SIN(DTE(I))*(ETEX4(I)-EPSX4(I))
      YEX4(I)= L5*COS(DTE(I))*(ETEX4(I)-EPSX4(I))
      ALPHX4(I) = ETEX4(I)-EPSX4(I)
C     DERIVATIVE OF XE,YE,ALPHAE, W.R.T. Y1
      THETY1(I) = -1./L1
      ETEY1(I)= COF1(I)*(SQRT(S2(I))-L3*L3+L4*L4-S2(I))*L2*SIN(PHI0(I))
     &       /(L3*S2(I))
      EPSY1(I)= ((L1-L2*COS(PHI0(I)))*L2*COS(PHI0(I))-(L2*SIN(PHI0(I)))
     &       *(L2*SIN(PHI0(I))))/(L1*S5(I))
      XEY1(I)=SIN(THETA0)-L5*SIN(DTE(I))*(THETY1(I)+ETEY1(I)-EPSY1(I))
      YEY1(I)= COS(THETA0)+L5*COS(DTE(I))*(THETY1(I)+ETEY1(I)-EPSY1(I))
      ALPHY1(I) =THETY1(I)+ETEY1(I)-EPSY1(I)
C     DERIVATIVE OF XE,YE,ALPHAE, W.R.T. Y2
      GUMAY2(I) = COF2(I)*(L3*COS(GUMAN1)-L5)*SIN(GUMAN1)/(L3*L5)
      XEY2(I) = -SIN(GUMAN1)*COS(DTE(I)) -L5*SIN(DTE(I))*GUMAY2(I)
      YEY2(I) = -SIN(GUMAN1)*SIN(DTE(I)) +L5*COS(DTE(I))*GUMAY2(I)
      OMEGY2 = 1./L3
      ALPHY2(I) =  OMEGY2
C     DERIVATIVE OF XE,YE,ALPHAE, W.R.T. Y3
      GUMAY3(I) = COF2(I)*SIN(GUMAN1)/L3
      XEY3(I) = -L5*SIN(DTE(I))*GUMAY3(I)
      YEY3(I) = L5*COS(DTE(I))*GUMAY3(I)
      OMEGY3 = -OMEGY2
```

```
      ALPHY3(I) =  OMEGY3
C     DERIVATIVE OF XE,YE,ALPHAE, W.R.T. Y4
      THETY4(I) = -THETY1(I)
      ETEY4(I) =-ETEY1(I)
      EPSY4(I) =-EPSY1(I)
      XEY4(I) = -L5*SIN(DTE(I))*(THETY4(I)+ETEY4(I)-EPSY4(I))
      YEY4(I) = L5*COS(DTE(I))*(THETY4(I)+ETEY4(I)-EPSY4(I))
      ALPHY4(I) = THETY4(I)+ETEY4(I)-EPSY4(I)
C     DERIVATIVE OF XE,YE,ALPHAE, W.R.T. GUMAN1
      GUMAM1(I)=1.
      XEGUM1(I) = -L5*SIN(DTE(I))
      YEGUM1(I) = L5*COS(DTE(I))
      ALPHM1 = 1.
C     DERIVATIVE OF XE,YE,ALPHAE, W.R.T. GUMAN2
      XEGUM2 = 0.
      YEGUM2 = 0.
      ALPHM2 = 1.
C
C     CALCULATE THE COEFFICIENTS OF THE CONSTRAINT FOR
C     OPTIMIZATION
      COEF1(3*I-2) = XEL1(I)**2
      COEF2(3*I-2) = XEL2(I)**2
      COEF3(3*I-2) = XEL3(I)**2
      COEF4(3*I-2) = XEL4(I)**2
      COEF5(3*I-2) = XEL5(I)**2
      COEF6(3*I-2) = XEX1(I)**2+XEY1(I)**2
      COEF7(3*I-2) = XEX2(I)**2+XEY2(I)**2
      COEF8(3*I-2) = XEX3(I)**2+XEY3(I)**2
      COEF9(3*I-2) = XEX4(I)**2+XEY4(I)**2
      COEF10(3*I-2) = XEGUM1(I)**2
      COEF11(3*I-2) = XEGUM2**2
C
      COEF1(3*I-1) = YEL1(I)**2
      COEF2(3*I-1) = YEL2(I)**2
      COEF3(3*I-1) = YEL3(I)**2
      COEF4(3*I-1) = YEL4(I)**2
      COEF5(3*I-1) = YEL5(I)**2
      COEF6(3*I-1) = YEX1(I)**2+YEY1(I)**2
      COEF7(3*I-1) = YEX2(I)**2+YEY2(I)**2
      COEF8(3*I-1) = YEX3(I)**2+YEY3(I)**2
      COEF9(3*I-1) = YEX4(I)**2+YEY4(I)**2
      COEF10(3*I-1) = YEGUM1(I)**2
      COEF11(3*I-1) = YEGUM2**2
C
      COEF1(3*I) = ALPHL1(I)**2
```

```
      COEF2(3*I) = ALPHL2(I)**2
      COEF3(3*I) = ALPHL3(I)**2
      COEF4(3*I) = ALPHL4(I)**2
      COEF5(3*I) = ALPHL5(I)**2
      COEF6(3*I) = ALPHX1(I)**2+ALPHY1(I)**2
      COEF7(3*I) = ALPHX2(I)**2+ALPHY2(I)**2
      COEF8(3*I) = ALPHX3(I)**2+ALPHY3(I)**2
      COEF9(3*I) = ALPHX4(I)**2+ALPHY4(I)**2
      COEF10(3*I) = ALPHM1**2
      COEF11(3*I) = ALPHM2**2
  100 CONTINUE
      RETURN
      END
C     ****************************************************************
      SUBROUTINE TOLMAIN
C     ****************************************************************
C     SUBROUTINE USED TO DECIDE THE TOLERANCE AND CLEARANCE
C     MOTION GENERATION
      DIMENSION COEF1(12),COEF2(12),COEF3(12),COEF4(12),COEF5(12),
     &COEF6(12),COEF7(12),COEF8(12),COEF9(12),COEF10(12),COEF11(12)
      DIMENSION TOLX(4),TOLY(4),TOLALP(4)
C     COMMON /DEPCOM/ NDP,NNDP
      COMMON /DEPCOM/ NDP
      DIMENSION X(12),VLB(12),VUB(12),G(12),IDG(12),IC(12),
     &DF(12),A(12,12),WK(1500),IWK(600)
      DIMENSION  TOL(5),CLEAR(4),TOLANG(2)
C     COMMON /DEPCOM/ NDP
      OPEN(FILE='EXAMPLE1.DAT',UNIT=7,FORM='FORMATTED')
      CALL COEFF(COEF1,COEF2,COEF3,COEF4,COEF5,COEF6,
     &           COEF7,COEF8,COEF9,COEF10,COEF11,TOLX,TOLY,TOLALP)
C     COMMON /DEPCOM/ NDP,NNDP
C     ARRAY DIMENSIONS.
      NRA=12
      NCOLA=3*NDP
      NRWK=1000
      NRIWK=500
C     PARAMETERS.
      IGRAD=0
      NDV=11
      NCON=3*NDP
C     INITIAL DESIGN.
C
      DO 200 J=1,12
```

```
      X(J)=0.0000001
      VLB(J)=1.E-11
      VUB(J)=.01
  200 CONTINUE
C     PI VALUE
      PI=4*ATAN(1.0)
C     IDENTIFY CONSTRAINTS AS LINEAR , INEQUALITY.
      DO 300 K=1,NDP
      IDG(3*K-2)=2
      IDG(3*K-1)=2
      IDG(3*K) =2
  300 CONTINUE
C     INPUT.
      WRITE(*,*) 'READ ISTART , IOPT, IONED IPRINT ! '
      READ(*,*) ISTART,IOPT,IONED,IPRINT
C     OPTIMIZE.
      INFO=0
C
  10  CALL ADS
(INFO,ISTART,IOPT,IONED,IPRINT,IGRAD,NDV,NCON,X,VLB,VUB,
     & OBJ,G,IDG, NGT,IC,DF,A,NRA,NCOLA,WK,NRWK,IWK,NRIWK)
C
      IF (INFO.EQ.0) GO TO 20
C     EVALUATE OBJECTIVE AND CONSTRAINTS.
      OBJ= 1./X(1)+1./X(2)+1./X(3)+1./X(4)
     &     +1./X(5)+1./X(6)+1./X(7)+1./X(8)+1./X(9)+1./X(10)+1./X(11)
C
C     EVALUATE THE CONSTRAINT
      DO 400 K=1,NDP
      G(3*K-2)= COEF1(3*K-2)*X(1) + COEF2(3*K-2)*X(2) +COEF3(3*K-2)*X(3)
     &         +COEF4(3*K-2)*X(4) + COEF5(3*K-2)*X(5) +COEF6(3*K-2)*X(6)
     &         +COEF7(3*K-2)*X(7) + COEF8(3*K-2)*X(8) +COEF9(3*K-2)*X(9)
     &         +COEF10(3*K-2)*X(10) + COEF11(3*K-2)*X(11) - TOLX(K)/3.0
C
      G(3*K-1)= COEF1(3*K-1)*X(1) + COEF2(3*K-1)*X(2) +COEF3(3*K-1)*X(3)
     &         +COEF4(3*K-1)*X(4) + COEF5(3*K-1)*X(5) +COEF6(3*K-1)*X(6)
     &         +COEF7(3*K-1)*X(7) + COEF8(3*K-1)*X(8) +COEF9(3*K-1)*X(9)
     &         +COEF10(3*K-1)*X(10) + COEF11(3*K-1)*X(11) - TOLY(K)/3.0
C
      G(3*K)= COEF1(3*K)*X(1) + COEF2(3*K)*X(2) +COEF3(3*K)*X(3)
     &         +COEF4(3*K)*X(4) + COEF5(3*K)*X(5) +COEF6(3*K)*X(6)
     &         +COEF7(3*K)*X(7) + COEF8(3*K)*X(8) +COEF9(3*K)*X(9)
     &         +COEF10(3*K)*X(10) + COEF11(3*K)*X(11) - TOLALP(K)/3.0
C
  400 CONTINUE
C     GO CONTINUE WITH OPTIMIZATION.
```

```
      GO TO 10
   20 CONTINUE
C
        WRITE(7,40) OBJ
        WRITE(7,41) G(1),G(2),G(3)
        WRITE(7,42) G(4),G(5),G(6)
        IF (K.EQ.3) THEN
        WRITE(7,43) G(7),G(8),G(9)
        ENDIF
        IF (K.EQ.4) THEN
        WRITE(7,43) G(7),G(8),G(9)
        WRITE(7,44) G(10),G(11),G(12)
        ENDIF
        WRITE(7,45) X(1),X(2)
        WRITE(7,50) X(3),X(4)
        WRITE(7,60) X(5),X(6)
        WRITE(7,70) X(7),X(8)
        WRITE(7,80) X(9),X(10)
        WRITE(7,85) X(11)
   30   FORMAT (4I5)
   40   FORMAT (//5X,7HOPTIMUM,5X,5HOBJ =,E12.5)
   41   FORMAT (/5X,6HG(1) =,E12.5,5X,6HG(2) =,E12.5,5X,6HG(3) =,E12.5)
   42   FORMAT (/5X,6HG(4) =,E12.5,5X,6HG(5) =,E12.5,5X,6HG(6) =,E12.5)
   43   FORMAT (/5X,6HG(7) =,E12.5,5X,6HG(8) =,E12.5,5X,6HG(9) =,E12.5)
   44   FORMAT (/5X,7HG(10) =,E12.5,5X,7HG(11) =,E12.5,5X,7HG(12) =,E12.5)
   45   FORMAT (/5X,6HX(1) =,E12.5,5X,6HX(2) =,E12.5)
   50   FORMAT (/5X,6HX(3) =,E12.5,5X,6HX(4) =,E12.5)
   60   FORMAT (/5X,6HX(5) =,E12.5,5X,6HX(6) =,E12.5)
   70   FORMAT (/5X,6HX(7) =,E12.5,5X,6HX(8) =,E12.5)
   80   FORMAT (/5X,6HX(9) =,E12.5,5X,7HX(10) =,E12.5)
   85   FORMAT (/5X,7HX(11) =,E12.5//)
      DO 11 J =1, 5
      TOL(J) = SQRT(X(J))*3.
      WRITE (7,*)'TOL(',J,') = ', TOL(J)
   11 CONTINUE
      DO 22 K =6, 9
      CLEAR(K) = SQRT(0.75*PI*X(K))
      WRITE (7,*)'CLEAR(',K,') = ', CLEAR(K)
   22 CONTINUE
      DO 33 I =10, 11
      TOLANG(I) = SQRT(X(I))*3.0*180./PI
      WRITE (7,*)'TOLANG(',I,') = ', TOLANG(I)
   33 CONTINUE
        CLOSE(7)
        STOP
        END
```